

TALES FROM THE CRYPTO:
PHAGOLYSOSOMAL PHENOMENA FEATURING FUNGI

by
Quigly Dragotakes

A thesis submitted to Johns Hopkins University in conformity with the requirements for the
degree of Doctor of Philosophy

Baltimore, Maryland

June 2020

© 2020 Quigly Dragotakes

All Rights Reserved

Front Matter

Abstract

Host-pathogen interactions are a cornerstone of microbiology and medicinal research. Many incredible cellular mechanisms evolved from arms races between pathogens and host defenses. Studying these mechanisms leads to significant advances in molecular biology (ex. CRISPR/Cas) and medicine (ex. Penicillin). By understanding the delicate balance of the damage-response framework of microbial disease and studying how microbes and host cells outmaneuver each other, we can better understand pathogenesis to develop therapeutic strategies against debilitating disease. I study the host-pathogen interactions of *Cryptococcus neoformans* and macrophages, sites of various cellular phenomena with far reaching implications in fields ranging from immunology to bioremediation.

I begin by describing phagolysosome acidification dynamics as a bet hedging strategy which macrophages employ to maximize fitness considering the variety of encounterable pathogens. Understanding this initial, broadly effective defense gives a frame of reference for downstream host-pathogen interactions. Phagolysosomal pH is an important aspect of this initial defense but is largely overlooked and undervalued.

Next, I focus on the mechanism of *C. neoformans* macrophage-to-macrophage transfer. The existence of this phenomenon has been previously reported, but its mechanism is undiscovered. Using fluorescent microscopy with reporters specific to cellular compartments, antibody blockades for surface receptors, and live cell microscopy to follow infection outcomes I focus on understanding the circumstances of this phenomenon and place its mechanism within known cellular processes.

Finally, I present work in progress toward understanding the interplay of *C. neoformans* and macrophages in the context of Dragocytosis. Using transcriptomics, fluorescence microscopy,

and simulations I outline how phagolysosome acidification and Dragocytosis are linked and provide evidence suggesting Dragocytosis is a survival mechanism to escape hostile phagolysosomes.

These data bring new understanding to several facets of *C. neoformans* pathogenesis and suggest mechanisms which may be common to other human pathogens.

Written under the advisory of Arturo Casadevall, Monica Mugnier, Dennis Wirtz, and Valeria Culotta.

Preface

Acknowledgements

I would like to acknowledge my scientific genealogy for helping to shape me into the scientist I am today. As a nuclear pharmacist and echocardiogram technician/zookeeper/science teacher both of my parents made sure our house was science friendly growing up. My brothers, for not being interested in research so I can pretend I'm the only doctorate in the family because I'm the smartest not because they got real jobs and don't need a Ph.D. The entire Ithaca College Chemistry and Biology departments which were filled with extremely dedicated, helpful, and straight up fun professors and excellent fellow students. Especially Scott Ulrich Ph.D. and Emily Garcia-Sega Ph.D. for being my research mentors throughout my four years. And Te-Wen Lo Ph.D. who became my second mentor and good friend in my senior year. Additionally, I do not think I would have been as successful without my friends Elitsa Stoyanova, Josh Messinger, Andrew Becker, Tom Dilcher, and especially Robert Nichols as colleagues and study group. The Greengard Laboratory at Rockefeller University, particularly Jean-Pierre Roussarie Ph.D., who mentored me the two years after graduation. The entire MMI department for which I am writing this dissertation, and my thesis committee for guiding me through this process. Specifically, I'd like to thank Monica Mugnier Ph.D. who has been an incredible help, an excellent mentor, and a good friend. Finally, the Casadevall Laboratory and Arturo Casadevall himself. I genuinely do not believe I would have achieved anything close to what I have here without Arturo's guidance.

I would also like to acknowledge the funding I received throughout my Ph.D. for these, and other, projects. The Achievement Rewards for College Scientists (ARCS) Metro-Washington Chapter. The National Institutes of Health which awarded our department a T32, and my department for accepting my application for funding on it. The BANG award, another MMI

department award. And I acknowledge BioRender for their service which I used to create some of my figures.

Additionally, there are several non-scientific acknowledgements I would like to make. Nina Grossman for suggesting the “Tales from the Crypto” title. Everyone who has been part of the Racquetball crew especially Ricardo (who taught me), Rada, Raghav, Daniel, Jenna, Jaime, and Leon. The Rat Tales (Nina, Daniel, Jamie, and Raghav) for giving me a weekly escape from boring normal life. I also unironically acknowledge videogames as one of the strongest influences on my problem solving and critical thinking abilities.

Contents

Front Matter	ii
Abstract.....	ii
Preface	iv
Acknowledgements.....	iv
List of Abbreviations	viii
List of Tables	x
List of Figures	xi
Introduction	1
<i>Cryptococcus neoformans</i>	1
Macrophages and the Host Response	2
Phagocytosis and Phagolysosome Acidification	3
The <i>C. neoformans</i> Containing Phagolysosome.....	5
Autophagy.....	8
Reactive Oxygen and Nitrogen Species.....	9
Extracellular pH Sensing in <i>C. neoformans</i>	11
A Gap in Knowledge – Summary of Significance.....	12
Part I: Acidification Dynamics of the Macrophage Phagolysosome	20
Abstract.....	20
Introduction	21
Materials and Methods.....	23
Results.....	31
Discussion.....	42
Part II: Dragocytosis.....	77
Abstract.....	77
Introduction	77
Materials and Methods.....	79
Results.....	87
Discussion.....	94
Part III: Triggers of Dragocytosis.....	119
Abstract.....	119
Introduction	119
Materials and Methods.....	122

Results.....	126
Discussion	130
Discussion	142
Summary.....	142
Relationship to Field	147
Limitations	148
Future Directions	150
Final Note.....	152
References	153
Curriculum Vitae	169

List of Abbreviations

Arg: arginase

BMDM: bone marrow derived macrophages

CR: complement receptor

DMEM: Dulbecco's modified Eagle medium

EEA1: early endosome antigen 1

ESCRT: endosomal sorting complex required for transport

FcR: Fc receptor

GAP: GTPase activating protein

GEF: guanine exchange factor

HBSS: Hank's balanced salt solution

IFN γ : gamma interferon

IACUC: Institutional Animal Care and Use Committee

IL-4: Interleukin 4

iNOS: inducible nitric oxide synthase

LAMP: lysosomal membrane associated protein

LC3: Microtubule-associated protein 1A/1B-light chain 3

LPS: lipopolysaccharide

M6PR: mannose-6-phosphate receptor

mAb: monoclonal antibody

NOX: NADPH oxidase

OG: Oregon Green

PAMP: pathogen associated molecular pattern

PBS: phosphate buffered saline

PtdIns3P/4P: phosphatidylinositol 3/4-phosphate

RILP: Rab interacting lysosomal protein

ROS: reactive oxygen species

Rra1: required for Rim101 activation 1

SAB: Sabouraud

SOD: superoxide dismutase

V-ATPase: vacuolar-type H⁺-ATPase

List of Tables

Table 1.....	19
Table 2.....	76
Table 3.....	117
Table 4.....	118

List of Figures

Figure 1	15
Figure 2	16
Figure 3	17
Figure 4	18
Figure 5	54
Figure 6	55
Figure 7	56
Figure 8	57
Figure 9	58
Figure 10	59
Figure 11	60
Figure 12	61
Figure 13	62
Figure 14	63
Figure 15	64
Figure 16	65
Figure 17	66
Figure 18	67
Figure 19	68
Figure 20	69
Figure 21	70
Figure 22	71
Figure 23	72
Figure 24	73
Figure 25	103
Figure 26	104
Figure 27	106
Figure 28	107
Figure 29	109
Figure 30	110
Figure 31	111
Figure 32	112
Figure 33	113
Figure 34	115
Figure 35	116
Figure 36	134
Figure 37	135
Figure 38	136
Figure 39	137
Figure 40	138

Figure 41	139
Figure 42	140
Figure 43	141

Introduction

Cryptococcus neoformans

Cryptococcus neoformans is a facultative intracellular fungal pathogen that resides in phagolysosomes within human hosts¹. It is responsible for a significant global health burden, most commonly among immune compromised populations, causing up to 1.5 million deaths each year². The human route of infection involves inhaling either yeasts or spores, likely from the environment³. Once inhaled, the yeasts can be opsonized by complement, surfactant, or antibody if present and are eventually ingested by alveolar macrophages¹. In an immune competent host, the yeasts are sequestered within granulomas and eventually cleared, with macrophages and neutrophils playing a significant role. In immune compromised hosts, however, *C. neoformans* can disseminate and eventually reach the brain where it results in cryptococcal meningitis, often fatal (Figure 1). It is currently unknown how *C. neoformans* passes the blood brain barrier, though the suggestion of a trojan horse method⁴ by escaping host macrophages after passing the barrier seems likely, supported by observing *C. neoformans* within phagocytes past the blood brain barrier⁵ and that the presence of *C. neoformans* containing phagocytes leads to increased brain dissemination⁶.

Early interactions between *C. neoformans* and macrophages are key to controlling infection⁷. Macrophages must inhibit pathogen growth before being overwhelmed. However, *C. neoformans* yeasts have an array of virulence factors and cellular processes which help combat

phagolysosomal defenses. Perhaps the most significant of which is the polysaccharide capsule, a protective layer of sugars and glycoproteins which excludes small particles, buffers environmental pH, modulates the host immune system, inhibits phagocytosis, and protects the yeast from desiccation as well as free radicals⁸⁻¹². In fact, even the initial size of the capsule can be a determinant of downstream control of infection, implying early events in macrophage-*Cryptococcus* interactions can have significant effects on overall disease outcome⁷. Previous investigations have established several other factors related to the outcome of *C. neoformans*-macrophage interactions. Phagolysosomal pH buffering via the polysaccharide capsule⁸ and urease¹³ activity, the process of capsule enlargement^{7,14,15}, proliferation⁷, melanization^{16,17}, and modulation of phagolysosomal integrity¹⁸ all play a role in these early interactions and have downstream effects on infection outcome. Later, during residence in the macrophage phagolysosome, *C. neoformans* exhibits the fascinating ability to exit the host macrophage through a variety of methods: host cell lysis, non-lytic exocytosis (Vomocytosis)¹⁹, or lateral transfer (herein named Dragocytosis)²⁰ (Figure 2).

Macrophages and the Host Response

The host of the host-pathogen interactions in *C. neoformans* infection is a complex and coordinated response involving all arms of the immune system, a notion supported by the prevalence of Cryptococcosis in immune compromised populations. It is known that Th1 vs. Th2 skewing in mouse models results in different disease outcomes²¹⁻²³. Specifically, this thesis focuses heavily on macrophages, as they are significant early responders to *C. neoformans* infection along with neutrophils and dendritic cells. Along with Th1/Th2 skewing, macrophage

polarization state also plays an important role in *C. neoformans*, with different polarizations promoting different disease outcomes. Notably, M1 macrophages are resistant while M2 are permissive to *C. neoformans* infection^{21,22,24}. Macrophages are polarized when they encounter certain cytokines and pathogen molecules, commonly IFN γ with LPS for M1 and IL-4 for M2²⁵. In reality the *in vivo* environment likely includes a spectrum of polarized macrophages rather than two distinct and extreme populations of either M1 or M2 polarized²⁶. These differences are generated, in part, by differences in the phagolysosome creation and maturation processes between the two types of macrophages. Acidity of the phagolysosome, speed of acidification, ROS activity, antigen cross-presentation, and timing of phagosome-lysosome fusion all differ between the two and all are important to inhibition of ingested pathogens²⁷⁻³¹. Therefore, while the Th1/Th2 paradigm is not a complete model of immune system function, studying polarization states can still provide insight into pathology, specific cellular processes, and potentially inform or predict infection outcome.

Phagocytosis and Phagolysosome Acidification

Phagocytosis is an ancient cellular process with various roles from nutrient acquisition to the ingestion and elimination of pathogens. More generally, phagocytosis refers to the ingestion of particles at least 5 μm in size. Before ingesting a target particle, the macrophage must first come into contact with it. Macrophages are constantly actively probing at their environment by extending and retracting pseudopods, projections of the plasma membrane formed through Arp2/3 directed branched actin polymerization and covered in various membrane bound receptors³². In this thesis we focus on receptor mediated phagocytic ingestion of *C. neoformans*,

a recognition-based process dependent on the presence and activation of various surface receptors. Specifically, we study the FcR and CR which bind constant regions of Immunoglobins and complement, respectively, and are the major players in *C. neoformans* recognition and ingestion³³.

The processes of FcR and CR based internalization differ slightly but both depend on receptor clustering signals and trigger internalization through a complex process involving pseudopod extension via ARP2/3 guided actin branching³⁴, which requires the activation of several other players including RhoA, WASP, WAVE, and Rac³⁵. Upon clustering, the FcR cytoplasmic tail phosphorylates, activating Syk and a signaling cascade which results in Rho activation via GEFs and further activates ARP2/3 guided actin polymerization leading to formation of a phagocytic cup via the plasma membrane surrounding the FcR opsonized particle. On the other hand, CR uses Rap and RhoA to recruit adapter proteins and activate mDia and Rac^{36,37}. Regardless of the initiation path, once the opsonized particle is surrounded, actin at the base of the phagocytic cup depolymerizes, pulling the surrounded particle inward and sealing the phagocytic cup. In short, macrophages recognize particles via surface receptors which, when clustered, transduce signals resulting in remodeling of the plasma membrane and actin cytoskeleton to engulf said target particle³⁸.

Once the particle has been ingested it is contained within the phagocytic cell in a single membrane organelle referred to as the phagosome³⁹. The phagosome undergoes maturation, progressing from early phagosome to late phagosome to phagolysosome. Maturation involves many changes

to both the membrane composition and interior contents of the organelle resulting in a hostile environment for ingested pathogens. Numerous endosomes and vesicles fuse with the newly formed phagosome, and evidence suggests some fuse even before the phagosome is fully formed⁴⁰. Rab5 acquisition and activation is a key marker of the transition to early phagosome along with remodeling of the lipid membrane to enrich PtdIns3P⁴¹⁻⁴⁴. These changes result in recruitment of EEA1^{45,46}, another early phagosome marker with a role in vesicle/membrane fusion⁴⁷. By fusing with late endosomes, the phagosome acquires V-ATPase, a membrane bound proton pump which begins to acidify the interior of the phagosome⁴⁸, as well as NOX2 which contributes reactive oxygen species for antimicrobial activity as well as pH modulation³¹. This marks the transition to the late phagosome, which can be visualized by the replacement of Rab5 with Rab7⁴⁹⁻⁵¹ or with the replacement of PtdIns3P with PtdIns4P⁵². Finally, the late phagosome becomes a phagolysosome, associated with the acquisition of new markers LAMP-1/2 and fusion with lysosomes^{53,54}. At this point the phagolysosome contains degradative proteins, reactive oxygen species, and is acidic in nature. The environment is incredibly harsh and inhospitable to any engulfed pathogens. The specifics of the phagolysosome can differ depending on the cell in which it is formed (macrophage, neutrophil, dendritic cell, etc.). The focus here is on the macrophage phagolysosome and its interactions with *C. neoformans*.

The *C. neoformans* Containing Phagolysosome

The phagolysosome is a membrane bound organelle found within the cytosol, the end result of *C. neoformans* ingested by a macrophage via receptor-mediated phagocytosis. As the late

phagosome matures to the phagolysosome, its membrane and interior both contain various and distinct proteins (Figure 3).

The GTPase Rab7 has important roles throughout the phagosome maturation process. It is essential for phagolysosome maturation, specifically by mediating the fusion of phagosome and lysosomes (or late endosomes) via membrane protrusions⁵⁵. Rab7 associates with RILP which includes a dynein-dynactin recruitment domain. RILP, in turn, promotes the projection of these membrane protrusions via microtubule action⁴⁹.

V-ATPase is a 14-subunit complex composed of two major structures: V_0 and V_1 . V_0 is associated with the actual transport of H^+ ions across the membrane while V_1 is associated with the ATP hydrolyzing action. V-ATPase is recruited to early phagosomes, acting quickly to acidify the compartment⁵⁶. It remains in the membrane as the organelle matures, maintaining the acidity of the compartment. It is not currently known how these V-ATPases are transported to the phagolysosome, but COPI vesicles have been shown to be required for phagolysosome maturation and acidification, suggesting the V-ATPases could be shuttled from the Golgi network⁵⁷.

NOX is a membrane bound protein which generates oxidative bursts of reactive oxygen species in various cell types for functions ranging from cell differentiation to anti-microbial activity^{58,59}. In terms of the phagolysosome and combatting *C. neoformans*, NOX is most relevant in its capacity for generating oxidative burst, specifically NOX2⁶⁰. NOX2 is recruited to the late phagosome by

VAMP7 and proceeds to generate $O_2^{\bullet-}$ from O_2 inside the phagosome by coupling NADPH hydrolysis in the cytosol^{61,62}.

LAMP-1 and LAMP-2 are transmembrane proteins found in abundance across the phagolysosome membrane. Knockouts of each individual LAMP do not show incredible differences in phagolysosome maturation but do result in upregulation of the still present LAMP, suggesting the two may share function and complement each other. However, knocking out both LAMPs inhibits the phagolysosome maturation process and the compartments are no longer acidified⁵⁴. Additionally, a double knockout does not abrogate the ability to form phagosomes from receptor mediated phagocytosis, supporting the conclusion that LAMPs are required for maturation rather than formation.

Cathepsins are lysosomal proteases which enter the phagosome upon fusion with lysosomes. They are a family of papain like proteases and some of the most well studied hydrolytic proteins of the lysosome⁶³. Cathepsins are mostly synthesized in a zymogen form to avoid uncontrolled proteolysis, with activation processing occurring in the lysosome itself⁶⁴. Should Cathepsins leak out of the phagolysosome they initiate apoptosis via caspase activation, as seen with Cathepsin D activation of caspase-8 in *C. neoformans* infection of macrophages due to a loss of phagosomal membrane integrity⁶⁵. Cathepsin B also plays an important role in *C. neoformans* defense and has been shown to inhibit cryptococcal growth in dendritic cells⁶⁶. Macrophages also generate Cathepsin B when activated, and it may account for a significant proportion of their *C. neoformans* killing ability⁶⁷.

The M6PR is a known lysosome addressing marker and its main function is to direct the delivery of lysosomal hydrolases⁶⁸. M6PR does not have a direct action related to *C. neoformans* infection but it remains an important marker for distinguishing the different phases of the phagosome as it matures.

Finally, *C. neoformans* containing phagolysosomes can sometimes be decorated with LC3, an autophagy marker⁶⁹. Specifically, LC3 decoration has been noted on subpopulations of antibody opsonized *C. neoformans* containing phagolysosomes, but not complement opsonized⁷⁰. Pathogen containing phagolysosomes decorated with LC3 are considered autophagolysosomes and can bridge the phagocytic and autophagic pathways, though the terminology is somewhat convoluted and debated⁷¹.

Autophagy

Autophagy is a cellular process responsible for degrading and removing waste products such as unwanted or damaged proteins and organelles. It is also relevant in combatting certain intracellular pathogens. Autophagy is triggered by the formation of the PI3K-III and ULK complexes which promote the formation of a phagophore. ATG16L, ATG12, and ATG5 promote the recruitment of LC3 to the phagophore as it loads with cargo. The phagophore then seals around the cargo forming an LC3 decorated autophagosome. This autophagosome then fuses with lysosomes resulting in an autolysosome and degradation of its contents.

The autophagy pathway is important to several aspects of *C. neoformans* cellular pathogenesis but the interactions are complicated and differ between host cell types. In BMDMs polarization state has a strong effect on autophagy and *C. neoformans* interactions. Using RNAi to knock down *atg5* expression results in decreased *C. neoformans* growth in M0 macrophages and increased growth in M1 polarized⁷⁰. In the *atg5*^{-/-} mouse model survivability is unchanged but there is a lower fungal lung burden and decreased inflammation⁷⁰. In immortalized murine macrophage like cells (J774) inhibiting ATG5 activity leads to decreased Vomocytosis and increased *C. neoformans* growth^{69,70}. Interestingly, a subpopulation of *C. neoformans* containing phagolysosomes associate with the autophagolysosomal marker LC3 only when the *C. neoformans* is ingested via antibody mediated phagocytosis^{72,73}. However, the experiments which observed only a subpopulation of phagolysosomes as LC3 positive were based on microscopy at set time points and it is possible that all *C. neoformans* phagolysosomes are LC3 positive but only at certain time points during infection. The relationship between autophagy and *C. neoformans* phagolysosomes is still poorly understood.

Reactive Oxygen and Nitrogen Species

One of the most powerful defense mechanisms phagocytic cells can employ against ingested pathogens is the creation of and exposure to ROS⁷⁴. In what is generally described as an “oxidative burst” or “respiratory burst”, phagocytic cells convert O₂ into O₂^{•-} and generate H₂O₂⁷⁵. While it is not fully known how ROS kill pathogens, ROS are extremely destructive to almost every type of biomolecule and can attack any oxidizable side group^{76,77}.

$O_2^{\bullet-}$ is generated from O_2 using the reductive potential of NADH via NOX, located at the phagolysosomal membrane. $O_2^{\bullet-}$ can later, spontaneously or enzymatically, generate H_2O_2 ⁷⁸. H_2O_2 can further reduce into 2 HO^{\bullet} by oxidizing other reagents, for example Fe^{2+} to Fe^{3+} . HO^{\bullet} is another particularly reactive species which can then go on to damage DNA or cellular proteins. Additionally, ROS are small polar molecules which allows them to permeate cellular membranes, making them difficult for pathogens to keep out. Reactive nitrogen species are intertwined with the reactive oxygen species generating system and fulfill a similar role in defense⁷⁹. PAMPS, cytokines, and other danger signals activate iNOS which converts O_2 and arginine into citrulline and NO^{\bullet} ⁸⁰. NO^{\bullet} can then react with $O_2^{\bullet-}$ to form $ONOO^{\bullet}$ or NO_2^{\bullet} , the reactive nitrogen species.

ROS are a natural byproduct of normal mitochondrial function and most eukaryotes have build in mechanisms for dealing with buildup of cellular ROS⁸¹. Usually this is achieved through the conversion of $O_2^{\bullet-}$ to H_2O_2 via SODs and then neutralization of H_2O_2 to H_2O and O_2 via catalase, peroxidase, peroxiredoxins, and thioredoxins⁸². *Cryptococcus neoformans* most notably uses SOD1 but is further able to defend itself from ROS via melanin, its polysaccharide capsule, and by scavenging reactive oxygen/nitrogen intermediates^{9,83-89}. Furthermore, the oxidative burst of macrophages is relatively weak in relation to that of neutrophils which may help explain *C. neoformans* ability to persist so well inside the macrophage phagolysosome⁹⁰.

Extracellular pH Sensing in *C. neoformans*

Survival across several environments of differing pH (soil, water, lungs, macrophage or amoeba phagolysosomes, etc.) requires *C. neoformans* to have efficient methods of sensing pH and responding accordingly. *C. neoformans* contain and express Rim/PalpH, a fungi conserved alkaline pH sensing system. Interestingly, this extracellular pH sensing pathway is also associated with the expression of virulence factors in many pathogenic fungi, and even contributes to capsule growth in *C. neoformans* specifically. In *C. neoformans* the Rim pathway is suspected to be controlled upstream by the Rra1 pH sensor, rather than the canonical Rim pH sensor Rim21, though other homologs of Rim upstream proteins have not yet been characterized.

In fact, the specifics of the *C. neoformans* pathway are largely unknown compared to the more well studied pathways of *Saccharomyces cerevisiae* or *Candida albicans*. Overall however, the pathways share many similarities. Generally speaking, Rim9 and Rim21/Dfg16 are embedded in the plasma membrane and are able to sense extracellular pH⁹¹. Rim8 associates with the cytosolic tail of Rim21/Dfg16 and, upon sensing alkaline pH, is ubiquitinated or phosphorylated allowing interaction with Rim23. The entire complex is endocytosed, allowing further interaction with the ESCRT complex, through which Rim20/Rim13 interact and recruit Rim101. Rim101 is then processed and activated (Figure 4A).

While a system explicitly for sensing acidic pH has not yet been described in *C. neoformans*, it would stand to reason the fungi have the ability to adapt to acidic environments since they

transfer rapidly from acidic environment, to neutral host blood, to acidic macrophage phagolysosomes in what can be fast and drastic pH changes. One explanation is that the inactivated Rim pathway is itself a signal for residing in an acidic environment, acting as a logic gate determining downstream cellular recognition of and reaction to acidic environments (Figure 4B).

A Gap in Knowledge – Summary of Significance

Generally speaking, many host-pathogen interactions can be summarized as either host and pathogen developing strategies to gain an advantage over one, and the other developing strategies to overcome that advantage. Many of these interactions occur at the phagolysosome, one of the macrophages' main defense against pathogens, and involve pathogens' strategies for evading, escaping, or surviving the phagolysosome. The macrophages develop a strategy to combat pathogens and the pathogens develop strategies to combat the phagolysosome. Therefore, to understand host pathogen interactions, we must understand what is happening on both sides, the macrophage and the pathogen.

However, the field lacks key information regarding some of the above macrophage-*C. neoformans* interactions. First, macrophages are initially able to inhibit pathogens by acidifying their phagolysosomes to inhospitable pH ranges, yet those macrophages would have no prior knowledge of what pathogen would be ingested and therefore would have no knowledge of what phagolysosome conditions will be most effective against said pathogen. Host defense

mechanisms are an important aspect of pathogenesis. Understanding these strategies is essential to studying host-pathogen interactions and *C. neoformans* infection is heavily influenced by the outcome of the macrophage-yeast interaction. Part one of this thesis explores how immune competent hosts can manage an infection without prior knowledge of a pathogen's weaknesses by modelling and observing a macrophage bet-hedging strategy used to combat pathogens using stochastic phagolysosomal acidification.

Second, as mentioned, *C. neoformans* is capable of transferring from one macrophage to another while contained in the phagolysosome but the mechanism for this process was not previously known. *C. neoformans* infection results in death due to invasion of the brain and resulting meningoencephalitis. It is believed that *C. neoformans* are able to enter the brain using a "Trojan Horse" method dependent on entering and subsequently transferring or exiting host macrophages^{4,6,92-94}. Understanding how *C. neoformans* can transfer between host cells can shed light on how the yeast is able to penetrate the blood brain barrier. Part two of this thesis uses fluorescence microscopy and receptor blockading to argue that the process of Dragotcytosis is a coordination of exocytosis and phagocytosis between two proximal macrophages.

Finally, it is also unknown why the Dragotcytosis process is triggered or specifically how the process benefits *C. neoformans*. *C. neoformans* is not the only intracellular pathogen capable of transferring between host cells, and the process appears to benefit the pathogen. Developing potential treatments to blockade this pathogen process requires understanding of how and why the yeast triggers the process in the first place. Part three of this thesis builds on observations

made in the first two parts to argue that Dragotcytosis can be triggered by inhospitable phagolysosomal pH and that even if a small proportion of *C. neoformans* undergo Dragotcytosis it will greatly increase their chances of survival.

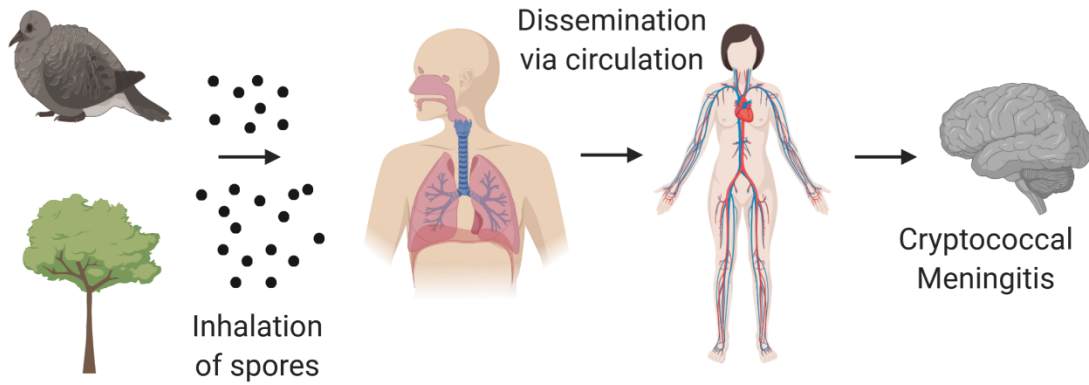


Figure 1

Cryptococcus neoformans pathogenesis. The yeast exists ubiquitously throughout the environment where spores can be spread by a variety of vectors. Spores are inhaled and the yeast propagates within the lungs. In immune compromised patients the yeast can spread via the bloodstream and invade the brain, likely through a Trojan horse mechanism, where it results in Cryptococcal meningitis.

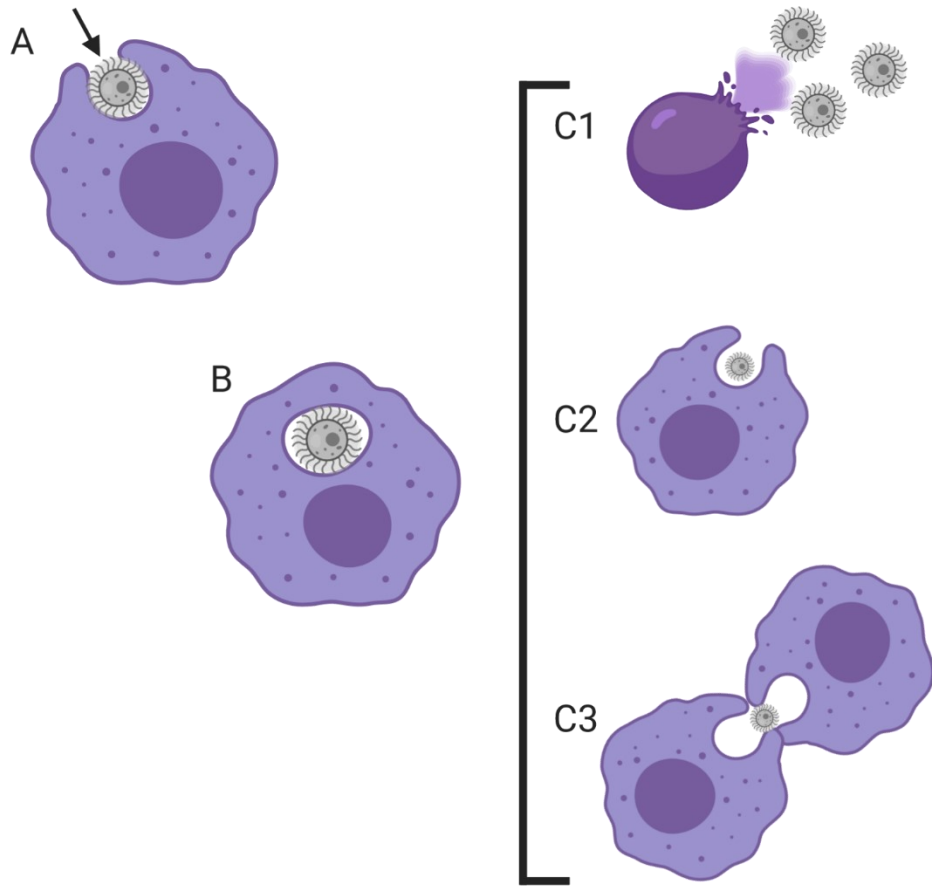


Figure 2

C. neoformans life cycle in macrophages. **A.** *C. neoformans* yeast is phagocytosed by the macrophage, via FcR or CR. **B.** Due to several survival strategies *C. neoformans* persists within the phagolysosome and can even replicate. **C.** *C. neoformans* exit their host macrophage via several strategies **1.** Lysis of the host cell **2.** Non-lytic exocytosis (Vomocytosis) **3.** Macrophage-to-macrophage transfer (Dragocytosis).

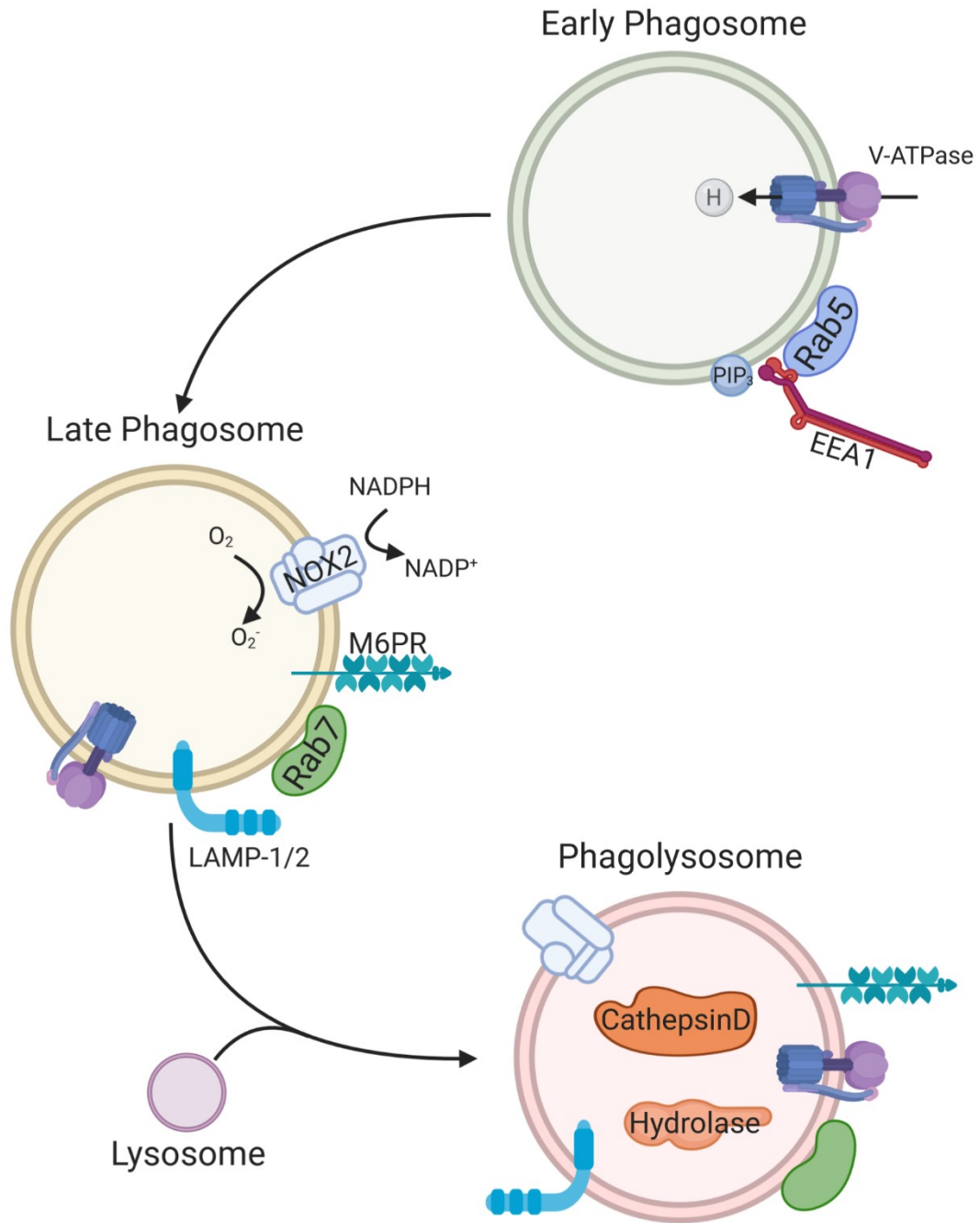


Figure 3

Maturation from early *C. neoformans* containing phagosome to autophagolysosome. Exchange and acquisition of various phagolysosomal membrane proteins allows us to select for or analyze phagosomes at different stages of maturation.

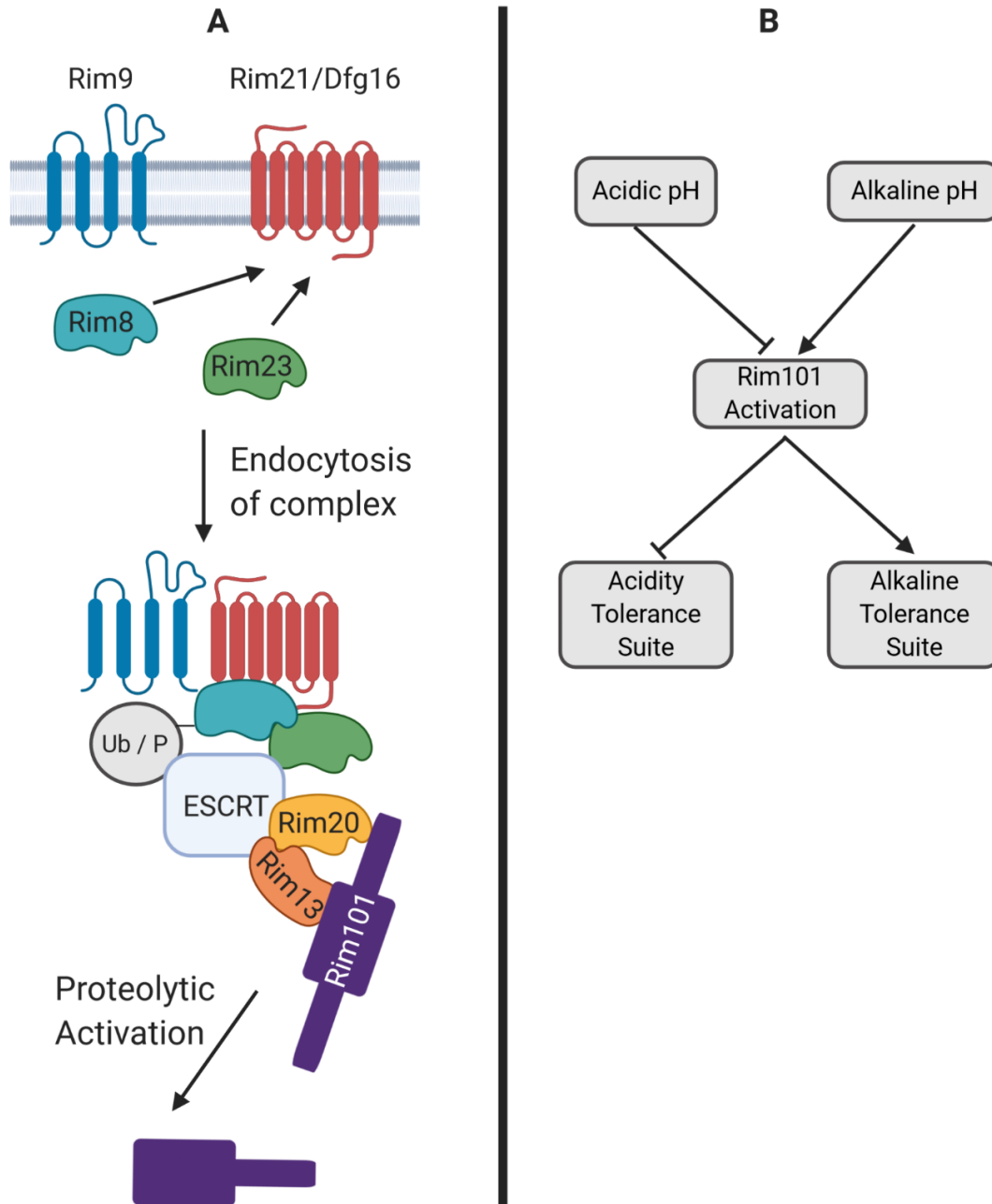


Figure 4

The Rim pathway is the most well-known and thoroughly studied fungal pH sensing pathway. Specifically, Rim is activated by alkaline environments, but inhibition of the Rim components can be just as much of a signal as activation. **A.** A general schema of the Rim pathway in fungi, depending on the species several proteins may be different, ubiquitination replaced by phosphorylation, but overall the pathway is conserved. **B.** A visualization of Rim inhibition as a cellular signal.

Protein	Early Phagosome	Late Phagosome	Autophagolysosome
Rab5	X		
EEA1	X		
V-ATPase	X	X	X
M6PR		X	
ESCRT		X	
Rab7		X	X
LAMP1/2		X	X
NOX2		X	X
Cathepsin D			X
Hydrolases			X
LC3			X

Table 1

Notable protein players in receptor-mediated phagocytosis of *C. neoformans*, from early phagosome to phagolysosome.

Part I: Acidification Dynamics of the Macrophage Phagolysosome

This chapter is published in the Journal of Clinical Investigations as “Macrophages utilize a bet-hedging strategy for antimicrobial activity in phagolysosomal acidification”

doi:10.1172/JCI133938

Abstract

Microbial ingestion by a macrophage results in the formation of an acidic phagolysosome but the host cell has no information on the pH susceptibility of the ingested organism. This poses a problem for the macrophage and raises the fundamental question of how the phagocytic cell optimizes the acidification process to prevail. We analyzed the dynamical distribution of phagolysosomal pH in murine and human macrophages that had ingested live or dead *Cryptococcus neoformans* cells, or inert beads. Phagolysosomal acidification produced a range of pH values that approximated normal distributions, but these differed from normality depending on ingested particle type. Analysis of the increments of pH reduction revealed no forbidden ordinal patterns, implying that the phagosomal acidification process was a stochastic dynamical system. Using simulation modeling, we determined that by stochastically acidifying a phagolysosome to a pH within the observed distribution, macrophages sacrificed a small amount of overall fitness to gain the benefit of reduced variation in fitness. Hence, chance in the final phagosomal pH introduces unpredictability to the outcome of the macrophage-microbe, which implies a bet-hedging strategy that benefits the macrophage. While bet hedging is common in biological systems at the organism level, our results show its use at the organelle and cellular level.

Introduction

***Audaces fortuna iuvat* (Fortune favors the bold) - Virgil**

Phagocytosis is a fundamental cellular process used by unicellular organisms for nutrient acquisition as well as by host immune cells for microbial defense. The parallels between food acquisition and immunity have led to the suggestion that these two processes had a common evolutionary origin⁹⁵. The process of phagocytosis results in the formation of a phagolysosome, a dynamic membrane bounded organelle, which represents a critical arena in the struggle between the host and ingested microbial cells⁹⁶. Microbial ingestion into phagosomes results in exposure to host cell microbicidal mechanisms, which leads to death for some microbes while others survive by subverting critical aspects of phagosome maturation and by damaging phagolysosome structural integrity.

The process of phagosomal maturation, encompassed by the fusion of the phagosome with lysosomes and lumen acidification, is a complex choreography that includes the recruitment of V-ATPase from lysosomes to the phagolysosome^{56,96} and many other protein components⁹⁷. Proton pumping into the phagolysosomal lumen results in acidification that inhibits microbes and activates antimicrobial processes. Consequently, some types of microbes, such as *Mycobacterium tuberculosis* and *Histoplasma capsulatum*, interfere with phagosomal maturation and acidification to promote their intracellular survival. The extent of phagosomal acidification is determined by numerous mechanisms that include proton flux through the pump, proton consumption in the phagosomal lumen, and backflow into the cytoplasm⁹⁸. Phagosome

acidification in macrophages is rapid with a pH of 6 being reached within 10 min after ingestion⁹⁹ and 5.4 by 15-20 min¹⁰⁰.

Cryptococcus neoformans is a facultative intracellular pathogen¹⁰¹. Upon ingestion by macrophages, *C. neoformans* resides in a mature acidic phagolysosome¹. The outcome of macrophage-*C. neoformans* interaction is highly variable depending on whether the fungal cell is killed, inhibited, or unaltered. If not killed, *C. neoformans* can replicate intracellularly, resulting in death and lysis of the host cell, non-lytic exocytosis^{102,103}, transfer to another macrophage^{20,104}, or phagosomal persistence. Maintenance of phagolysosomal membrane integrity is a critical variable in determining the outcome of the *C. neoformans*-macrophage interaction, with loss of integrity leading to host cell death¹⁸.

Prior studies of *C. neoformans* phagosomal acidification measured great variation in the pH of individual phagolysosomes^{13,18,105}. The pH of cryptococcal phagolysosomes is affected by several microbial factors including urease expression¹³, phagosomal membrane integrity¹⁸, and the presence of the cryptococcal capsule with glucuronic acid residues⁸. In addition, the capsule of *C. neoformans* increases in diameter as part of a stress response which can potentially affect the phagolysosomal pH through increasing the phagolysosome volume, thus diluting its contents and promoting membrane damage through physical stress¹⁸.

In this study, we analyzed the time dependence of the phagolysosomal pH distribution in murine and human macrophages and conclude that acidification is a stochastic process in which macrophages default to a range of pHs with random variation. We demonstrate that, in doing so, macrophages employ a *bet-hedging* strategy by sacrificing a small amount of overall fitness to ensure broad survivability. Thus, we suggest that chance, in the form of stochastic dynamics, could be an important strategy which benefits the macrophage by bet hedging against a range of pathogens, and could echo through the immune process to introduce a fundamental uncertainty in the outcome of microbe-macrophage interactions.

Materials and Methods

Cell Strains and Culture Conditions

Cryptococcus gattii species complex strains R265, WM179, and WM161 were obtained from ATCC (Manassas, VA), and *Cryptococcus neoformans* species complex serotype A strain H99 as well as *ure1Δ* (lacking urease, derived from H99) were originally obtained from John Perfect (Durham, NC). The strains were stored at 80°C. Frozen stocks were streaked onto Sabouraud dextrose agar (SAB) and incubated at 30°C. Liquid suspensions of cryptococcal cultures were grown in SAB overnight at 30°C. Cryptococcal cultures were heat killed by incubating at 65 °C for 1 h.

Macrophage cells were either mouse bone marrow-derived macrophages (BMDM) obtained from 6 week old C57BL/6 female mice from The Jackson Laboratory (Bar Harbor, ME), J774.16 macrophage-like cells, or human monocytes isolated from PMBCs. BMDMs were isolated from hind leg bones and for differentiation were seeded in 10 cm tissue culture treated dishes (Corning,

NY) in Dulbecco's Modified Eagle Medium (DMEM, Corning) with 10% FBS (Atlanta Biologicals, Flowery Branch, GA), 1% nonessential amino acids (Cellgro, Manassas, VA), 1% penicillin-streptomycin (Corning), 2 mM Glutamax (Gibco, Gaithersburg, MD), 1% HEPES buffer (Corning), 20% L-929 cell conditioned supernatant, 0.1% beta-mercaptoethanol (Gibco) for 6 days at 37 °C and 9.5% CO₂. BMDMs were used for experiments within 5 days after differentiation. J774.16 cells were cultured in DMEM with 10% FBS, 1% nonessential amino acids, 10% NCTC109 (Gibco), and 1% penicillin-streptomycin at 37 °C with 9.5% CO₂. For human peripheral blood mononuclear cells (hPBMCs), CD14⁺ monocytes were isolated using Dynabeads Untouched Human Monocytes Kit (Thermo Fisher Scientific) according to the manufacturer protocol. The isolated cells were differentiated in RPMI-1640 medium (RPMI) with 10% FBS (Atlanta Biologicals, Flowery Branch, GA), 1% penicillin-streptomycin (Corning), and 25 ng/mL of human granulocyte-macrophage colony-stimulating factor (GM-CSF, Sigma-Aldrich) for five days. Human cells were further cultured in RPMI (RPMI) with 10% FBS (Atlanta Biologicals, Flowery Branch, GA), 1% penicillin-streptomycin (Corning), and activated with 0.5 ug/mL lipopolysaccharide (LPS; Sigma-Aldrich) and 10 ng/mL interferon gamma (IFN- γ ; Roche) for M1 polarization or 20 ng/mL IL-4 for M2 polarization.

Phagolysosomal pH measurement

Phagolysosomal pH was measured using ratiometric fluorescence imaging involving the use of pH-sensitive probe Oregon green 488 as described in prior studies¹³. The pH values analyzed here were collected in part during prior studies of *C. neoformans*-macrophage interactions^{13,18,105}. Briefly, Oregon green 488 was first conjugated to monoclonal antibody (mAb) 18B7, which binds

C. neoformans capsular polysaccharide, using Oregon Green 488 Protein Labeling Kit (Molecular Probes, Eugene, OR). The labeling procedure was done by following the manufacture's instruction. BMDMs were plated at a density of 1.25×10^5 cells/well or differentiated human macrophages were plated at a density of 2.5×10^5 cells/well on 24-well plate with 12 mm circular coverslip. Cells were activated with 0.5 $\mu\text{g/ml}$ LPS and 100 U/ml IFN- γ or 20 ng/mL IL-4 as previously described at 37 °C in a 9.5% CO₂ (BMDM) or 5% CO₂ (Human macrophage) atmosphere overnight. Prior to infection, 2 d old live, heat killed H99, R265, WM179, ure1, cap59, or anti-mouse IgG coated polystyrene bead (3.75×10^6 cells or beads/ml) were incubated with 10 $\mu\text{g/ml}$ Oregon green conjugated mAb 18B7 for 15 min. Macrophages were then incubated with Oregon green conjugated mAb 18B7-opsionized particles in 3.75×10^5 cryptococcal cells or beads per well (BMDM) or 2.5×10^5 cell/well (Human macrophage). For drug treatment experiments the macrophage cell media was supplemented with 3 μM chloroquine. Cells were either centrifuged immediately at 350 x g for 1 min or incubated at 4 °C for 30 min to synchronize ingestion and cultures were incubated at 37 °C for 10 min to allow phagocytosis. Extracellular cryptococcal cells or beads were removed by washing three times with fresh medium, a step that prevents the occurrence of new phagocytic events. As an additional safeguard against new phagocytic events fresh media was supplemented with AlexaFluor 568 conjugated mAb 18B7 for 1 h to label extracellular particles. Samples on coverslip were collected at their respective time points after phagocytosis by washing twice with pre-warmed HBSS and placing upside down on MatTek petri dish (MatTek, Ashland, MA) with HBSS in the microwell. Images were taken by using Olympus AX70 microscopy (Olympus, Center Valley, PA) with objective 40x at dual excitation 440 nm and 488 nm, and emission 520 nm. Images were analyzed using MetaFluor Fluorescence Ratio Imaging Software (Molecular Devices, Downingtown, PA). Fluorescence intensities were used to

determine the ratios of Ex488 nm/Ex440 nm that were converted to absolute pH values using a standard curve where the images are taken as above but intracellular pH of macrophages was equilibrated by adding 10 μ M nigericin in pH buffer (140 mM KCl, 1 mM MgCl₂, 1 mM CaCl₂, 5 mM glucose, and appropriate buffer \leq pH 5.0: acetate-acetic acid; pH 5.5-6.5: MES; \geq pH 7.0: HEPES. Desired pH values were adjusted using either 1 M KOH or 1 M HCl). The pH of buffers was adjusted at 3-7 using 0.5-pH unit increments.

Immunofluorescence Microscopy

BMDMs were seeded on 12 mm circular coverslips in 24 well tissue culture plates at 2.5×10^5 cells per well. Cells were activated with 0.5 μ g/ml lipopolysaccharide and 100 U/ml interferon gamma at 37 °C in a 9.5% CO₂ atmosphere overnight. Anti-mouse IgG coated beads were opsonized with 10 μ g/mL and added to cells at MOI 1. Phagocytosis was synchronized by centrifuging the plate at 350 x g for 1 min before being incubated at 37 °C. At each timepoint media was replaced with 4% paraformaldehyde (PFA) and incubated for 10 min at room temperature to fix cells. PFA was removed and cells were washed three times with 1 mL PBS (1X). Coverslips were blocked for 1 h at room temperature with 2% BSA in PBS. Primary incubation was performed with Rb α EEA1 (ThermoFisher Scientific MA5-14794) at 1:100 dilution or Rb α V-ATPase (ThermoFisher Scientific PA5-29899) at 1:100 dilution in blocking buffer for 1 h at room temperature. Coverslips were washed with blocking buffer before secondary incubation with Goat α Rb AlexaFluor 488 (1:100) in blocking buffer for 1 h at room temperature. Coverslips were washed once more with dH₂O and mounted on glass slides using Prolong Gold mounting agent. Slides were imaged via Zeiss Axiovert 200M microscope and intensity was analyzed using Zeiss Lite Blue Version. A region of interest

was generated by outlining the ingested bead via phase contrast channel then measuring mean fluorescence intensity of the secondary antibody.

Trained macrophage experiments

BMDMs were plated at a density of 2×10^5 cells/well on 24-well plate with 12 mm circular coverslip. Cells were activated with 0.5 $\mu\text{g/ml}$ LPS and 100 U/ml IFN- γ ; Roche and incubated at 37 °C in a 9.5% CO₂ atmosphere overnight. Prior to the infection, H99 were stained with 0.01% Uvitex 2B for 10 min. BMDMs were then infected with H99 (2×10^5 cells/well) in the presence of 10 $\mu\text{g/ml}$ 18B7. After 1 h of infection, 5 $\mu\text{g/ml}$ of amphotericin B were added to each well and the culture were incubated for overnight. On the following day, the cultures were washed three times with PBS, and incubated in PBS for 2 h. After the incubation, the cultures were further washed three times with PBS. A fresh overnight culture of H99 were incubated with 10 $\mu\text{g/ml}$ Oregon green conjugated mAb 18B7 for 15 min. Macrophages were then incubated with Oregon green conjugated mAb 18B7-opsonized H99 in 2×10^5 cells per well. Cells were centrifuged immediately at 350 x g for 1 min to synchronize ingestion. Phagolysosomal pH were then measured using Olympus AX70 microscopy.

Time-lapse imaging and intracellular replication

The time of intracellular replication here were collected in time-lapse imaging during prior studies of *C. neoformans*-macrophage interactions¹³. For imaging BMDM (5×10^4 cells/well) were plated on poly-D-lysine coated coverslip bottom MatTek petri dishes with 14mm microwell (MatTek).

Cells were cultured in completed DMEM medium and stimulated with 0.5 µg/ml LPS and 100 U/ml IFN-γ overnight at 37 °C with 9.5 % CO₂. On the following day, macrophages were infected with cryptococcal cells (H99 or ure1; 1.5 × 10⁵ cells/well) opsonized with 18B7 (10 µg/ml). After 2 h incubation to allow phagocytosis, extracellular cryptococcal cells were removed by washing the culture five times with fresh medium. Images were taken every 4 min for 24 h using a Zeiss Axiovert 200M inverted microscope with a 10x phase objective in an enclosed chamber at 9.5 % CO₂ and 37 °C. The time intervals to initial replication of individual cryptococcal cells inside macrophage were measured in time-lapse imaging.

Data Processing

Phagolysosome pH intervals were calculated by subtracting measured pH levels of phagolysosomes from a starting pH of 7.2, the pH of the surrounding media, and individual interval measurements were concatenated into a single dataset for each time point examined.

Data analysis

Discrimination of deterministic vs. stochastic dynamics was achieved using the previously characterized permutation spectrum test¹⁰⁶. In this method, the processed datasets were segmented into overlapping subsets of 4 data points using a sliding window approach, as detailed in figure 4, and assigned 1 of 24 (4!) possible ordinal patterns based on the ordering of the 4 terms in the subset. The frequencies with which each unique ordinal pattern occurred in the dataset were then calculated and plotted. Deterministic dynamics were characterized by the occurrence

of “forbidden ordinals”, equal to ordinal patterns that doesn’t occur in the dataset whereas stochastic dynamics were characterized by the presence of all ordinals. Measured phagolysosomal pHs were subtracted from an initial pH value (7.2) based on cell media pH and placed in a vector. Subsets of 4 data points were generated using a sliding window approach in which the first four values were grouped, the window shifted by one, and the subsequent set of 4 values grouped. Each subset was prescribed an “ordinal pattern” based on the relative values of the data points in the subset to each other with, for instance, the lowest value assigned a “0” in the ordinal pattern and the highest a “3”. Further characterization of deterministic dynamics was achieved using the previously characterized point count plot¹⁰⁷, in which periodic vs. chaotic dynamics were differentiated based on the distribution of “peaks” in the calculated power spectrum of each dataset. Power spectrums were estimated with Matlab’s Lomb-Scargle power spectral density (PSD) estimate function and subsequently normalized. From the normalized power spectrum, “point count plots” were generated by counting the number of peaks above a set threshold—the point threshold—with values of the point threshold ranging from 0 to 1. Periodic dynamics were characterized by “staircase” point count plots whereas chaotic dynamics were characterized by point count plots with a decreasing exponential shape.

Distribution and normality analysis

Each set of sample data was fit to a series of distributions using the R package “fitdistrplus” with default parameters for each distribution type, generating the histograms and Quantile-Quantile (Q-Q) plots. Normality and significance were calculated via the base R Shapiro-Wilk test.

Generating and Analyzing Simulations

Let $f(x)$ be the probability distribution of the host's pH. For simplicity, we assume that f is $\text{Normal}(\mu, \sigma)$. Let $F(x)$ be the corresponding cdf. At every time-point, we randomly sample a pathogen i from a set of pathogens. The pathogen has a range (a_i, b_i) of viable pH, which differs among pathogens. Minimum tolerable pH values were obtained from the literature as described, while a constant value of 8 was used for maximum since most pathogens were inhibited as high pH as well as phagolysosomes being unlikely to alkalize. The host, in turn, randomly chooses a pH by sampling from the distribution $f(x)$. If the host's pH x falls in the interval (a_i, b_i) , then there is a probability p of the host dying. We can think of the host's survival rate p as its fitness, which is a random variable that depends on the randomness in pathogens. As a function of i , we have $p(i) = p * (F(b_i) - F(a_i))$; the random variable p assumes the values $p(i)$ with equal probability. Additionally, since biologically relevant phagolysosome pH values will only fall within a certain range, we decided to limit the possible pH values between 2 and 7.2 (pH of associated cell media). Any values generated outside those limits were instead recorded as their respective limit. Thus, distributions become less normally distributed at the extremes, sacrificing normality for biological practicality, as real phagolysosomes would not alkalize or be likely to acidify below 2. In these situations, we calculated outputs based on 1,000 replicates of 10,000 simulated phagolysosomes each.

Statistics

A variety of tests were used throughout this manuscript. All tests used an a priori P cutoff of 0.05 to determine significance. Comparing multiple phagolysosomes within a single cell used a two-

tailed student's t-test to determine differences between the initial populations. To test the normality of distributions, we used the Shapiro-Wilk normality test. To determine linear correlation between fluorescence intensity and hours post infection, we employed a linear regression according to the model Intensity \sim Hours Post Infection. To investigate the differences in pH between trained and untrained macrophages we used the two-tailed student's t-test.

Study Approval

The present studies in animal and/or human cell lines were reviewed and approved by an appropriate institutional review board. Murine macrophages were harvested from mice under protocols approved by the Animal Care and Use Committee for Johns Hopkins University (1620 McElderry Street, Baltimore, MD). Human peripheral blood monocytes were a generous gift from the Laboratory of Dr. Andrea Cox from de-identified human leuko packs obtained from the Anne Arundel Medical Blood Center (Anne Arundel, Maryland) in protocols approved by the Johns Hopkins IRB (1620 McElderry Street, Baltimore, MD).

Results

We previously reported a wide distribution of phagolysosomal pH after the ingestion of *C. neoformans* by murine bone marrow derived macrophages (BMDMs)^{13,18}. Given that the growth rate of *C. neoformans* is highly affected by pH^{10,13} and that the outcome of the *C. neoformans*-macrophage interaction is determined in the phagolysosome^{18,108,109}, we decided to analyze the distribution of phagolysosomal pH mathematically to gain insight into the dynamics of the

acidification process. Understanding the fundamental process of phagolysosomal acidification, and if there are overarching rules or determinism involved, could provide key insights to disease pathology of any pathogen, which would interact with the phagolysosome. A scheme of the method used to determine phagosomal acidification with representative data from polystyrene bead phagocytosis experiments are shown in Figure 5. To determine the pH of a phagolysosome, particles are opsonized with an Oregon Green conjugated Ab. Oregon Green is pH insensitive at Ex440/Em520 and pH sensitive at Ex488/Em520, allowing pH to be measured by quantifying the ratio of fluorescent intensity between each wavelength. We were able to establish robust standard curves from known pH controls and calculate unknown phagolysosome measurements (Figure 5B).

Murine macrophage phagolysosomes acidify stochastically

To determine whether phagolysosomal acidification is a deterministic or stochastic dynamical process, we employed a permutation spectrum test¹⁰⁶ in which the distribution of ordinal patterns occurring in subsets of our full dataset was analyzed (Figure 5C). Ordinal patterns simply refer to the order of each measurement in terms of value, in our case the phagolysosomal pH, within a scanning window, which parses all measurements within each condition, exemplified in Figure 5¹¹⁰⁻¹¹³. Here we found a 4-unit window size to be the most appropriate. We found no forbidden patterns at any time evaluated for any of the pH distributions resulting from the synchronized ingestion of beads, alive *C. neoformans*, or heat-killed *C. neoformans*, which implies that the acidification is a stochastic process (Figure 6). A forbidden ordinal is an ordinal pattern that does not appear during the time frame of our experiment. Despite the overall population of

macrophages showing chaotic dynamics, we considered whether the Chaotic signatures occurred at the individual cellular level. That is, whether slight differences at the initiation of phagocytosis propagated through maturation and acidification resulting in two phagolysosomes within the same cell with different acidifications. To determine if this was the case, we analyzed the phagosomal pH in pairs of bead containing phagolysosomes for which each pair was within a single macrophage. We chose macrophages in which the ingested beads were visibly separated. We found that the differences between phagolysosomal pH measurements of this cohort of phagolysosomes yields a normal distribution centered at 0 with non-zero values, suggesting each individual phagosome has an independent target phagolysosomal pH (Figure 7). The ordinal pattern analysis was repeated on several other strains and conditions throughout the project and at no point did we observe forbidden ordinal patterns (Figure 8A), again suggesting the process exhibits no signature of deterministic chaos¹¹³⁻¹¹⁶. Given that beads are inert and cannot modify pH, we reasoned that their corresponding phagolysosomes would be the closest approximation of a default acidification state and would therefore represent a “baseline” to which we could compare phagolysosome acidification dynamics in other conditions.

Bead ingested murine macrophage phagolysosomes stabilize to a normally distributed pH

To probe the dynamics of the phagolysosomal acidification system at this baseline, we analyzed several hundred individual phagolysosomal pH measurements at various time intervals after BMDMs had ingested inert beads (Figure 9A). To determine whether phagolysosome pH measurements followed a normal distribution, the measured relative pH values were fit to a predicted normal distribution using the “fitdistrplus” R statistical package then analyzed via Q-Q

plots and the Shapiro-Wilk normality test. We found that phagolysosome pH value distributions did not approximate normality at early times (15 and 30 min), but mostly did at intervals of and past 1 h post infection. We were able to reject the Shapiro-Wilk null hypothesis only at 15 min, 30 min, and 3 h (Figure 9B). We hypothesized that not all phagolysosomes were fully mature before 1 h and reasoned that the bimodal appearance of pH at early time intervals is likely due to the population of phagosomes being at different stages of maturity. Interestingly, the pH distribution for the phagolysosomes containing live or dead *C. neoformans* did not approximate normality even at later times, nor did other live yeast containing phagolysosomes (Figure 10). We rejected Shapiro-Wilk normality for each of these samples except for dead *C. neoformans* at 3 h. Q-Q plots supported the notion that each sample skews further from normality compared to bead ingested macrophage phagolysosome pH distributions (Figure 11). Considering that macrophages default to a random pH from a particular normal distribution and that *C. neoformans* invest in disrupting this process, we hypothesized that this system must confer some host benefit. Thus, we decided to compare the pH distribution of mature bead ingested phagolysosomes to a range of pHs tolerated by relevant potential pathogens.

Acidification Dynamics are Closely Related to Maturation

To probe whether the observed normality and stochasticity is a result of dynamics in acidification or in the maturation process, we analyzed the intensity of two phagolysosomal maturation markers, EEA1 and V-ATPase, over the same time course. Using relative intensity of each immunofluorescent staining as a surrogate measurement of maturation, we found that, again, no samples had forbidden ordinal patterns, suggesting phagolysosomal maturation, when measured

by the accumulation of these markers, is also stochastic in nature (Figure 12). However, neither of the fluorescence intensity measurements from these markers approximated normality at any time, with sufficient skewing to reject the Shapiro Wilk null hypothesis (Figure 13). Skewing of these measurements away from normality could reflect cytoplasmic speckling, limitations of fluorescent microscopy resolution, non-linearity of fluorescence signals and the inherent complexity of such a system, such that we are not confident to reject the notion that these processes indeed demonstrate a normal distribution. We hypothesized that macrophages may experience limited resources in terms of the number of available V-ATPase pumps at any given time and that we might see a correlation between intensity of V-ATP staining around individual phagosomes in cells that had ingested one versus multiple beads. We found no evidence of a correlation between V-ATPase staining, or EEA1 for that matter, and total number of ingested particles (Figure 14).

BMDM phagolysosomes acidify to a pH range suboptimal for growth of soil and pathogenic microbes

The pH of soils varies greatly from acidic to alkaline based on a variety of conditions that, in turn, determine the associated microbiome¹¹⁷. Soils contain many pathogenic microbes including *C. neoformans*. Since the phagolysosome is an acidic environment, we reasoned that microbes that thrive in acidic soils could proxy for the types of microbes that hosts, and thus macrophages, could encounter, and pose a threat to the cell/host due to their acidophilic nature (ex. *Cryptococcus neoformans*). Hence, we compared^{118,119} the distribution of pH values from mature phagolysosomes (HPI ≥ 1 h) which had ingested latex beads, as a measure of the range of acidities

generated in the absence of microbial modulation, relative to published soil microbe growth data as a function of pH (Figure 15). The latex bead pH distribution is narrow and centered at a pH of about 4.5, which corresponds to a pH that significantly reduces the optimal growth even for microbes in acidic soils. To generate a more relevant comparison to human disease models, we also searched out the pH tolerance of 27 significant human pathogens which macrophages are likely to encounter during human infectious diseases (Supplemental Table I). We then compared these distributions to the pH distribution in bead ingested macrophage phagolysosomes (Figure 15). The distribution of this default macrophage pH heavily overlaps with the more inhibitory pH regions when compared to both soil and known pathogen pH tolerances. Taken together these data suggest that the low phagosomal pH is itself a defense mechanism, with a distribution that manifests bet hedging by defaulting to a range, rather than single value, inhibitory to most of the spectrum of pathogens the macrophage is likely to encounter.

Simulations of macrophage populations show stochastic pH as a bet-hedging strategy

Bet hedging is generally understood as a strategy whereby an organism decreases variation in fitness at the expense of a small decrease in mean fitness. To test whether variation in macrophage phagolysosome pH constitutes a diversified bet-hedging strategy, we first modeled host survival rate as a function of final phagolysosomal pH in the context of a pathogen randomly selected from Table 2. This analysis modeled phagolysosomal pH as a normal distribution with mean μ and standard deviation σ varied over a range of possible values in order to test how bet hedging depends on these parameters. To each phagolysosomal pH, we associated a fitness value which models survival likelihood against pathogens, using the list of pathogens (Table 2), with

their viable pH ranges collected from the literature, and we computed the distribution of fitness (ρ) as phagolysosomal pH varies (Figure 16A,B). As expected in bet hedging, we observed decreases in standard deviation of fitness with increasing σ of phagolysosomal pH (Figure 16C). Mean fitness was mostly unchanged with changing standard deviation, such that even in the most extremes deviations in phagolysosomal pH there were only slight changes in fitness in either direction.

Another way to formalize the emergence of bet hedging as an evolutionary strategy is by considering the average long-term rate of growth. Thus, we considered a multiplicative model, in which the growth rate (r_T) over a span of time (T) is defined as the geometric mean of ρ_1, \dots, ρ_T , where for each t ranging from 1 to T , ρ_t is the fitness at time t . Taking logs, $\log(r_T)$ is the average of $\log(\rho_1), \dots, \log(\rho_T)$. By the law of large numbers, if we assume each ρ_t is independent and identically distributed, this average will approach $E(\log(\rho))$. Thus $E(\log(\rho))$ is the operative quantity to be maximized, rather than $E(\rho)$. Note that applying the log transformation has the effect of placing heavier penalties on fitness values that are close to 0, so that maximizing mean log fitness will tend to encourage lower standard deviation in fitness¹²⁰. Thus, increased mean log fitness is another indication of bet-hedging which directly relates to long-term growth. We indeed observe increased mean log fitness with increasing σ of phagolysosomal pH (Figure 16D).

To probe whether our simulations would reflect biological responses, we analyzed macrophage phagolysosomal pH in which cells treated with Chloroquine, a weak base that localizes to the phagolysosome. According to our model the increased shift in mean pH from chloroquine would result in a lower overall mean log fitness as a result of shifting the mean pH closer to 6, a more tolerable region for most of the candidate pathogens. Thus, we compared previously reported

data¹ of *C. neoformans* containing phagolysosomes treated with chloroquine to our data from the respective time interval and found that chloroquine treatment results in a drastically reduced overall mean log fitness (-5.323) compared to the mean log fitness of our non-chloroquine treated data of the respective condition (-2.486).

Time intervals from ingestion of C. neoformans to initial budding are stochastic

C. neoformans replication rate is highly dependent on pH¹³. Consequently, we hypothesized that if phagolysosomal acidification followed stochastic dynamics, this would be reflected on the time interval from ingestion to initial replication. Analysis of time intervals to initial fungal cell budding events revealed stochastic dynamics with no evidence of forbidden ordinal patterns (Figure 8B). Similar results were observed for initial budding of wild type and urease negative strains of *C. neoformans*, which reside in phagolysosomes that differ in final pH as a result of ammonia generation from urea hydrolysis. Acidification intervals for both strains were stochastic, despite the fact that phagolysosomes of urease deficient strains are approximately 0.5 pH units lower than those of wild type strains¹³.

Trained murine macrophages have inverse acidification dynamics

Trained immunity has recently been shown to influence repeated infection in monocyte populations not exposed to the adaptive immune system¹²¹. To determine whether initial exposure to a pathogen has an effect in the dynamics of this system we exposed BMDMs to *C. neoformans*, resolved the infection with antifungals, and measured phagolysosome acidification

dynamics upon reinfection. We found that pH distribution of phagolysosomes from macrophages previously trained as described also exhibited stochastic behavior (Figure 17A), veering away from a normal distribution of pH (Figure 17B, Figure 18). However, trained BMDMs on average exhibited a significantly lower initial pH, which became significantly higher compared to untrained BMDMs over time (Figure 17C). Fully understanding this system will require significant further study outside the scope of this manuscript. In this regard we note that amphotericin B is a powerful activator of macrophages¹²² and that *C. neoformans* residence inside macrophages is associated with host cell damage^{123,124}. Hence, the effects we observe could be the aggregate of several influences in the system. Nevertheless, there is a clear suggestion of a historical effect on which pH distribution a macrophage will employ. This may also suggest an adaptive component to the macrophage bet-hedging strategy.

Differently polarized macrophages acidify stochastically but not using this bet hedging system

To probe whether M0 and M2 polarized macrophages acidify with the same dynamics of M1 macrophages, we repeated these experiments with macrophages that were either not stimulated, or stimulated with IL-4 to skew towards M2. First, we found that regardless of the polarization skew all macrophages acidified stochastically (Figure 19A). Second, we found that the phagolysosomal pH distributions differed overall with M2 macrophages having the highest mean pH, followed by M0 and then followed by M1 skewed (Figure 19B). Most striking was the observation that M0 and M2 skewed macrophages did not manifest a normally distributed pH range as observed with M1 skewed macrophages. Instead, M0 macrophages consistently yield a bimodal distribution even after 1 h. The M2 macrophages phagosomal pH distribution started

with a heavy tail of higher pH and eventually stabilize to a bimodal distribution. These data suggest that while the macrophages have the same underlying acidification dynamics, they do not share the betting strategy of M1 skewed macrophages. Thus, we estimated each population of macrophages likelihood to survive when faced with the same list of human pathogens modeled after bimodal distributions estimated from the observed data (Figure 20). After comparing these simulations, we found that M1 macrophages by far have the highest mean log fitness, followed by M0, followed by M2 (Figure 19C). Our model shows M1 macrophages as resistant to these infectious agents with M2 permissive.

Human monocytes acidify stochastically and approximate normality

To determine how closely the murine system resembled human acidification dynamics, we isolated macrophages from human peripheral blood monocytes and repeated these experiments with beads and live *C. neoformans*. We found that acidification intervals in human cells were also stochastic in nature (Figure 21A). Additionally, human cells that ingested inert beads were normally distributed at the 15 min and 1 h time intervals. Even though the times skewed away from normality, the skew was not as severe as that observed in yeast containing phagolysosomes (Figure 8B). We hypothesize that some of this skewing could result from different dynamics due to the different background inherent to human donors, which differ from the mouse system in which cells are isolated from genetically identical individuals (Figure 22). Furthermore, within the context of our simulation, if we model the phagolysosome pH values of a population of human macrophages as a normal distribution with mean and standard deviation determined from pH

values observed across all time points (5.08 and 1.08, respectively), the resulting mean log fitness is high with dramatically reduced deviation in fitness (Figure 16).

Pathogens skew phagolysosome acidification towards conditions less favorable to the macrophage

Cryptococcal cells buffer the phagolysosome pH toward 5.5, a value optimal for yeast growth¹⁸. We therefore hypothesized that *C. neoformans* could use this buffering capability to disrupt the host acidification strategy. We found that phagolysosomes containing live *C. neoformans* and live *C. gattii* acidified to distributions of pH less normally distributed and more permissive to general fungal replication by increasing the average observed phagolysosomal pH.

To probe host fitness with regard to *C. neoformans* specifically, we modified our model by declaring the inhibitory pH as ≤ 4 , which inhibits *C. neoformans* replication¹²⁵, and calculated the likelihood of each population of macrophages to achieve an inhibitory pH, assuming phagolysosome pHs were normally distributed around the observed mean and standard deviation. Here we analyzed the combined data for all time intervals, reasoning that in actual infection interactions between *C. neoformans* and host macrophages early phagosomes would be important as well, rather than focusing only on mature phagolysosomes.

We estimated the proportions of inhibitory phagolysosomes and found that bead-containing phagolysosomes were more likely to acidify to ≤ 4 , followed by heat-killed and $\Delta ure1$ *C. neoformans*, followed by live *C. neoformans*, with capsule deficient *Cap59* being particularly likely, and trained macrophages or *C. gattii* containing phagolysosomes being particularly unlikely to

achieve inhibitory pH (Figure 23A). Our actual data was not normally distributed with non-bead samples though, as *C. neoformans* actively modulates phagolysosomal pH. The starkest difference we observed is that, in reality, killed and live *C. neoformans* phagolysosomes had the same proportion of inhibitory phagolysosomes, suggesting the capsule has a more significant effect on pH modulation than we initially expected. This finding is corroborated by the high proportion of inhibitory phagolysosomes in *Cap59* containing phagolysosomes, a strain incapable of modulating pH since it has no capsule (Fig 9C). Additionally, the expected and observed increased likelihood of bead containing phagolysosomes to inhibit *C. neoformans* replication compared to live *C. neoformans* phagolysosomes was consistent between murine and human cells (Figure 23B,D).

To probe whether this phenomenon was applicable to pathogens other than *C. neoformans*, we repeated this analysis with published phagolysosomal pH data from *Mycobacterium avium*¹²⁶. We found that like *C. neoformans*, live *M. avium* bacteria modified their resident phagolysosomal pH to be more favorable toward them. In contrast, the estimated mean log fitness for the host macrophage population increased when they ingested killed mycobacteria, which are unable to modulate pH (Figure 24).

Discussion

The complexity and sequential nature of the phagolysosomal maturation process combined with the potential for variability at each of the maturation steps, and the noisy nature of the signaling networks that regulate this process, have led to the proposal that each phagolysosome is a unique and individual unit¹²⁷. In fact, the action of kinesin and dynein motors that move phagosomes along microtubules exhibits stochastic behavior, adding an additional source of randomness to

the process¹²⁸. Hence, even when the ingested particle is a latex bead taken through one specific type of phagocytic receptor there is considerable heterogeneity in phagolysosome composition, even within a single cell¹²⁷. Since the phagolysosome is a killing machine used to control ingested microbes, this heterogeneity implies there will be differences in the microbicidal efficacy of individual phagolysosomes. This variability raises fundamental questions about the nature of the dynamical system embodied in the process of phagosomal maturation.

In this study, we analyzed the dynamics of phagolysosome pH variability after synchronized ingestion of live yeast cells, dead yeast cells, and latex particles. We sought to characterize the acidification dynamics as either stochastic—an inherently unpredictable process with identical starting conditions yielding different trajectories in time, or deterministic—a theoretically predictable process with identical starting conditions leading to identical trajectories. In particular, we focused our analysis on differentiating stochastic vs. chaotic signatures in the trajectories of phagolysosomal pH. While both dynamics might yield highly divergent trajectories for similar starting conditions (i.e. only one of 100 variables differing by only a minuscule amount), a chaotic system is inherently deterministic, such that if strictly identical starting conditions were replicated, the same trajectory would follow from those conditions each time. A chaotic system is defined as one so sensitive to initial conditions that, in practice, initial conditions cannot be replicated precisely enough to see these same trajectories followed. The dynamical signatures of such systems are unique and can be differentiated from that of other deterministic or stochastic dynamics.

Irrespective of the nature of the ingested particle, we observed that the distribution of the increment of phagolysosomal pH reduction was random, indicative of a stochastic process. We found no evidence that phagosome acidification was a chaotic process. Systems in which a large number of variables each contribute to an outcome tend to exhibit 'noise', which gives them the characteristics of a stochastic dynamical system. Additionally, while particle size and shape affects ingestion time¹²⁹ the mean time to ingestion for beads and *C. neoformans* particles have been shown to be 2.5 and 4.18 min, respectively^{129,130}. Since phagocytosis was synchronized and our observations were made over a period of hours, it is unlikely that the effects described here are due to noise from differences in uptake time differences. In this regard, our finding that phagolysosomal pH demonstrates stochastic features is consistent with our current understanding of the mechanisms involved. Quantile-Quantile (Q-Q) plots revealed that most phagolysosomal pH distributions in this study manifested significant deviations from normality in several instances. Specifically, this stochastic normal distribution was generated at the phagolysosomal level, as evident by the fact that different phagosomes within the same macrophage manifested different pH values. Hence, each macrophage contains phagolysosomes with a different pH rather than each macrophage containing multiple of the same pH, such that the normal distribution observed was generated at the organelle level. The most normally distributed pH sets were those resulting from the ingestion of latex beads, particles that cannot modify the acidity of the phagolysosome. We note that for the three *C. gattii* strains the pH distributions revealed more skewing in Q-Q plots than for the H99 *C. neoformans* strain. Although the cause of this variation is not understood and the strain sample size is too small to draw firm conclusions, we note that such variation could reflect more microbial-mediated modification of the phagolysosomal pH by the *C. gattii* strains. In this regard, the capsular polysaccharide of *C.*

gattii strains has polysaccharide triads that are more complex¹³¹ and, given that the cryptococcal polysaccharide capsule contains glucuronic acids that can modify phagolysosomal pH via acid-base properties⁸, it is possible that this skewing reflects differences in phagolysosome to phagosome capsular effects.

We attempted to separate the dynamics of phagolysosomal maturation from acidification by investigating the accumulation of phagolysosomal maturation markers, EEA1 and V-ATPase after ingestion. Analyzing the same time intervals where pH populations stabilized, namely 1 to 4 h post ingestion, we found no forbidden ordinal patterns, suggesting that phagosome maturation was also a stochastic process. However, the acquisition of these two maturation markers did not approximate a normal distribution at any of the four time intervals, with all samples manifesting heavy right skewing. This is especially interesting considering V-ATPase is responsible for pumping protons into the phagolysosome and maintaining acidity. If the number of V-ATPase molecules translated directly to the number of protons pumped into the phagolysosome we would expect correlation between V-ATPase staining intensity and pH, and thus expect normal distributions in both. The different dynamics observed with V-ATPase immunofluorescence implies the pH heterogeneity is regulated by additional mechanisms. For example, it is possible that the efficacy of the V-ATPase pumps on the phagolysosomal membrane differs from pump to pump and that these differences also contribute to the distribution of phagolysosomal pHs observed.

For most microbes, maintenance of an acidic environment in the phagolysosome is critically determinant on the integrity of the phagolysosomal membrane, keeping protons in the

phagolysosomal lumen whilst excluding more alkaline cytoplasmic contents. For example, with *C. albicans*, the rupture of the phagolysosomal membrane is followed by rapid alkalization of the phagolysosomal lumen¹³². For *C. neoformans*, phagolysosomal integrity is compromised by secretion of phospholipases that damage membranes as well as the physical stress on membranes resulting from capsular enlargement in the phagolysosome¹⁸. However, for *C. neoformans*, loss of phagolysosomal membrane integrity does not immediately result in loss of phagolysosomal acidity, which is attributed to buffering by glucuronic acid residues in the *C. neoformans* capsule⁸. Adding to the complexity of the *C. neoformans*-macrophage interaction is the fact that the phagolysosomal pH in the vicinity of 5.5 matches the optimal replication pH for this fungus¹³, which can be expected to place additional stress on the organelle membrane through the increased volume resulting from budding cells. Treating macrophages with chloroquine, which increases phagosomal pH¹³³, potentiates macrophage antifungal activity against *C. neoformans*¹³⁴. Hence, phagosomal acidification does not inhibit *C. neoformans* replication but is critical for activation of mechanisms involved in antigen presentation¹³⁵. In the cryptococcal-containing phagolysosome the luminal pH is also likely to reflect a variety of microbial-mediated variables which include ammonia generation from urease, capsular composition, and the integrity of the phagolysosomal membrane.

Analysis of the normality of phagolysosomal pH distributions as a function of time by the Shapiro-Wilk test produced additional insights into the dynamics of these systems. Phagolysosomes containing inert beads manifested pH distributions that met criteria for normality at most time intervals after 1 h post infection (HPI). We hypothesize that at 0.25 and 0.5 HPI there are two

populations of phagolysosomes, mature and maturing, with the latter having not yet fully acidified and thus resulting in the observed bimodal distributions. Additionally, it has been shown that phagolysosomes of macrophages undergo active alkalization, regulated in part by NOX2 activity^{29,30,136}. It is likely that these early time points veer away from normality due to a combination of phagolysosomes maturing at a different rate and a subpopulation of phagolysosomes which are actively alkalized, both contributing noise to early phagolysosomal dynamics. In contrast, the pH distribution of phagolysosomes containing dead *C. neoformans* cells initially veered away from normality at 15 min, 30 min, and 1 h but in later time intervals approached normality, meeting the criteria for normality at 3 h. One interpretation of this result is that the process of phagocytosis is itself a randomizing system with Gaussian noise resulting from phagolysosome formation and kinetics of the initial acid-base reactions between increasing proton flux and quenching glucuronic acids in the capsular polysaccharide. With time, the titration is completed as all glucuronic acid residues are protonated, as dead cells did not synthesize additional polysaccharide, which moved the phagolysosomal pH distribution towards normality. A similar effect may have occurred with strains R265, W179, and *ure1Δ*. Convergence to or away from normality could reflect a myriad of such variables affecting phagolysosomal pH including the intensity of acidification, the volume of the phagolysosome (largely determined by the yeast capsule radius), the glucuronic acid composition of the capsule, the production of ammonia by urease, and the leakiness of the phagolysosome to cytoplasmic contents with higher pH. Although our experiments cannot sort out the individual contributions of these factors, they suggest that, in combination, they produce Gaussian noise effects that push or pull the resulting distribution to or from normality. Additionally, human phagolysosome acidification dynamics resembled those of mouse cells but noted significant differences in the distributions of phagolysosomal pH

between individual human donors. This donor-to-donor variation could reflect differences in polymorphisms in Fc receptor genes or other genetic variables and is an interesting subject for future studies.

When a phagocytic cell ingests a microbe, it has no information as to the pH range tolerated by the internalized microbe. A stochastic dynamical process for phagolysosomal acidification could provide phagocytic immune cells and their hosts with the best chance for controlling ingested microbes. The acidic pH in the phagolysosome activates microbicidal mechanisms and acidity is not generally considered a major antimicrobial mechanism in itself. However, our analysis of pH tolerances of 27 pathogenic microbes revealed that the majority are inhibited by phagolysosomal pH with the caveat that some, like *C. neoformans*¹⁰ and *Salmonella typhimrium*¹³⁷, thrive in acidified phagolysosomes. On the other hand, a less acidic phagosomal pH is conducive to intracellular survival for *M. tuberculosis*¹³⁸. During an infectious process when the immune system confronts numerous microbial cells the random nature of the final phagosomal pH will result in some fraction of the infecting inoculum being controlled, and possibly killed, by initial ingestion allowing antigen presentation. In this regard, the mean number of bacteria in the phagolysosomes and cytoplasm of macrophages infected with the intracellular pathogen *Francisella tularensis* exhibits stochastic dynamics¹³⁹, which in turn could result from the type of stochastic processes in phagolysosome formation noted here. Hence, chance in phagolysosomal pH acidification provides phagocytic cells with a mechanism to hedge their bets such that the stochastic nature of the process is itself a host defense mechanism.

In biology, bet-hedging was described by Darwin as a strategy to overcome an unpredictable environment¹⁴⁰, which is now known as diversified bet-hedging: diversifying offspring genotype to ensure survival of at least some individuals at the expense of reducing the mean inclusive fitness of the parent. The main idea behind any bet-hedging strategy, under the assumption of multiplicative fitness, is that to maximize long-term fitness, an organism must lower its variance in fitness between generations^{141–143}. For example, varying egg size and number in a clutch can bank against years with a hostile environment in a form of diversified bet-hedging¹⁴⁴. During any given “good year” fewer of the offspring will thrive because some are specifically designated for survival in “bad years”, drastically increasing fitness during bad years at the cost of a slight fitness reduction during good. Our observations suggest that, as a population, macrophages perform a bet-hedging strategy by introducing a pH level as inhospitable to pathogens as possible, while still maintaining biologically possible levels. However, such an approach could select for acid-resistant microbes. Our observation suggests that to avoid an arms-race, the macrophage not only lowers the pH level to a level that is unfavorable to most microbes, since the reduction in pH level reduces the optimal growth condition to around 70% of the optimum (see Figure 3 red line under the blue shaded curve), but it also introduces randomness in the achieved pH, such that ingested microbes are less likely to adapt to the potentially hostile environment. In other words, tightly controlled pH reduction by the host without increased variation, might introduce an evolutionary arm-race between pathogens and their host cells, leading towards deleterious outcome of selecting microbial acid resistance. A similar evolutionary arms race would occur between environmental *C. neoformans* and the amoebas who prey upon them. Previous studies indicate that acidification in amoebas closely resembles that of macrophages with similar final pH and time to acidification^{145,146}. Thus, phagocytic predators in soils would face the same problem as

macrophages in not knowing the pH tolerance of their prey and it is conceivable that they employ a similar defense strategy to that observed in macrophages, likely to have been honed in by eons of selection in soil predator-prey interactions.

Additionally, our model shows that even at the lower extreme mean pH, macrophage populations still benefit in the long run by increasing their phagolysosomal pH variance. We note that the pH of other mammalian fluids such as that of the blood are tightly regulated such that their physiological variance is very small¹⁴⁷. For example, human plasma pH averages 7.4 with a range of only 0.05 units. Hence, organisms can maintain tight pH control when it is physiologically important, implying that the comparatively large range of phagolysosomal pHs measured in all conditions studied is a designed feature of this system. In other words, one can envision the macrophage's first line of defense of bet-hedging phagolysosomal pH as a roulette wheel, where the payout is likelihood of macrophage survival and the placed bet is a range of possible pH. Placing multiple bets across the table (increasing standard deviation of pH distribution) increases the chance of winning at the cost of a lower payout (mean fitness), resulting in a more profitable long-term strategy (increased mean log fitness). In fact, the most profitable roulette strategy is broad color bets with lower payouts but the best winning probability. The most profitable betting strategy would of course be to play Blackjack instead, but macrophages do not have that luxury.

We observed that this bet hedging strategy was displayed in M1 polarized macrophages, dependent on a normal distribution of phagolysosomal pH with a high variance. M2 macrophages, which acidify with different dynamics to M1¹⁴⁸, do not acidify to a normal distribution and thus

do not engage in this bet hedging strategy. Additionally, we found that M2 skewed macrophage populations on average acidify to a higher pH than M1 skewed populations and are overall more favorable to *C. neoformans*, an observation supported by previous literature^{148,149}. This hypothesis, while requiring more investigation, may help explain why M2 skewed macrophages are unable to control *C. neoformans* infection, as their phagolysosomes acidify to a pH range that is optimal for *C. neoformans* growth¹³.

Additionally, intracellular pathogens have developed their own ways to disrupt or game the macrophage betting system. For *C. neoformans*, which can manipulate phagolysosomal pH through several mechanisms, our model shows that the fungal-mediated changes in the distribution of phagolysosomal pH favors the pathogen overall, disrupting the bet hedging system and resulting in lower macrophage population fitness. This phenomenon can also be observed with *M. avium* in which previously reported phagolysosomal pH values¹²⁶ show a marked increase in mean log fitness when the ingested pathogen is killed and unable to modulate pH. This finding is emphasized by our analysis of phagolysosomes whose pH has been pharmacologically manipulated to a region favorable to pathogens. We found that disrupting the macrophage betting system this way led to a drastically reduced overall mean log fitness of the macrophage population.

Given that acid has potent antimicrobial properties, one might wonder why phagolysosomal acidification does not reach even lower and more acidic pHs. There are several explanations for observed lower limits in pH. Acidification is achieved by pumping protons into the vacuole and

achieving lower pHs against an ever-increasing acidity gradient could prove thermodynamically difficult. There is also evidence that the integrity of the cell membrane lipid bilayer is compromised by acidity at pHs of 3 and below^{150,151} which could promote leakage of phagolysosomal contents into the cytoplasm with damage to the host cell. Consequently, we propose that a larger variation in macrophage phagolysosomal pH acts as a diversified bet-hedging strategy against the stochasticity of the potential pH tolerances of ingested microbes within the physiological limits of achievable acidification. This hypothesis is supported by simulated data in which an increase in standard deviation of the pH distribution slightly lowers the expected mean but significantly decreases the standard deviation of host survival. Fully analyzing the consequences and evolutionary tradeoff of this strategy would require a closer analysis that considers the costs and benefits with regard to the host. Though outside the scope of our current work, our observations suggest this line of investigation for future studies.

Our results delineate new avenues for investigation. Most perplexing is how a random phagolysosomal pH is established and maintained. One can imagine various mechanisms including variation in the number of ATPase molecules and/or differences in activity of individual pumps depending on location and adjoining structures. To resolve this would require sophisticated technology allowing the measurement of pH in individual phagolysosomes as a function of pump occupancy and efficacy. Such techniques are likely beyond the current technological horizon but suggests new fertile areas of scientific investigation. From a clinical perspective, a drug that increases variation in phagolysosomal pH could be useful in enhancing macrophage anti-microbial efficacy in situations that one cannot anticipate which specific microbes will be encountered. On

the other hand, drugs that specifically modulate pH may be useful in situations with specific microbes that express marked acid/base tolerance. In this regard, chloroquine alkalizes *C. neoformans* phagolysosomes, moving away from optimal inhibitory pH. This drug has been shown to enhance macrophage activity against *C. neoformans*^{1,152}, an outcome predicted by our model.

In summary, we document that phagolysosomal acidification, a critical process for phagocytic cell efficacy in controlling ingested microbial cells, manifests stochastic dynamics that permit a bet-hedging strategy for phagocytic cells ingesting microbes of unknown pH tolerance. These observations establish that the use of bet-hedging strategies in biology extends to the sub-organism level to involve cells and their organelles. This, in turn, implies a significant role for chance in the resolution of conflict between microbes and host phagocytic cells in individual phagolysosomes. We have recently argued that chance is also a major determinant of individual susceptibility to infectious diseases at the organismal level¹⁵³. Variability in the outcome of infectious disease between individual hosts may reflect the sum of innumerable chance events for host-microbe interactions at the cellular level, which include the process of phagosome acidification.

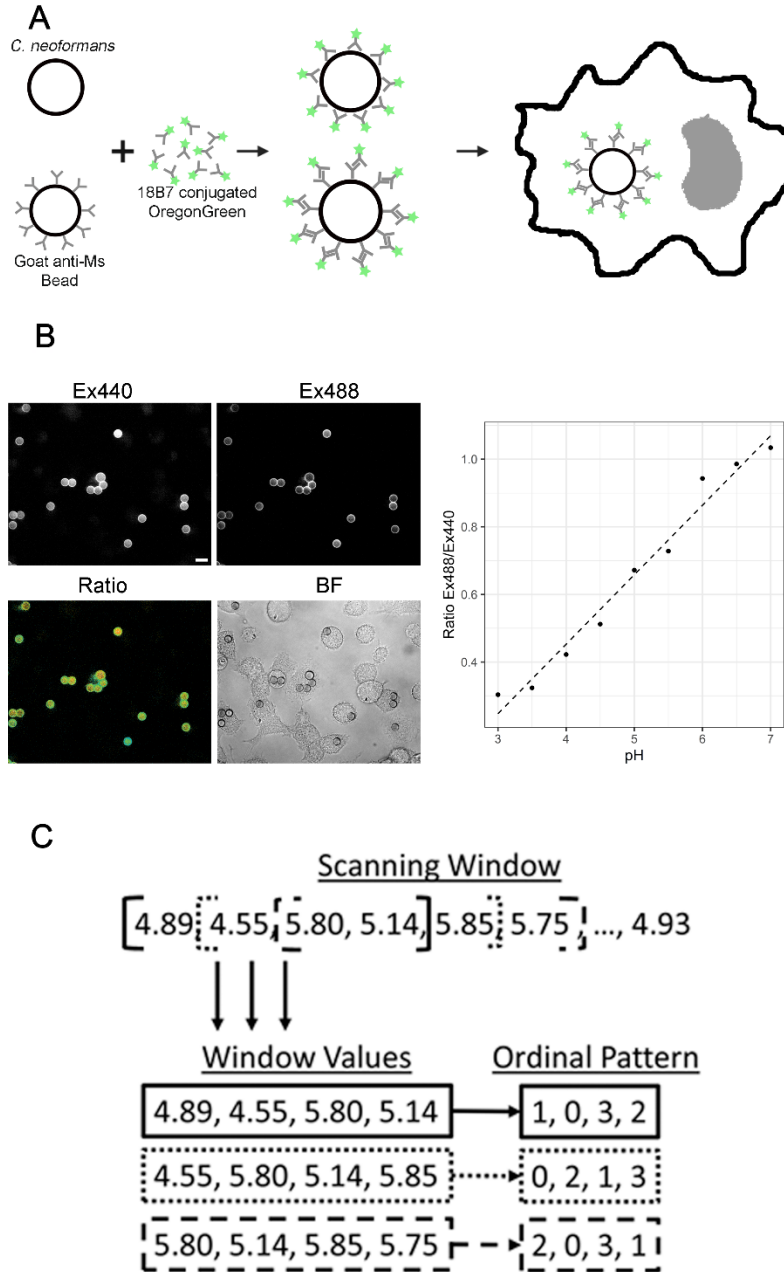


Figure 5

Experimental designs for described methods. **A.** Experimental design for phagolysosomal pH measurement. Particles are opsonized with mAb 18B7 conjugated to fluorophore Oregon Green. **B.** Measurement of phagolysosomal pH. Measurements are based on ratiometric measuring of Ex440/Em520 and Ex488/Em520. **C.** Experimental design for the detection of Chaos within a system. A scanning window generates sets of windows values. Ordinal patterns are then generated by ordering the terms in each scanning window from least to greatest.

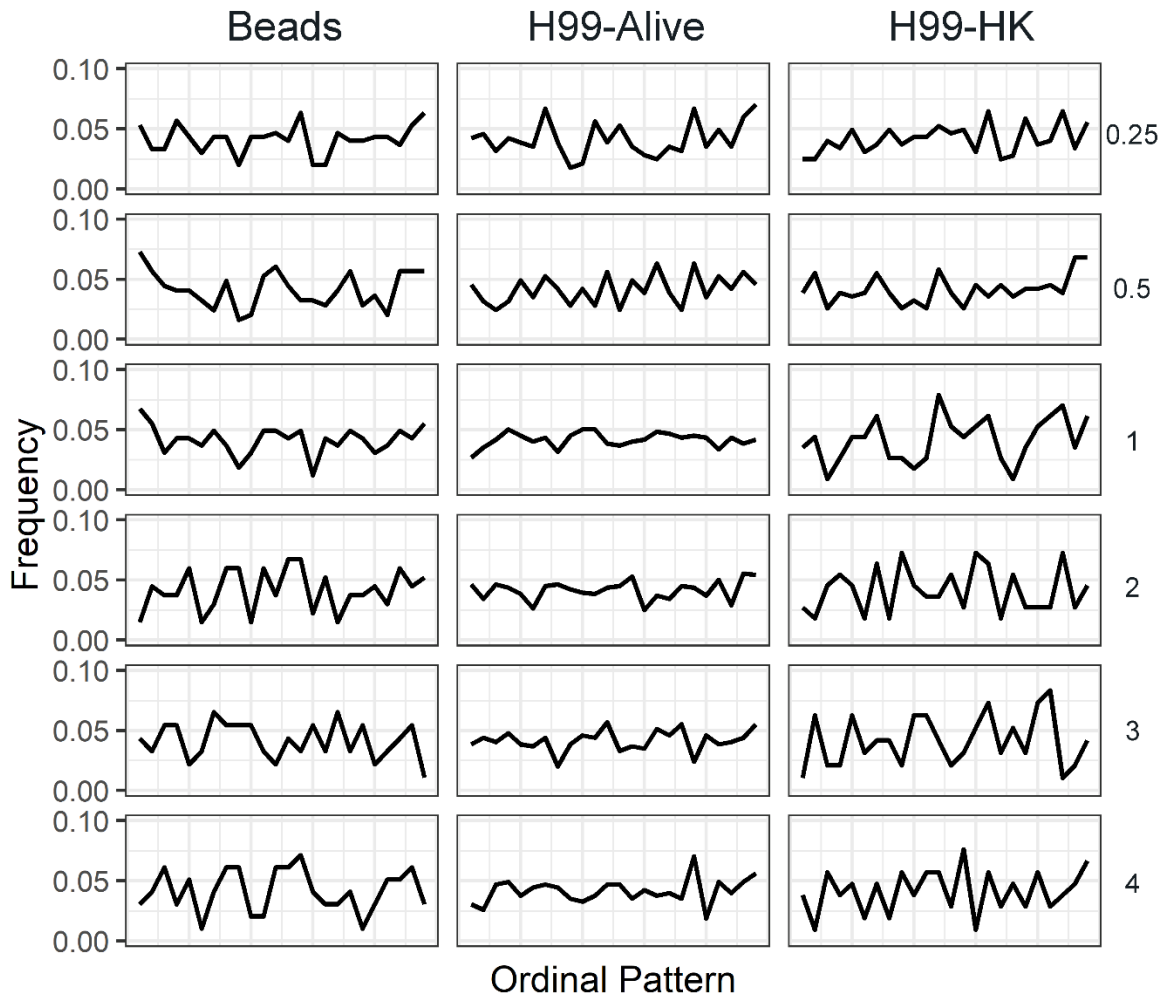


Figure 6

Murine macrophage phagolysosomes acidify stochastically. The frequency of each 4-unit ordinal pattern for each ingested particle: beads, live *C. neoformans*, and dead *C. neoformans* at various HPI. Note that all ordinal patterns have a non-zero frequency.

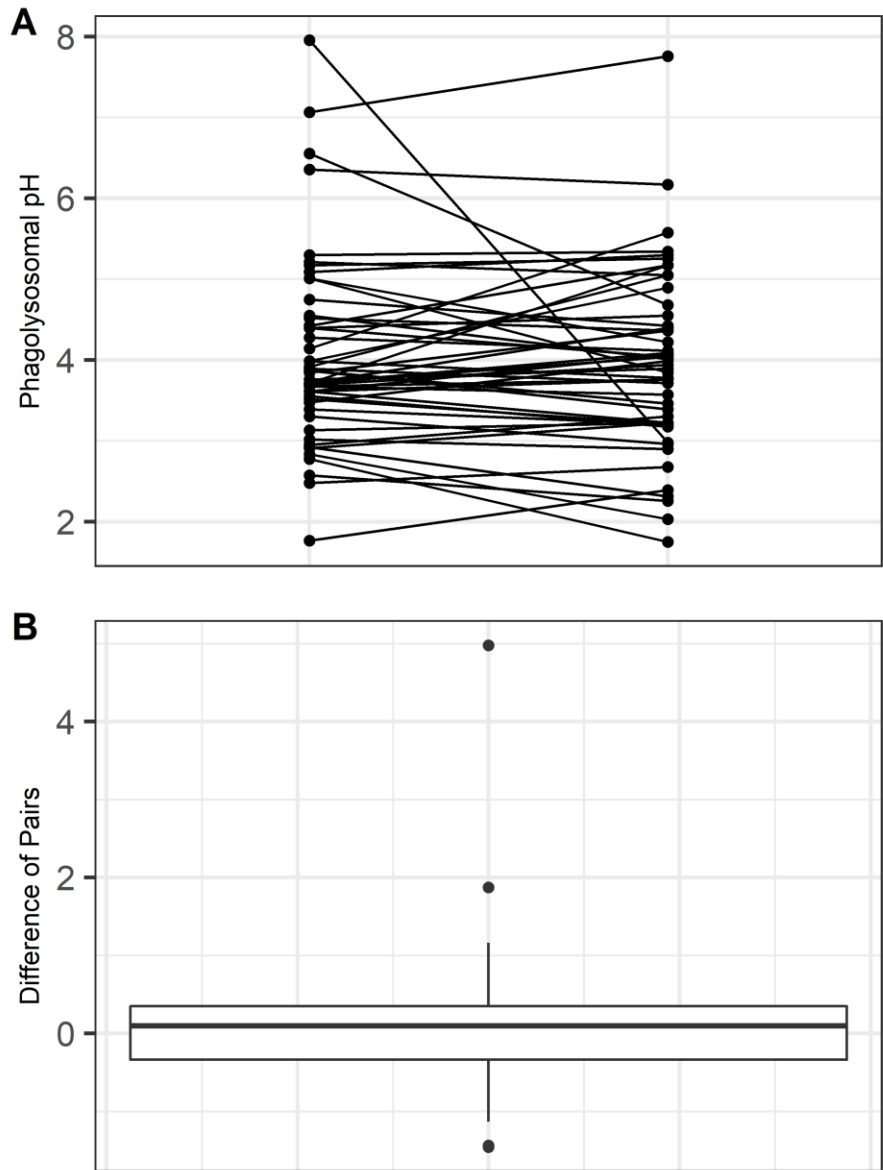


Figure 7

Analysis of 80 pairs of phagolysosomes within single cells. **A.** Measured phagolysosomal pH of multiple beads located in the same macrophage but non-proximal phagolysosomes. Lines indicate particles within the same macrophage. Phagolysosomes were measured in no particular order. **B.** Differences of each phagolysosomal pH pair approximate a normal distribution centered around 0 with non-zero values despite being generated within the same macrophage at a synchronized starting time.

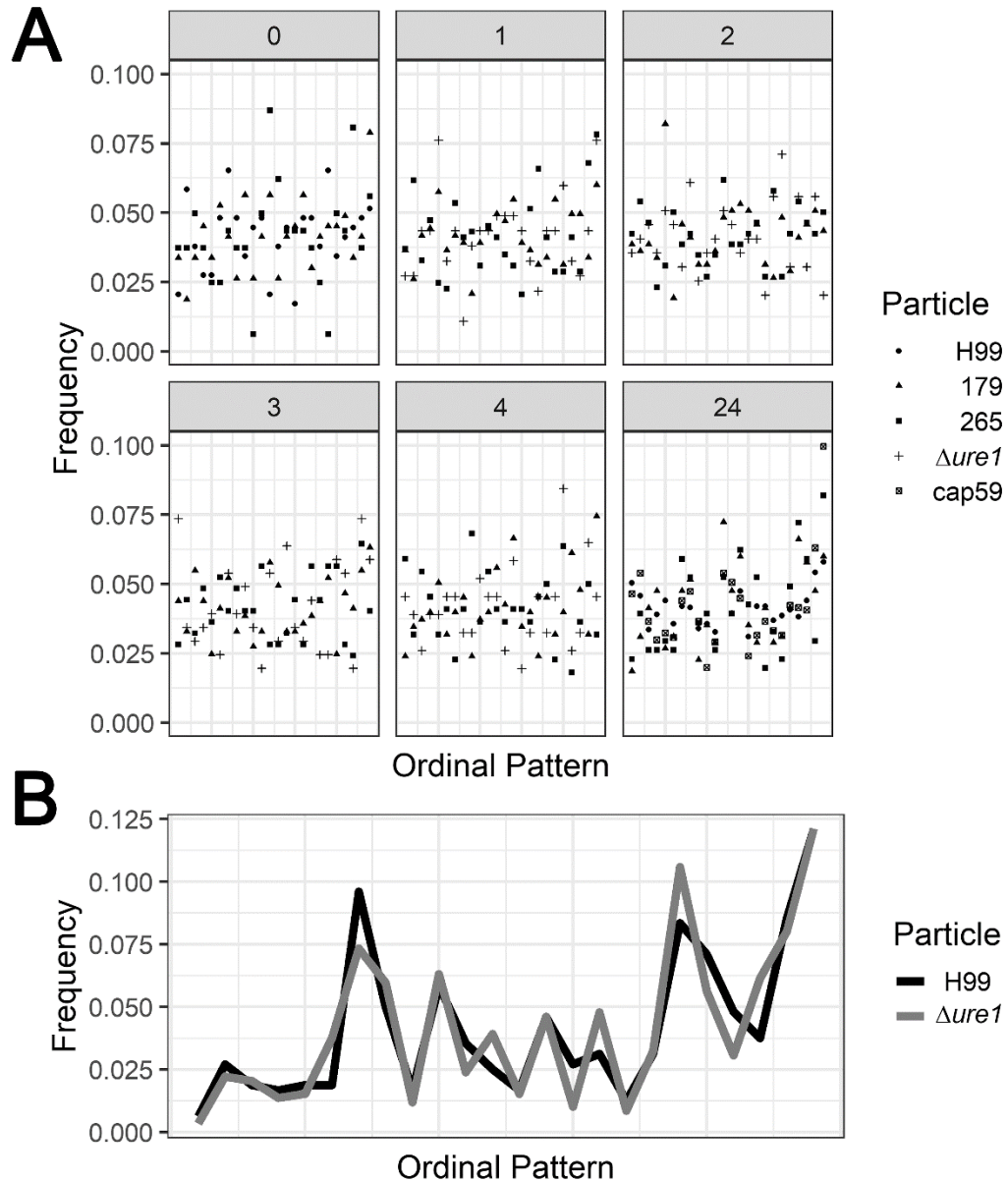


Figure 8

Ordinal pattern analysis for expanded samples. **A.** Ordinal pattern frequencies for phagolysosomal acidification intervals in BMDMs infected with various particles at various hours post infection (gray box values). **B.** Ordinal pattern frequencies for time elapsed before initiation of budding for yeast strains ingested by BMDMs.

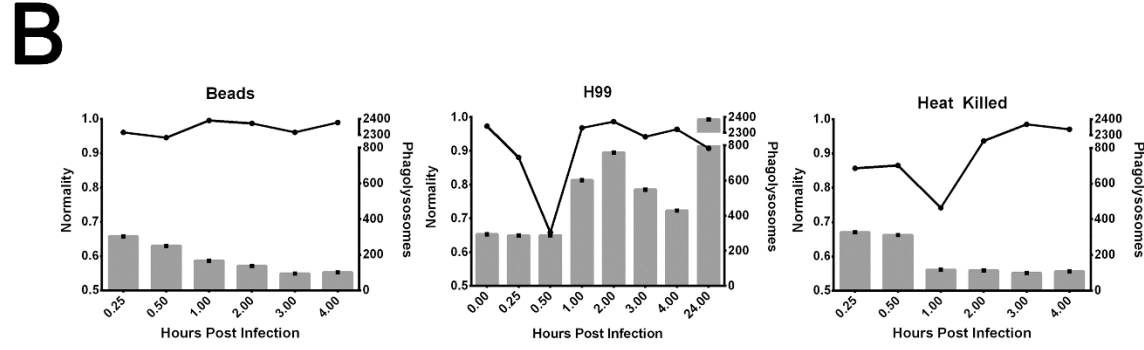
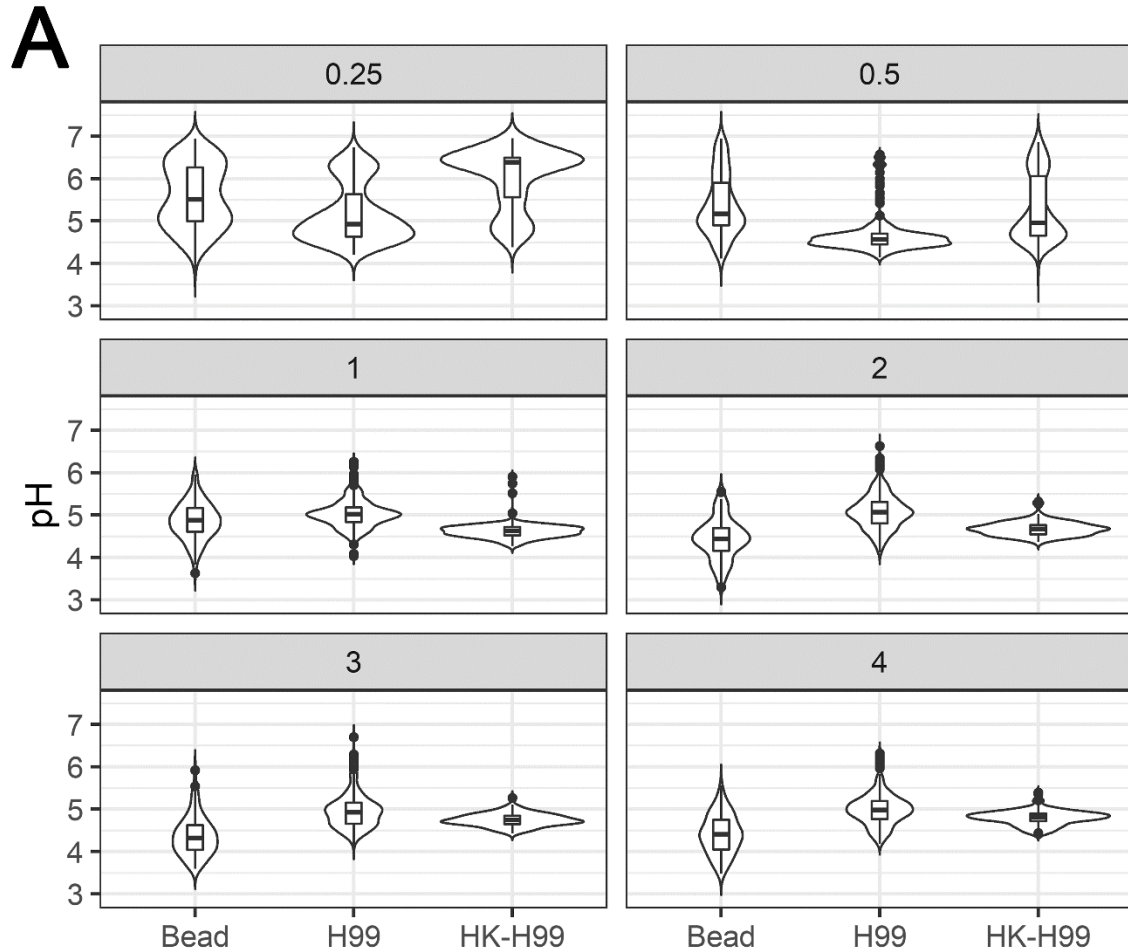


Figure 9

Bead ingested murine macrophage phagolysosomes stabilize to a normally distributed pH. **A.** Distributions of measured phagolysosomal pH after ingestion of various particles by BMDMs at various hours post infection (gray box value) for bead, live *C. neoformans* (H99), and dead *C. neoformans* (HK-H99). **B.** Visualization of estimated normality via Shapiro-Wilk (line) and total phagolysosome count (bar) for each sample.

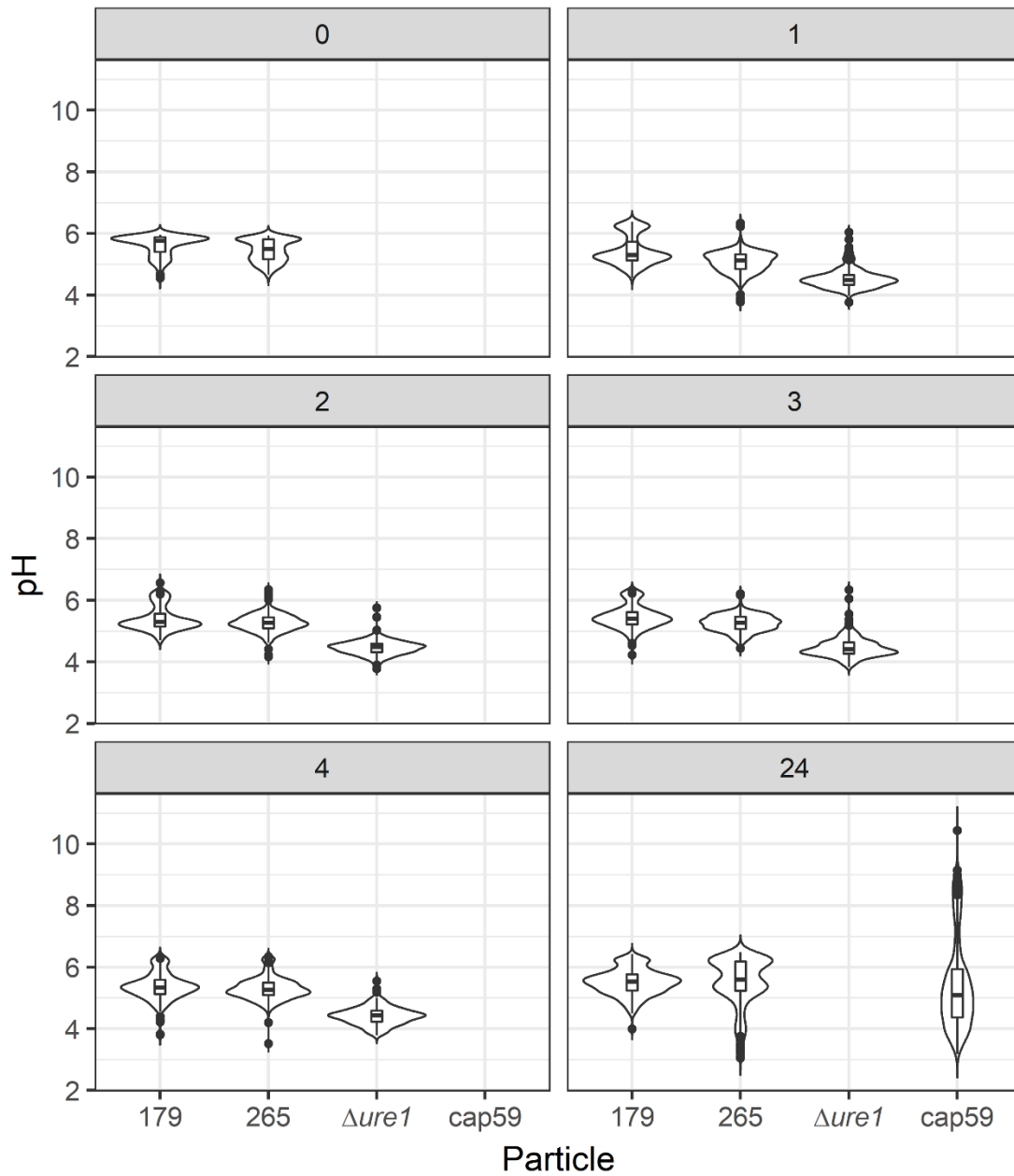


Figure 10

Phagolysosomal pH distributions for expanded samples. Two strains of *C. gattii* (179 and 265), a urease deficient H99 mutant ($\Delta ure1$), and a capsule deficient H99 mutant ($cap59$) were analyzed at various hours post infection (gray box value).

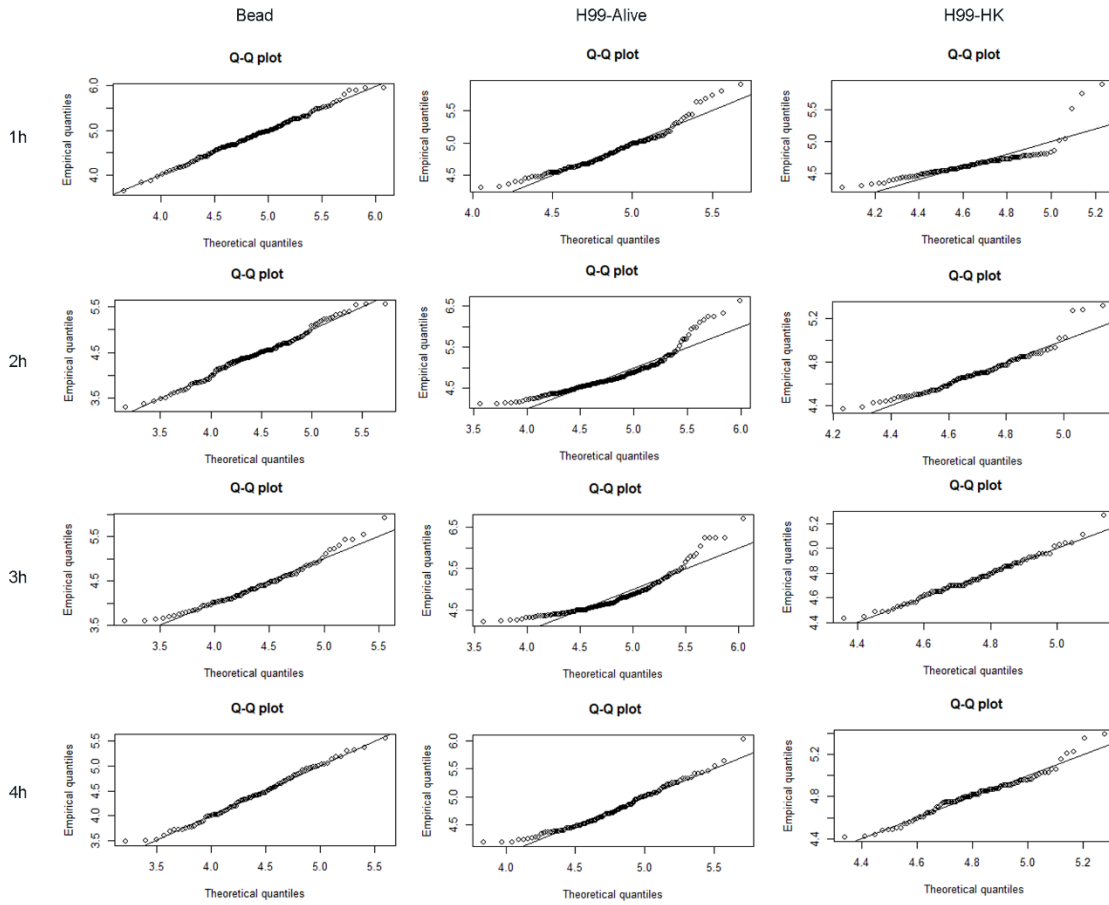


Figure 11

Q-Q plots of macrophages 1-4 HPI after ingesting various particles. Note that bead containing phagolysosomes closely approximate a normal distribution, while *C. neoformans* containing phagolysosomes have heavy tails, regardless if the particle is live or dead.

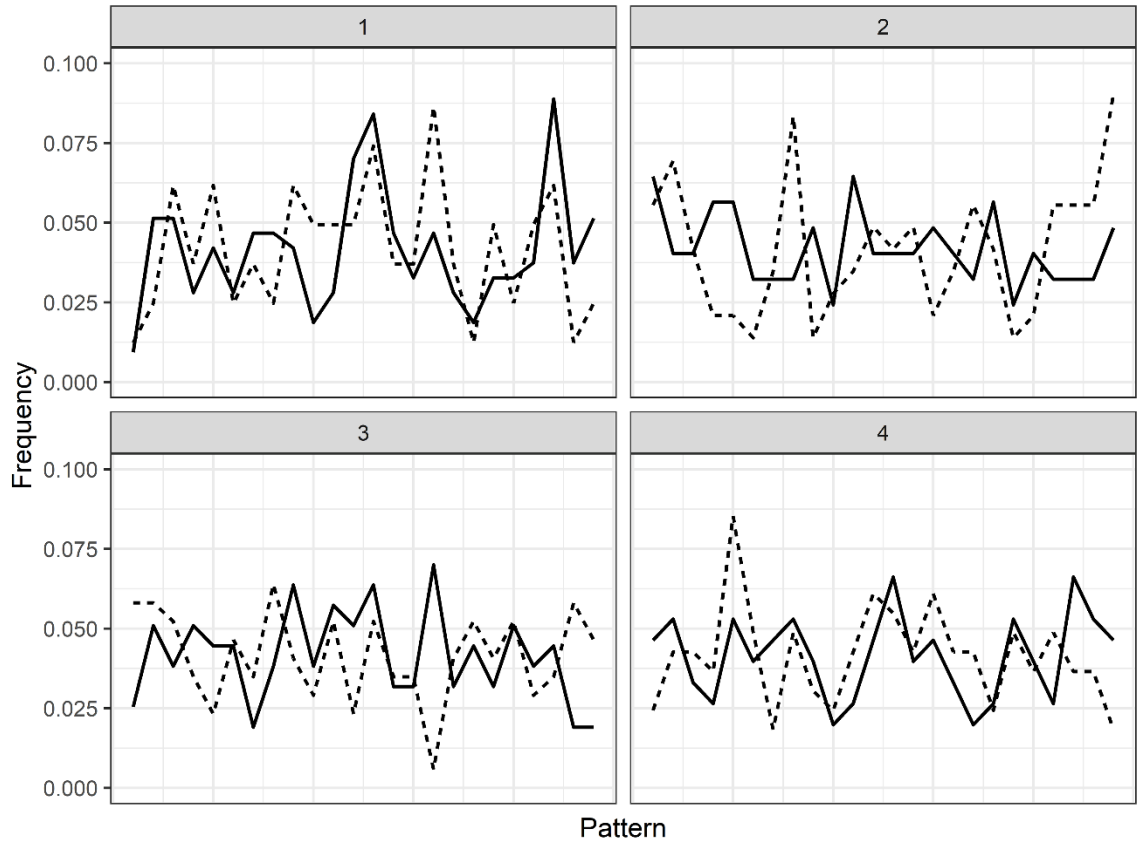


Figure 12

Ordinal pattern analysis for EEA1 (solid) and V-ATPase (dashed) immunofluorescent staining for bead containing macrophage phagolysosomes at various hours post ingestion (gray box values). No forbidden ordinal patterns were detected for any samples, suggesting phagolysosomal maturation marker acquisition is a stochastic process.

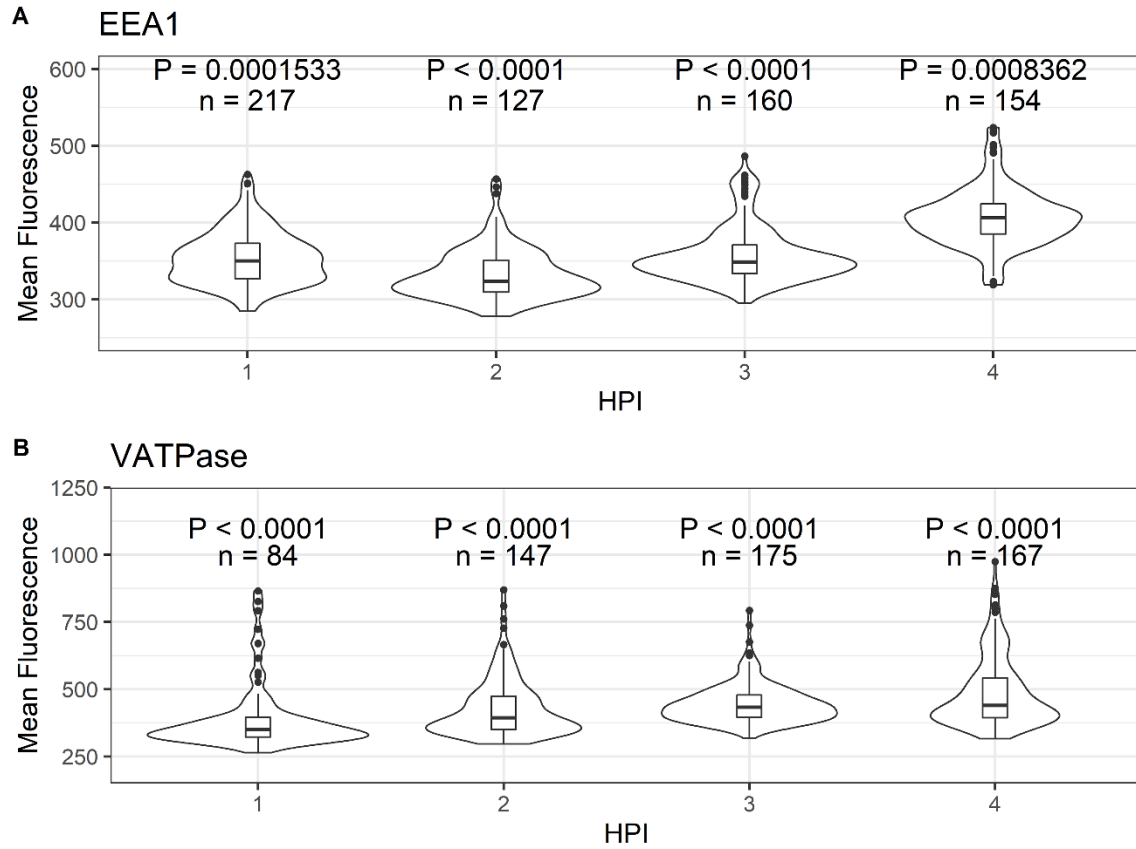


Figure 13

Mean fluorescence intensity values for EEA1 and V-ATPase immunofluorescent staining. The acquisition of these phagolysosomal maturation markers does not resemble that of bead containing phagolysosomal pH, as no samples here are normally distributed. P values were determined via Shapiro-Wilk normality test.

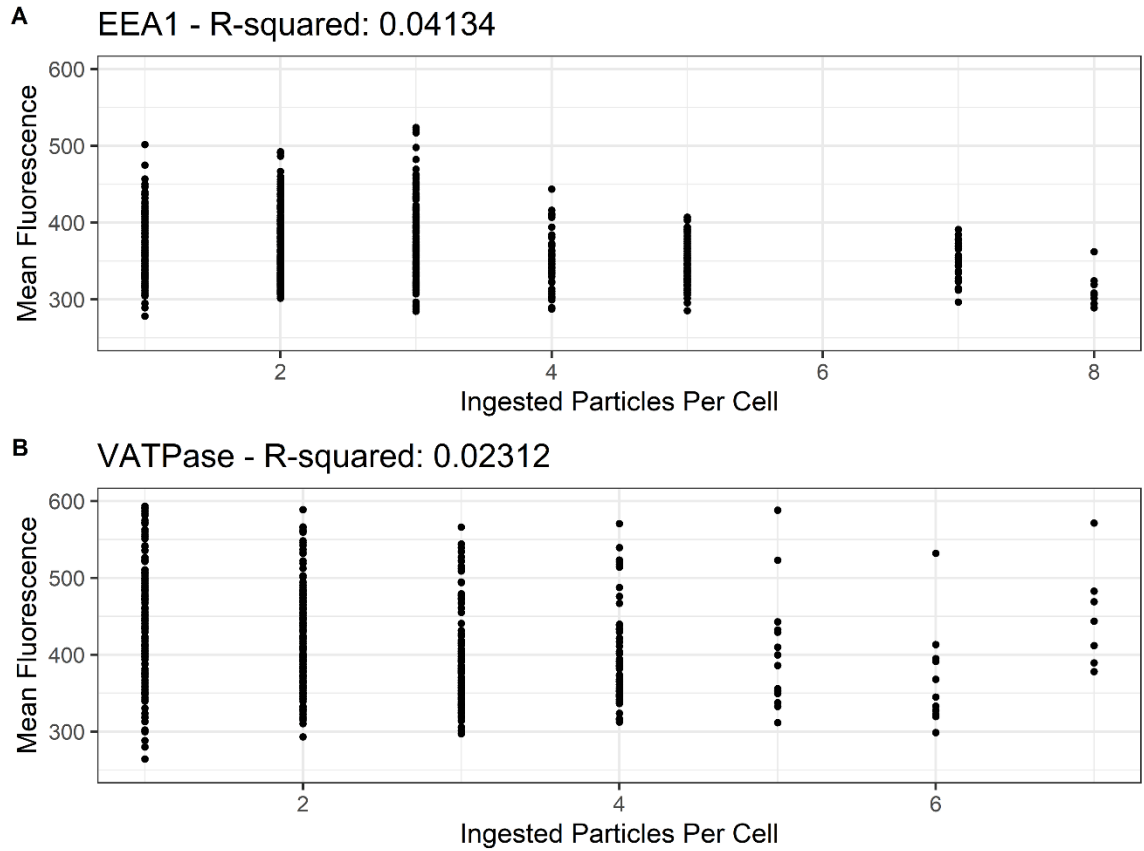


Figure 14

Mean fluorescent intensity of macrophage ingested beads stained for EEA1 and V-ATPase, sorted according to total ingested particles per cell. Linear regressions were calculated for each sample set but clearly there is no significant correlation between total ingested particles and number of EEA1 or V-ATPase molecules as measured by fluorescent intensity.

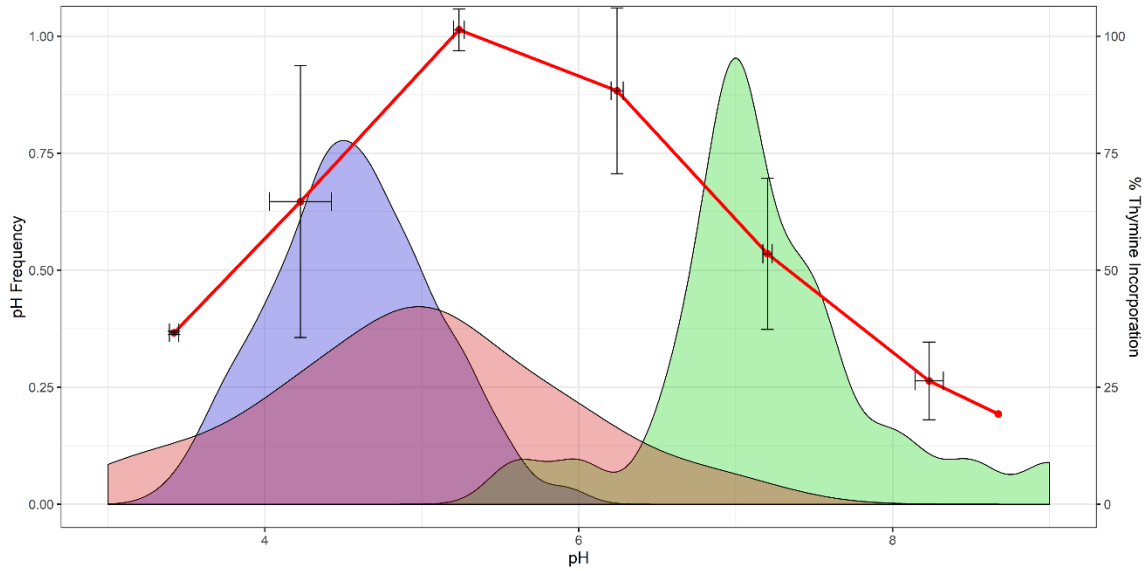


Figure 15

BMDM phagolysosomes acidify to a default pH range suboptimal for soil microbe and pathogen growth. Growth rates of soil bacteria^{118,119} as percent thymine incorporation (red line) and distribution of minimal culturable pH for 27 human pathogens (red fill) compared to the distribution of observed phagolysosomal pH after bead ingestion and phagolysosome maturation, 1-4 HPI (blue fill). The bead pH distribution overlaps unfavorably with minimal growth conditions of microbes, and only minimally overlaps with the optimal growth pH range of the same 27 pathogens (green fill).

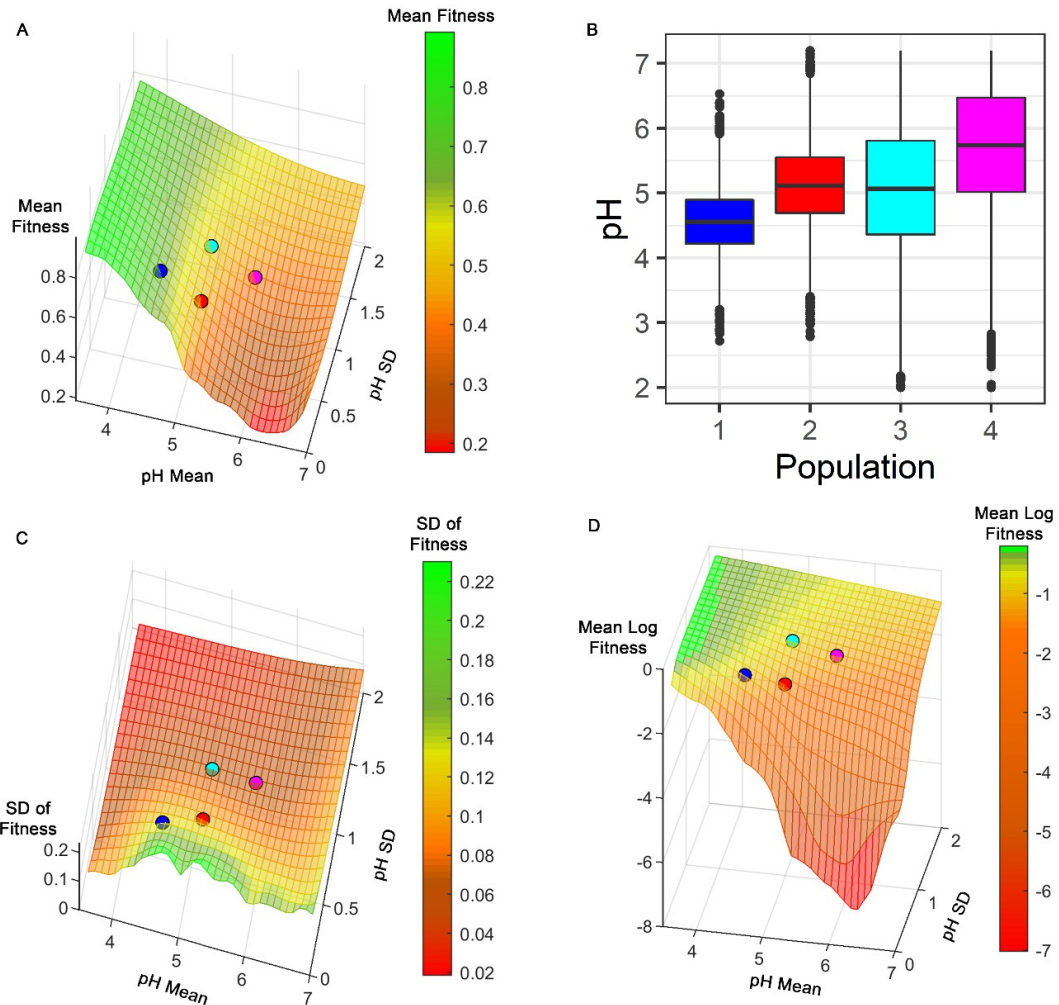


Figure 16

Simulated macrophage populations show stochastic pH as bet-hedging strategy. Success of host-microbe interactions are visualized as macrophage populations faced with randomly selected pathogens and acidified to random pHs from normal distributions of mean μ and standard deviation σ . Meshes represent host macrophage fitness, deviation in fitness, and log mean fitness. Plotted points represent measured data of H99 containing murine (red) and human (magenta) or bead containing murine (blue) and human (cyan) phagolysosomes. **A.** Mean macrophage survival (Z axis, colorbar) increases significantly as pH lowers, and mostly unchanged with standard deviation. **B.** Examples of simulated populations based on colored points in panel A. Each combination of mean and SD from the axes of panel A represent a unique population of macrophages with a fitness represented by the Z axis and colored mesh. **C.** Deviation in host fitness (Z axis, colorbar) dramatically decreases by increasing standard deviation of pH, and mostly unaffected by shifts in mean pH. **D.** Logarithmic measurement of host fitness (Z axis, colorbar) to observe long term trends applicable to a bet-hedging strategy.

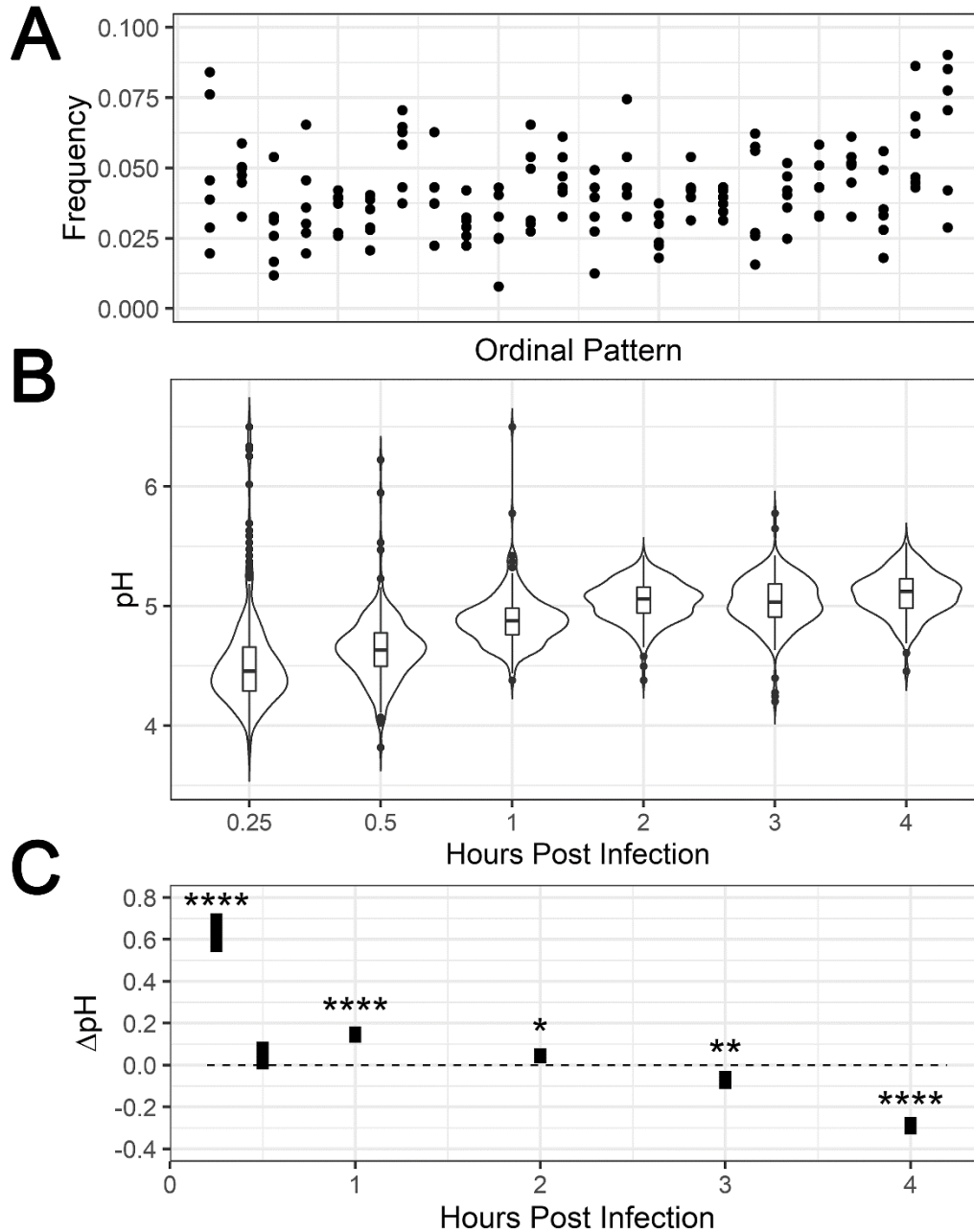


Figure 17

Trained murine macrophages have inverse acidification dynamics. **A.** Ordinal pattern analysis of phagolysosome pH in trained BMDMs. All ordinal patterns appear at a non-zero frequency. **B.** pH distributions of phagolysosomes at various HPI. **C.** Difference (95% CI) after subtracting mean trained phagolysosome pH from mean untrained phagolysosome pH at each timepoint. *, **, **** denote $P < 0.05$, 0.01 , and 0.0001 respectively via two tailed t-test.

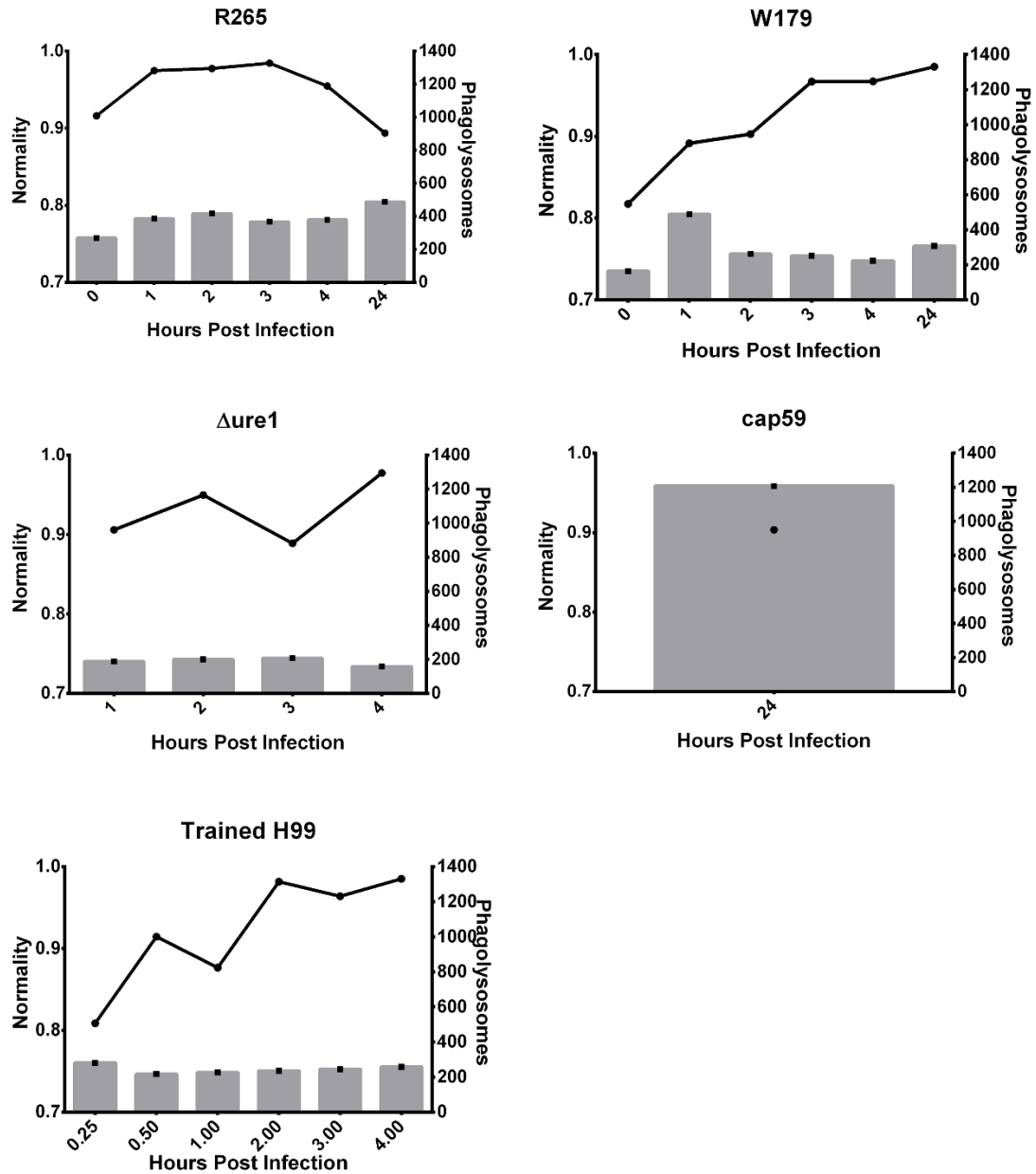


Figure 18

Normality analysis for expanded samples. Shapiro-Wilk normality values (lines) alongside total phagolysosome sample sizes (bars) for two strains of *C. gattii* (179 and 265), a urease deficient H99 mutant (*Δure1*), a capsule deficient H99 mutant (*cap59*), and trained BMDMs on reinfection.

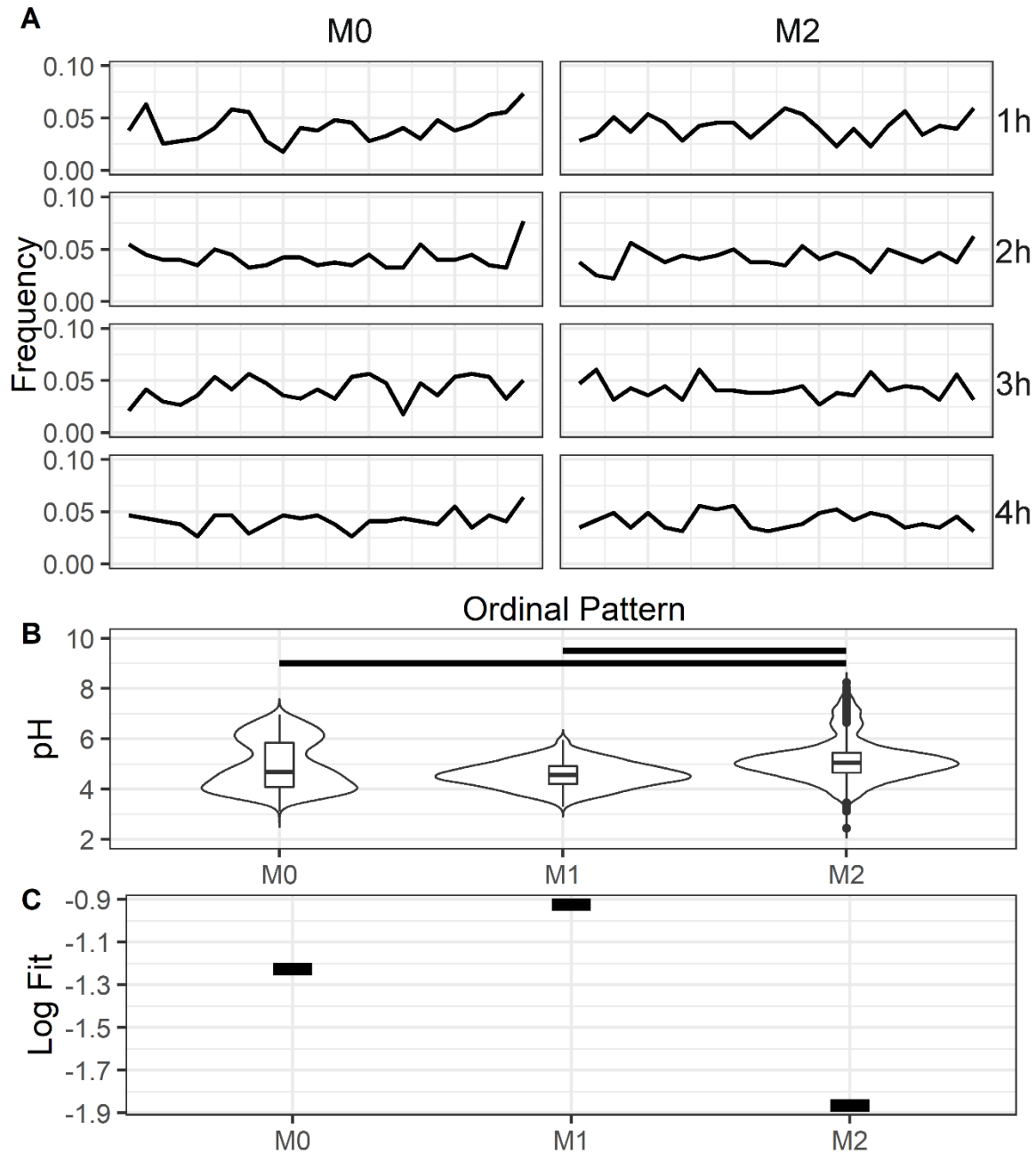


Figure 19

Phagolysosome dynamics of macrophages skewed toward different polarization states. **A.** Ordinal patterns of bead containing phagolysosomes at various HPI. **B.** Bead containing phagolysosome pH distributions of differently polarized macrophages. Black bars represent $P < 0.0001$ via Kruskal-Wallis test with Wilcox rank pairing test. **C.** Mean log fitness of bead containing phagolysosomes according to our bet hedging model.

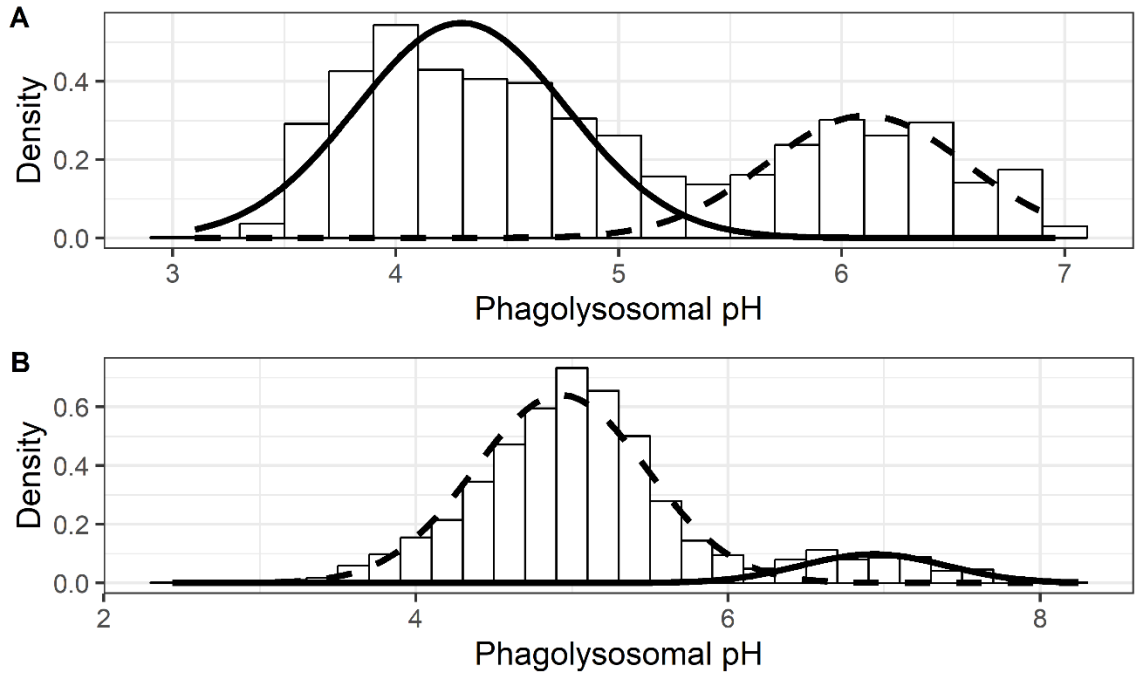


Figure 20

Bimodal models fitted to the observed data for **A.** M0 and **B.** M2 skewed macrophages. Models are attempted fits of two mixed Gaussian distributions. Histogram bars visualize the observed data while solid and dashed lines depict the relative contributions of the two hypothetical Gaussian distributions.

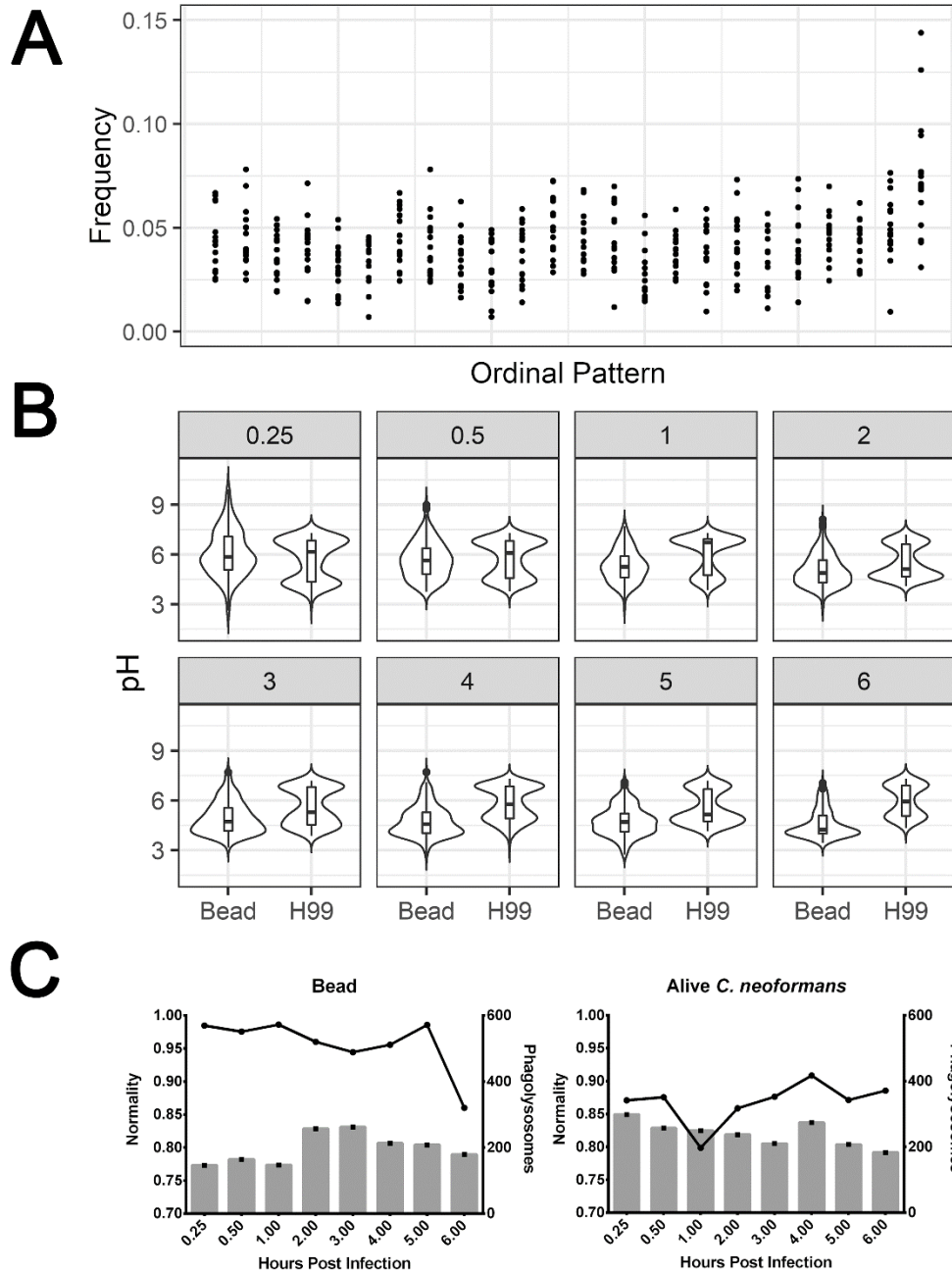


Figure 21

Isolated human monocytes acidify stochastically and approximate normality. Human macrophages were infected with inert beads or live *C. neoformans*, and their pH analyzed at various timepoints. **A.** Ordinal Pattern analysis for all conditions. All patterns exist at non-zero frequencies for all timepoints. **B.** Distributions of phagolysosome pH at different timepoints. **C.** Shapiro-Wilk normality and total sample count for each condition.

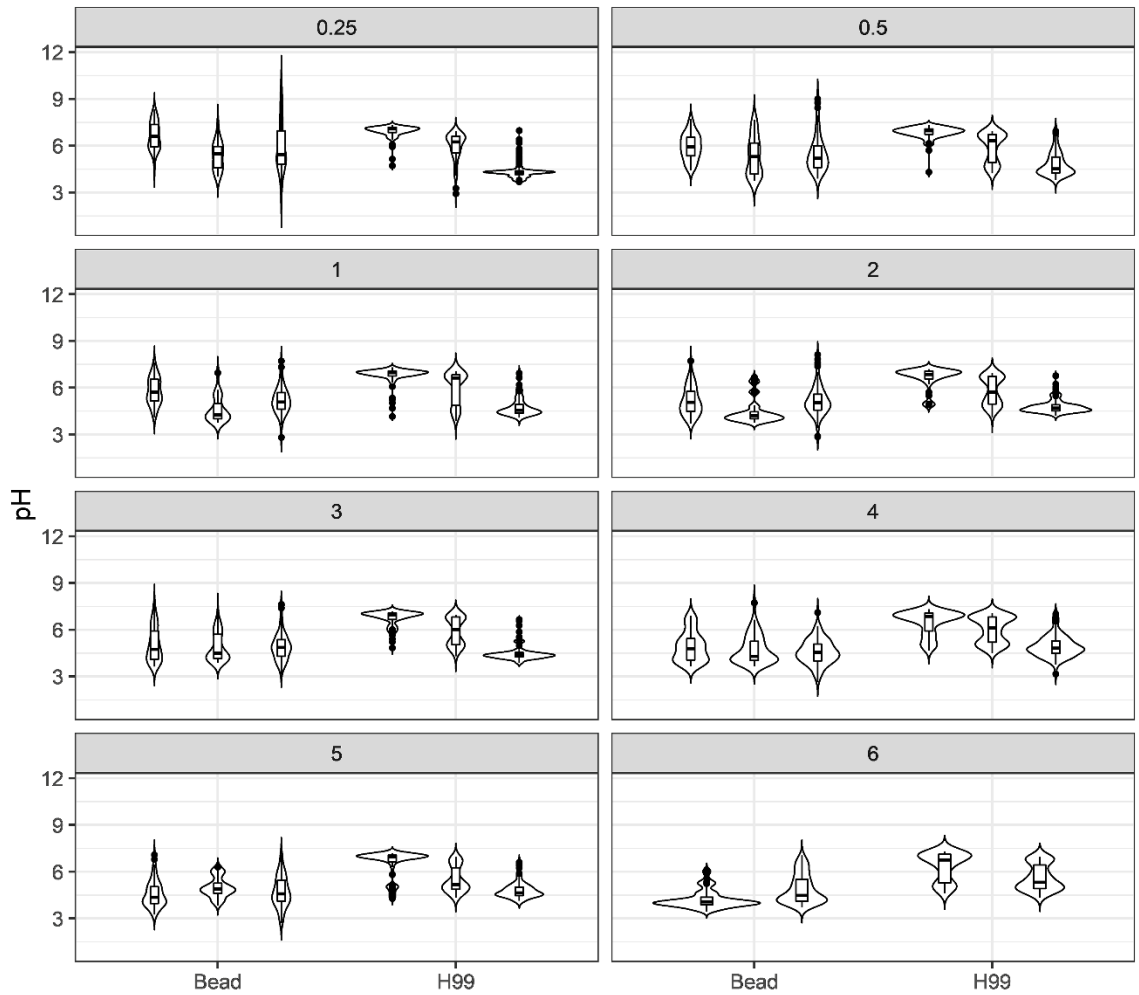


Figure 22

Phagolysosomal pH distributions for human macrophages infected with H99 separated by individual donor. Human macrophages were analyzed after ingesting either H99 or inert beads at various hours post infection (gray box value).

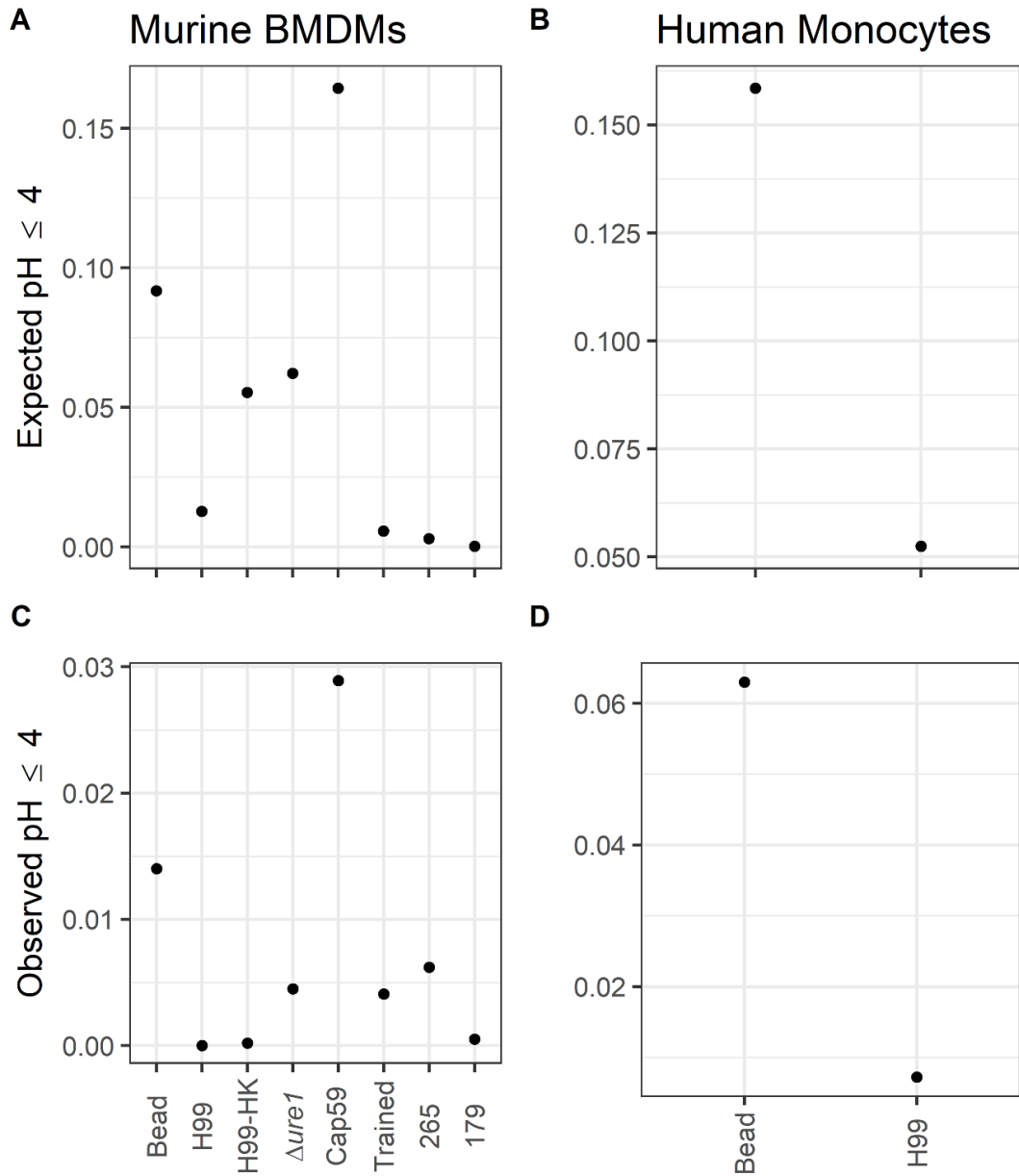


Figure 23

Expected and observed likelihood of phagolysosomes to achieve $\text{pH} \leq 4$. **A.** The expected proportions of murine BMDM phagolysosomes to achieve $\text{pH} \leq 4$ assuming a normal distribution based on all observed data. **B.** The expected proportions of human macrophage phagolysosomes to achieve $\text{pH} \leq 4$ assuming a normal distribution based on the observed data. Expected proportions of macrophages to achieve $\text{pH} \leq 4$ were calculated by assuming a normal distribution centered around a mean and standard deviation calculated from the observed data. **C.** The observed proportions of murine BMDM phagolysosomes to achieve $\text{pH} \leq 4$. **D.** The observed proportions of human macrophage phagolysosomes to achieve $\text{pH} \leq 4$.

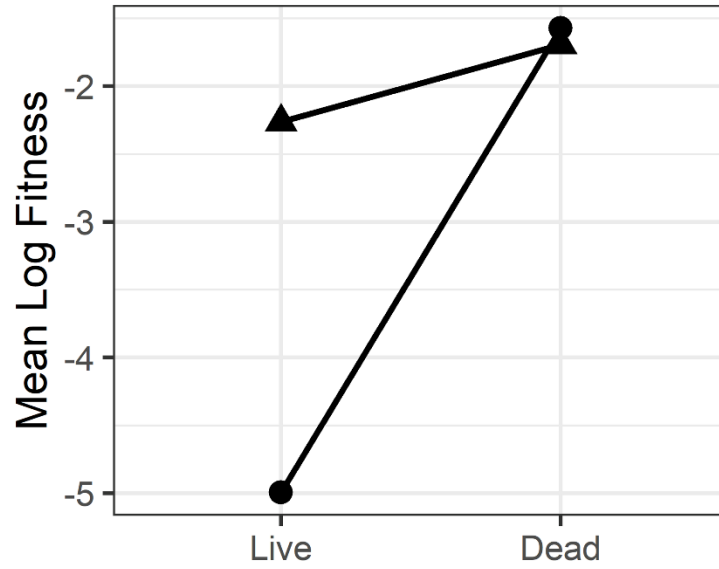


Figure 24

Estimated mean log fitness of macrophages containing live or killed *M. avium*. Phagolysosomal pH data was gathered from literature using either video microscopy (triangles) or confocal microscopy (circles).

Table 2

A list of human pathogens which would commonly be encountered by alveolar macrophages. Inhibitory and optimal pH for each pathogen were acquired from literature where available.

Microorganism	Inhibitory pH	Optimal Growth pH (range, average)	Reference
<i>Acetivobacter baumannii</i>	5	7	154
<i>Bacillus cereus</i>	4.3	6.75	155
<i>Bartonella henselae</i>	<6.6	6.8-7.2 (7.0)	156
<i>Bacteroides fragilis</i>	5	7-7.5 (7.25)	157
<i>Bordetella pertusis</i>	6	7-7.5 (7.25)	158
<i>Brucella spp.</i>	3.5	6.6-7.4 (7.0)	159
<i>E. coli</i>	~4	6-8 (7.0)	160
<i>Campylobacter jejuni</i>	4	6.5-7.5 (7.0)	161
<i>Enterococcus spp.</i>	4.5	7.5	162
<i>Group A Streptococcus</i>	5.5	7.5	163,164
<i>Group B Streptococcus</i>	4.3	7	165
<i>Histoplasma capsulatum</i>	5	6-9 (7)	166
<i>Legionella pneumophila</i>	5	5.5-9.2 (7.35)	167
<i>Listeria monocytogenes</i>	3.3	5.6	168,169
<i>Mycobacterium tuberculosis</i>	6.0	7.0	170
<i>Mycobacterium avium</i>	4.6	6	126,171
<i>Neisseria gonorrhoea</i>	5.8	6.7	172,173
<i>Neisseria meningitidis</i>	6	7.2-9.0 (8.1)	174
<i>Pseudomonas aeruginosa</i>	5.4	6-7.5 (6.75)	175
<i>Salmonella typhimurium</i>	5	7	176
<i>Staphylococcus aureus</i>	4.3	6.5	177

<i>Streptococcus pneumoniae</i>	7.0	7.9	178
<i>Serratia marcesens</i>	3.0	9.0	179,180
<i>Shigella flexneri</i>	5.5	7.5	181
<i>Vibrio cholerae</i>	5.0	8.5	182,183
<i>Yersinia enterocolitica</i>	5.0	N/A	184
<i>Yersinia pestis</i>	5	7.6	185,186

Table 2

Part II: Dragotcytosis

This chapter is published in the Journal of Immunology as “Dragotcytosis: Elucidation of the Mechanism for *Cryptococcus neoformans* Macrophage-to-Macrophage Transfer”

doi:10.4049/jimmunol.1801118

Abstract

Cryptococcus neoformans is capable of a unique and intriguing form of cell-to-cell transfer between murine macrophage cells. The mechanism for cell-to-cell transfer is not understood. Here we imaged macrophages with CellTracker Green CMFDA-labeled cytosol to ascertain whether cytosol was shared between donor and acceptor murine macrophages. Analysis of several transfer events detected no transfer of cytosol from donor to acceptor murine macrophages. However, blocking Fc and complement receptors resulted in a major diminution of cell-to-cell transfer events. The timing cell-to-cell transfer (11.17 min) closely approximated the sum of phagocytosis (4.18 min) and exocytosis (6.71 min) times. We propose that macrophage cell-to-cell transfer represents a non-lytic exocytosis event followed by phagocytosis into a macrophage that is in close proximity and name this process Dragotcytosis (Dragot is a Greek surname meaning ‘Sentinel’) as it represents sharing of a microbe between two sentinel cells of the innate immune system.

Introduction

C. neoformans infects and reproduces inside of macrophages, making the macrophage a key cell in the pathogenesis of cryptococcosis, and the outcome of the *C. neoformans*-macrophage interaction can determine the outcome of the infection^{1,39,92,101,148}. The cryptococcal pathogenic

strategy is remarkable in that it involves fungal cell survival in a mature phagosome and the phenomenon of non-lytic exocytosis (or Vomocytosis), which is characterized by expulsion of the fungal cells from the macrophage with the survival of both cells^{20,104,187}. In addition, *C. neoformans* is capable of being transferred from an infected to a non-infected macrophage^{20,104}. Cell-to-cell transfer is generally believed to be a process different from non-lytic exocytosis, with these two events being referred to as Type III and Type II exocytosis, respectively¹⁸⁸, denoting the fact that all these events share in common the exit of a fungal cell from an infected macrophage. Non-lytic exocytosis has been described in mammalian^{20,104}, fish¹⁸⁹, insect⁶⁹, and amoeba¹⁹⁰ cells and appears to be a highly conserved strategy for *C. neoformans* cells to escape host and environmental predatory phagocytic cells. Non-lytic exocytosis has been described in other pathogenic microbes, including *Burkholderia cenocepacia*¹⁹¹, *Candida albicans*¹⁹, and *Mycobacterium tuberculosis*¹⁹², suggesting that it may be a widespread strategy for microbial escape from phagocytic cells.

Little is known about the mechanism of cell-to-cell transfer, which could facilitate the spread of infection in anatomical sites where macrophages are in close apposition to one another, such as cryptococcal granulomas and infected lymph nodes. Macrophage to endothelial cell transfer of *C. neoformans* was described in blood-brain barrier models⁹⁴. Whether cell-to-cell transfer favors control of infection, or promotes it, it is likely to depend on the circumstances of the host-microbe interaction. For example, transfer of a single fungal cell between two macrophages would appear to be a debit for the host, since *C. neoformans* residence in macrophages is associated with host cell damage¹²⁴ and thus could damage two host cells. Conversely, transfer of fungal cells from a

macrophage infected with many yeasts could help in the control of infection since it would reduce the multiplicity of infection per cell.

C. neoformans cell-to-cell transfer has received relatively little attention, largely because it is difficult to study. We investigated the mechanism of macrophage-to-macrophage transfer of *C. neoformans* cells and found that it involves a coordinated non-lytic exocytosis event from one cell followed by immediate phagocytosis by an adjacent cell. The results implicate non-lytic exocytosis in cell-to-cell transfer.

Materials and Methods

C. neoformans Strain and Culture Conditions

Cryptococcal cultures were prepared by inoculating 10 mL Sabouraud Dextrose Broth [SAB; Becton-Dickenson, Franklin Lakes, NJ] media with a stab of frozen *C. neoformans* var. *grubii* serotype A strain H99 stock. Cultures were incubated at 30 °C shaking at 150 rpm for 2 d before use in infections. Cultures were heat killed by incubating for 1 h at 60 °C in a water bath.

Macrophage culture

BMDM were generated from hind leg bones of 5- to 8-wk-old co-housed C57BL/6 female mice [Jackson Laboratories, Bar Harbor, ME] or Fc receptor knockout (Fcr1g) mice (Taconic model 583) of the same age. For the macrophage differentiation, cells were seeded in 100 mm tissue culture-

treated cell culture dishes [Corning, Corning, NY] in Dulbecco's Modified Eagle medium [Corning] with 20 % L-929 cell-conditioned medium, 10 % FBS (Atlanta Biologicals, Flowery Branch, GA), 2mM Glutamax [Gibco, Gaithersburg MD], 1 % nonessential amino acid [Cellgro], 1 % HEPES buffer [Corning], 1 % penicillin-streptomycin [Corning] and 0.1 % 2-mercaptoethanol [Gibco] for 6-7 d at 37 °C with 9.5 % CO₂. Fresh media in 3 ml were supplemented on day 3 and the medium were replaced on day 6. Differentiated BMDM were used for experiments within 5 days after completed differentiation.

Murine macrophage-like J774.16 cells were maintained in DMEM with 10 % NCTC109 medium [Gibco], 10 % FBS, 1 % nonessential amino acid, 1 % penicillin-streptomycin at 37 °C with 9.5% CO₂. All murine work was done using protocols reviewed and approved by IACUC. All experimental work in this study was done with BMDM except for the high-resolution movie shown in Figure S1, which was filmed using J774.16 cells.

Acquisition of Supplemental Video

J774.16 cells were seeded (5×10^4 cells/well) on poly-D-lysine coated coverslip bottom MatTek petri dishes with 14mm microwell [MatTek Brand Corporation] in medium containing 0.5 µg/ml LPS [Sigma] and 0.02 µg/mL (100 U/ml) IFN γ [Roche]. Cells were then incubated at 37 °C with 9.5 % CO₂ overnight. On the following day, macrophages were infected with cryptococcal cells (1.5×10^5 cells/well) in the presence of 10 µg/ml mAb 18b7. After 2 h incubation to allow phagocytosis, culture was washed five times with fresh medium to remove extracellular cryptococcal cells.

Images were taken every 4 min for 24 h using a Carl Zeiss LSM 780 confocal microscope with a 40 x 1.4 NA Plan Apochromat oil-immersion DIC objective and a spectral GaAsP detector in an enclosed chamber under conditions of 5.0 % CO₂ and 37 °C. Acquisition parameters, shutters and focus were controlled by Zen black software [Carl Zeiss].

Macrophage Infections and Videos for Cytosol Exchange and Inhibitor Trials

BMDMs were seeded (2.5×10^4 cells/well) in MatTek dishes and 24-well plates [Corning]. Cells in one MatTek dish and one well from the 24-well plate were activated overnight (16h) with IFN γ (0.02 μ g/mL) and (0.5 μ g) LPS. Cells in the MatTek dish were stained with CellTracker Green CMFDA [ThermoFisher] according to manufacturer's protocol before infecting with Uvitex 2B (5 μ m/mL ; Polysciences Inc., Warrington, PA) labeled and 18B7 (Generated in lab; 10 μ g/mL) or guinea pig complement (20% ; MilliPore) opsonized *Cryptococcus* at an MOI of 1 for 1 h. Cells from the 24-well plate were labeled with CellMask Orange [ThermoFisher] according to manufacturer's protocol, then raised and seeded over the MatTek dish after washing with 2mL fresh cell media three times to reduce extracellular cryptococcal cells. Inspection of MatTek monolayers immediately after washing and before starting the experiments revealed no extracellular *C. neoformans*. Cells were incubated for 30 additional minutes to allow for adhesion before supplementing the plate with 2 mL fresh cell media. MatTek dishes were then placed under a Zeiss axiovert 200M 10X magnification, incubated at 37 °C and 9.5% CO₂, and imaged every 2 min for a 24 h period. Images were then manually analyzed to identify clear transfer events. For each transfer event donor and acceptor cells were outlined according to cell membranes visible in phase contrast. CellTracker and Uvitex 2B channel intensities were then collected for each pixel

within the cell outline and compared using unpaired two-tailed t tests between pre and post transfer quantifications.

Receptor inhibitor experiments used a single MatTek dish with 5×10^4 macrophages activated overnight with IFN γ (0.02 $\mu\text{g}/\text{mL}$) and LPS (0.5 $\mu\text{g}/\text{mL}$). Cells were infected with *C. neoformans* at an MOI of 1 for 1 h followed by three washes of 2 mL fresh media to reduce extracellular cryptococcal cells. Cells were incubated for 1h with aCD16/32 anti-Fc receptor antibodies (0.5 $\mu\text{g}/\text{mL}$; BD Biosciences 553142) and anti-CD11b antibodies (0.5 $\mu\text{g}/\text{mL}$; BD Biosciences 553308) or Cytochalasin B (2, 4, or 10 μM ; Sigma C6762), or Cytochalasin D (2 or 4 μM ; Sigma C8273) before beginning 24 h imaging under the Zeiss axiovert 200M 10X magnification at 37 °C with 9.5 % CO $_2$ overnight to analyze total cellular exit events.

Fc receptor knockout experiments used a single MatTek dish with 5×10^4 macrophages activated overnight with IFN γ (0.02 $\mu\text{g}/\text{mL}$) and LPS (0.5 $\mu\text{g}/\text{mL}$). Cells were infected with *C. neoformans* at an MOI of 1 for 1 h followed by three washes of 2 mL fresh media to reduce extracellular cryptococcal cells. Cells were then imaged for 24 h under the Zeiss axiovert 200M 10X magnification at 37 °C with 9.5 % CO $_2$ overnight to analyze total cellular exit events. For inhibitor trials, cells were incubated for 1h with CD11b anti-complement antibodies (0.5 $\mu\text{g}/\text{mL}$) before beginning 24 h imaging under the Zeiss axiovert 200M 10X magnification at 37 °C with 9.5 % CO $_2$ overnight to analyze total cellular exit events.

Phagocytosis and non-lytic exocytosis timing experiments were set up as above except using an MOI of 1 for 2 h at 4 °C, then MatTek dishes were placed on the microscope stage, and images were immediately taken every 1 min for 24 h immediately after adding mAb 18B7 (10 µg/mL) directly to the dish.

For experiments in which we explored dye acquisition during exposure to the extracellular environment, BMDMs were seeded in a single MatTek dish with 5×10^4 macrophages activated overnight with IFN γ and LPS. Cells were infected with *C. neoformans* at an MOI of 3 for 1 h followed by three washes of 2 mL fresh media to reduce extracellular cryptococcal cells. Uvitex 2B (50 µm/mL) and 18B7 conjugated to Oregon Green (100 µg/mL) was supplemented to the extracellular media. Cells were then imaged for 24 h under the Zeiss axiovert 200M 10X magnification at 37 °C with 9.5 % CO $_2$ overnight to analyze cryptococcal cell acquisition of each dye.

BMDM mRNA Gene Expression Array

BMDMs were seeded in 6-well dishes at 10^6 cells per well. Cells were activated overnight with IFN γ and LPS. Cells were then treated for 1 h with or without Fc receptor blocking antibody, or harvested before the incubation for a baseline. Cells were lifted from the dishes, pelleted, and resuspended in TRizol reagent [ThermoFisher]. The supernatant was then flash frozen and stored at -80 °C.

Total RNA was extracted using a PureLink RNA minikit (Ambion/Life Technologies) according to the manufacturer's protocol, including on-column DNase treatment. Following elution of purified RNA from the PureLink columns with nuclease-free water, quantitation was performed using a NanoDrop spectrophotometer, and quality assessment was determined by RNA LabChip analysis on an Agilent Bioanalyzer 2100 system or with RNA Screen tape on an Agilent TapeStation 2200 system. One hundred nanograms of total RNA was processed for hybridization to Agilent SurePrint G3 mouse (v2) 8x60K gene expression arrays according to Agilent's one-color microarray-based analysis (low-input QuickAmp labeling) protocol, including cDNA synthesis, cRNA synthesis with Cy3 labeling and purification, fragmentation, hybridization, and post-hybridization washing. Spike-In controls were utilized and processed according to Agilent's one-color RNA Spike-In kit protocol. The arrays were scanned in an Agilent G2600D SureScan microarray scanner using scan protocol AgilentG3_GX_1color. Agilent's Feature Extraction software was used to assign grids, provide raw image files per array, and generate quality control (QC) metric reports from the microarray scan data. The QC metric reports were used for quality assessment of all hybridizations and scans. Txt files from the Feature Extraction software were imported into the Partek Genomics Suite (v7.0; Partek) for detailed analyses of gene expression. Within Partek, the gProcessedSignal was imported and the intensity values were normalized to the 75th percentile, lower expressed genes were filtered out, and log transformation base 2.0 was performed. The batch effect removal tool (analysis of variance [ANOVA]) was used to correct for effects of array (slide). A two-way ANOVA with linear contrasts for treatment (Antibody) and time (1hr) versus the control (No Antibody 1hr or No Antibody 0hr) was performed with outputs of *P* value, fold change, and mean ratio. The cutoff criteria for filtering gene lists were significant *P* values ($P < 0.05$) with the fold changes of greater than 2 or less than -2. Heatmaps were generated from the filtered gene lists,

as well as lists from Venn diagram comparisons. Microarray data has been deposited to the NCBI Gene Expression Omnibus (GEO) repository (GEO dataset # GSE126977) <https://www.ncbi.nlm.nih.gov/geo/query/acc.cgi?acc=GSE126977>.

Quantification of Temporal Kinetics

Each type of event (phagocytosis, non-lytic exocytosis, and cell-to-cell transfer) was given a start and end based on the movie frame when beginning and ending was observed. The total number of frames spanning from start to end were counted to estimate the duration of the event. The start of phagocytosis was defined as the first frame in which a cryptococcal cell was attached to a macrophage cell, no longer free moving through the media. The end of phagocytosis was defined as the first frame in which it is undeniably clear that the cryptococcal cell has been fully engulfed and is no longer touching the plasma membrane. The start of non-lytic exocytosis was defined as the frame immediately prior to a cryptococcal cell within a macrophage moving toward the plasma membrane. The end of non-lytic exocytosis was defined as the frame in which that cryptococcal cell is fully outside of its host macrophage and no longer in contact with the plasma membrane. The start of a cell-to-cell transfer event was defined in the same way as non-lytic exocytosis, that is the frame immediately prior to movement toward the plasma membrane. The end of a cell-to-cell transfer event was defined in the same way as phagocytosis, that is the frame in which the cryptococcal cell is fully engulfed by the acceptor macrophage and is no longer in contact with the plasma membrane.

C. neoformans Inhibition Assay

BMDMs were seeded (1×10^6 cells/well) in 6-well tissue culture treated plates [Corning]. Cells in one MatTek dish and one well from the 24-well plate were activated overnight (16 h) with IFN γ (0.02 $\mu\text{g}/\text{mL}$) and (0.5 μg) LPS. Cells were then infected with *C. neoformans* opsonized with 18B7 (10 $\mu\text{g}/\mu\text{L}$) at MOI 3 and incubated a further 24 h. Wells were washed twice with 1 mL HBSS then lifted with CellStripper and pelleted via centrifugation (350 x g for 10 min). Macrophages were then lysed via resuspension in 500 μL dH $_2\text{O}$ for 10 min. Released *C. neoformans* were then plated on a SAB agar plate in a serial dilution of 8 x 1/3 dilutions. SAB agar plates were incubated at 30 °C for 2 d. To quantify, the smallest dilution with at least 1 colony was identified for each sample. Colony counts were back calculated to the highest common dilution and compared.

Statistics

Statistical differences between dye channels for both cytosolic (CellTracker Green) and cryptococcal (Uvitex 2B) were determined by two-tailed unpaired t-test between cells pre and post transfer. The region of interest was manually defined by the exterior of the host cell plasma membrane via phase contrast channel. Each pixel within the designated region was measured for intensity in its respective channel. Graphs are a depiction of pixel intensity values with bars representing minimum and maximum values. Statistics were calculated on these groups of pixel intensity values. For inhibitor trials significance was calculated using a one-sided test of proportions for each condition compared to the control (18B7 opsonized with no inhibiting antibody treatment).

Results

High Resolution Imaging of Cell-to-Cell Transfer

Cryptococcal cell-to-cell transfer was observed by imaging J774.16 cells infected with *C. neoformans* overnight with phase contrast microscopy (video available in online publication). The coordination apparently involved in this event suggests an underlying mechanism involving both the donor and acceptor cell.

Cytosol Transfer was not Detected During Cryptococcal Transfer

To determine whether cytosol was transferred from donor to acceptor cell along with *Cryptococcus* cells during fungal macrophage-to-macrophage cell transfer, we visualized transfer events in which only the donor cell was stained with a permanent cytosolic dye in BMDMs. BMDMs were used in this and all proceeding experiments described in this manuscript. Upon identifying a transfer event the microscopic images were isolated before, during, and after the transfer event (Figure 25). This experiment was repeated until ten independent events were identified, and the individual fluorescent channels were quantified at each frame before and after Cryptococcal cell transfer. We ensured donor (positive) and acceptor (negative) cell populations were distinguishable by cytoplasmic stain intensity, even at the upper dynamic range of the assay (Figure 26). We found that cytosolic dye signal remained constant in the donor (Figure 27A) and was not observable above background in the acceptor (Figure 2B) cell throughout the event. However, fluorescence intensity corresponding to cryptococcal cells decreased in the donor cell

(Figure 27C) and increased in the acceptor cell (Figure 27D) after transfer. This analysis was repeated for every event. Taken together these data showed no evidence that host cell cytosol was transferred during cryptococcal cell-to-cell transfer. Additionally, we performed experiments supplemented with a plasma membrane stain (CellMask Orange; ThermoFisher) and identified two transfer events. There was no intensity difference between plasma membrane staining before and after transfer, suggesting that there is no mixing between donor and acceptor cell plasma membranes during transfer events (Figure 28).

Cell-to-Cell Transfer Requires FcR and/or Complement Receptor

No cytosolic dye transfer between macrophages during transfer events suggests two hypotheses:

1. Cryptococcal cells are transferred via coordinated exocytosis followed by phagocytosis between the two macrophages; or
2. Only the phagosome is directly transferred between macrophages in a manner that excludes cytosol. Given that the *C. neoformans* capsule prevents phagocytosis^{193,194}, that opsonin is required for ingestion¹⁹⁵, and that capsule-associated antibody is present after exocytosis¹⁹⁶, we designed experiments to test the first hypothesis. Specifically, we investigated whether cell-to-cell transfer was blocked by the addition of an anti-CD16/32 monoclonal antibody, which prevents FcR function, in BMDMs. Transfer events were drastically reduced by blocking the FcR but interestingly, occasional cell transfer events were still observed. Additionally, lytic and non-lytic exocytosis events were both unexpectedly reduced in anti-CD16/32 incubated BMDMs compared to control. It is known that opsonized cryptococcal cells can be phagocytosed via complement receptor by a mechanism where antibody modifies the capsule and allows direct interaction with this receptor in the absence of complement¹⁹⁷. To

investigate whether this was the case, the experiments were repeated with complement inhibiting antibody (anti-CD11b) and both inhibiting antibodies. The frequency of cell-to-cell transfer was significantly reduced compared to control when each of the FcR and CR were inhibited and completely abrogated when both were inhibited together, with $P < 0.01$, 0.05 , and 0.001 , respectively (Figure 29A, Table 3).

To investigate whether the reduction in observed effects was a consequence of antibody incubation we extracted RNA from BMDMs incubated with or without the Fc receptor blocking antibody and analyzed mRNA gene expression levels between the cells. We found that no genes were significantly differentially regulated with an FDR threshold of 0.05 , and only 10 uniquely significantly differentially regulated genes when the cutoff was loosened to an unadjusted P value < 0.05 (Table 4). The data suggests incubation of BMDMs with receptor blocking antibodies had no significant effect on the transcriptional profile relative to cells and thus the reduction in transfer events measured is not likely to be due to an effect of the antibody itself on the host macrophage.

To further explore this phenomenon, we infected BMDMs harvested from Fc receptor knockout mice (Fcer1g) opsonized with 18B7 antibody. We found that Fcer1g BMDMs experienced cell-to-cell transfer significantly less than the control, $P < 0.01$, and at a similar rate as wild-type cells incubated with the anti-FcR antibody (Figure 29A, Table 3). These data suggested that both Fc and complement receptor mediated phagocytosis can be utilized in cell-to-cell transfer.

We hypothesized that the initial phagocytic event may have downstream effects on whether Cryptococcal cells can undergo cell-to-cell transfer. To explore a potential effect of complement mediated phagocytosis, we repeated these experiments with guinea pig complement opsonized *C. neoformans* on wild type BMDMs. We found that BMDMs which had ingested *C. neoformans* via complement experienced abrogated cell-to-cell transfer compared to control and in frequencies similar to both wild-type BMDMs inhibited with anti-FcR antibodies and Fcγ1g BMDMs with no inhibiting antibodies (Figure 29A, Table 3).

Finally, we also performed experiments supplemented with cytochalasin B, an actin inhibitor, reasoning that actin activity is required for exocytosis. We observed no transfer events, with $P < 0.001$ compared to control, further supporting the idea that transfer relies on exocytosis events (Figure 29A, Table 3). Interestingly, previous reports suggested that transfer events were inhibited¹⁰⁴ but non-lytic exocytosis events were present¹⁰² or even increased¹⁸⁷ with cytochalasin D treatment at low concentrations, 4 μM and 2 μM in J774 cells. In both cases, however, this was simply a noted observation without in depth experimental analysis. Additionally, in these cases non-lytic exocytosis events were observed almost immediately after adding cytochalasin D, 3-5 min, whereas our experiments included a 1 h incubation with cytochalasin B before starting image acquisition. Additionally, these experiments used different host cells and/or *C. neoformans* strains. We therefore sought to replicate these experimental conditions utilizing our primary BMDM cells. Surprisingly, treating BMDMs with 4 μM cytochalasin D resulted in the formation of extremely large, bulbous, vacuole-like organelles around cryptococcal cells (Figure 30). These

formations would sometimes rupture, leading to lysis of the host macrophage. Regardless, we observed neither transfer events nor non-lytic exocytosis events and given these results, we favored the first hypothesis as the continued presence of a phagosome around the cryptococcal cell would block antibody-receptor interactions.

C. neoformans Cells Must be Alive for Cell-to-Cell Transfer

To determine whether macrophage-to-macrophage transfer is an active process on the part of *C. neoformans*, we infected BMDMs with heat killed *C. neoformans* yeasts opsonized with 18B7. We found no examples of lytic exocytosis, non-lytic exocytosis, or cell-to-cell transfer events when macrophages were infected with heat killed *C. neoformans* (Figure 29A, Table 3). Additionally, when macrophages were infected with heat killed *C. neoformans* and treated with cytochalasin D we did not observe the above described bulbous vacuole-like organelle development.

Temporal Kinetics of Cell-to-Cell Transfer

If Cryptococcal cells are transferred via exocytosis followed by phagocytosis it would follow that the total time of transfer events should resemble the length of exocytosis plus the length of phagocytosis. Cell-to-cell transfer time was estimated by counting the total number of frames immediately prior to immediately after transfer, as each frame represented a set number of minutes progression in time. Each image was taken at two-minute intervals, and so the total time of transfer was directly calculated by the number of frames. We found that the median and mean transfer times were 11 and 11.17 minutes, respectively, from twelve total analyzed events (Figure

29B). To our knowledge the timing of neither phagocytosis nor non-lytic exocytosis of *C. neoformans* by BMDMs has been previously carefully measured. To investigate whether the timing of cell-to-cell transfer matched the times of exocytosis and phagocytosis, we visualized phagocytosis by repeating the infection movie protocol but only adding opsonizing antibody immediately before starting image acquisition. We observed phagocytic events and counted the number of frames (taken each minute) to determine an experimental estimate of phagocytosis ingestion time. Based on eleven observed phagocytic events we determined ingestion occurred over approximately 4.18 minutes (Figure 29B). We then timed non-lytic exocytosis events. Based on seven observed non-lytic exocytosis events we determined a total expulsion time of approximately 6.71 minutes (Figure 29B). Adding the time required for non-lytic exocytosis (6.71 minutes) to that required for phagocytosis (4.18 minutes) yielded 10.9 minutes, which is tantalizingly close to the measured average time of 11.17 minutes for cell-to-cell transfer, $P > 0.05$ (Figure 29C). Our measured time for cell-to-cell transfer is close to the 10 minutes reported in the initial description of this phenomenon²⁰. In fact, the relatively short time involved in cell-to-cell transfer precluded us from using either the cell wall dye (Uvitex 2B) or fluorophore conjugated antibody in to stain *C. neoformans* cells during the brief time that they would presumably be exposed to cytoplasm in an exocytosis-phagocytosis event. The time needed for either Uvitex or antibody cellular staining exceeded the longest observed time for cell-to-cell transfer, requiring an average time of 30 and 65 minutes to gain appreciable signal, respectively (Figure 31). However, we made the interesting observation that incubation of macrophages containing ingested *C. neoformans* led to Uvitex staining of yeast cells in some phagosomes, particularly larger ones containing multiple yeast cells (Figure 32). Whether this reflects some mechanism for

leakage of Uvitex into cells or dye transport into the phagosome in a mechanism involving pinocytosis and delivery to phagosome¹⁹⁸, this observation may be worthy of future study.

Additionally, we investigated the amount of time required post-infection for transfer events to start occurring. We found that cell-to-cell transfer events predominantly occur within the first 9 hours of the experiment, with an average initiation time of approximately 6.7 h (Figure 29D).

Host Macrophages Establish Contact Before Transfer

It was previously reported that host macrophage membranes contact each other before cryptococcal cell-to-cell transfer^{104,188}. We investigated this further by investigating each of 38 transfer events for whether the donor and acceptor macrophages appeared to establish membrane contact before transfer. We found that in every situation the donor and acceptor cells came in close proximity at least two minutes (one frame) prior to transfer, remained in contact during transfer, and maintained contact for a short time after transfer as well (Figure 33).

A Model for Macrophage-to-Macrophage Cellular Transfer

Our results indicate that cell-to-cell transfer is a coordinated process between two macrophages, that it does not involve the transfer of cytosol (e.g. Trogocytosis), and that it does not occur when the opsonic Fc and complement receptors are blocked. The time required for cell-to-cell transfer closely approximates addition of the times required for non-lytic exocytosis and ingestion.

Although no single observation provides a mechanism, when our results are considered in combination, the most parsimonious interpretation is that *C. neoformans* cell-to-cell transfer results from sequential non-lytic exocytosis events followed by subsequent phagocytosis of expelled yeast cells by an adjacent macrophage. (Figure 34).

Blockading Fc and Complement Receptors Leads to Increased C. neoformans Intracellular Inhibition

To investigate the potential physiological relevance of this phenomenon, we decided to quantify and compare the ability of receptor blocked BMDMs to kill ingested *C. neoformans*. BMDMs were seeded, activated, and infected for a 24 h interval supplemented with Fc receptor inhibitory antibodies, both Fc and C receptor inhibitory antibodies, or simply additional cell media. When surviving intracellular *C. neoformans* were quantified we found reduced numbers of viable *C. neoformans* cells when BMDMs were incubated with either Fc or Fc and C receptor inhibitory antibodies (Figure 35). These data support the hypothesis that cryptococcal macrophage-to-macrophage favors pathogen survival and spread.

Discussion

Cell-to-cell transfer was described simultaneously by two independent groups, including our own, in 2007^{20,104}. Both groups noted that donor and acceptor cells established contact and that actin was involved at the membrane interface between macrophages. There was speculation about membrane fusion as a preliminary step in cell-to-cell transfer, but this was never experimentally

established. Little progress has been made in unraveling the mechanism primarily because cell-to-cell transfer events are relatively rare, occurring sporadically and unpredictably. In fact, the mechanism by which a fungal cell transfers between intact macrophages has been difficult to envision given that it would involve a yeast cell in a membrane-bound phagosome crossing two plasma membranes.

We considered several hypotheses for the mechanism of cryptococcal cell-to-cell transfer. Initially we were intrigued by the possibility that transfer occurred via Trophocytosis, a cellular communication process in which cytosol and surface proteins are shared between macrophages¹⁹⁹. Trophocytosis was previously shown to be a mechanism that intracellular pathogens can utilize and promote to spread between macrophage cells²⁰⁰. However, when we labeled the cytosol of cryptococcus-infected macrophages we detected no cytosol transfer from donor to acceptor cell during cryptococcal transfer. It should be noted that the shift in Uvitex 2B signal is immediately apparent despite the Uvitex 2B positive population (corresponding to the cryptococcal cell) accounting for a particularly small subset of the entire region of interest. Therefore, even a small amount of dye transferred to the donor cell would noticeably shift the distribution post-transfer. Similarly, we detected no transfer of plasma membrane between macrophages in the experiments supplemented with membrane dye. Obviously, one cannot rule out that an iota of cytosol transferred since that would involve proving a negative, but the absence of any signal indicating cytosol transfer is strong evidence against a mechanism involving a cell-to-cell channel or bridge where donor and acceptor cytoplasm contact. These experiments essentially rule out Trophocytosis as the mechanism of cryptococcal cell-to-cell transfer.

Next, we investigated whether cell-to-cell transfer was a non-lytic exocytosis event followed by ingestion of the expelled yeast by a proximal macrophage. Supporting this hypothesis was the observation that expelled yeast cells have residual opsonizing antibody bound to their capsule even after phagosomal residence, which could support subsequent phagocytosis¹⁹⁶. When both Fc receptor and complement receptor were blocked no transfer events were observed. Although our conditions did not contain complement-derived opsonin, antibody binding to *C. neoformans* capsule results in structural changes that allow complement-independent phagocytosis via complement receptor¹⁹⁷. The measured length of transfer also supports the exocytosis-phagocytosis hypothesis. We determined the average length of non-lytic exocytosis events to be approximately 7 min, consistent with the prior reported 4-12 min²⁰¹. Macrophage phagocytosis of *C. neoformans* took approximately 4 min. Last, we found that complete transfer required approximately 11 min, close to the time required for both phagocytosis and non-lytic exocytosis of *C. neoformans*. These observations imply that cell-to-cell transfer is a sequential non-lytic exocytosis event followed by immediate phagocytosis by a nearby macrophage.

When macrophages were incubated with FcR and CR blocking antibodies non-lytic exocytosis events were reduced, but not completely abrogated, compared to controls. This finding suggests that receptor blocking also affects exocytosis, raising the possibility that reduced transfer in the presence of blocking antibody is a consequence of fewer potential donor cells. Consequently, we performed a microarray experiment comparing the transcriptome of macrophages treated with blocking antibody to a control population and were unable to detect significant differences. In

addition, we analyzed cell-to-cell transfer using FcR knockout mice macrophages. As previously noted, opsonizing *C. neoformans* with 18B7 allows phagocytosis via CR so these macrophages can still be infected are unable to undergo cell-to-cell transfer via FcR. As hypothesized, transfer events in FcR knockout mice were reduced to levels similar to macrophages inhibited via FcR blocking antibody, while lytic and non-lytic events were not significantly reduced compared to wild type macrophages.

Based on the incomplete inhibition of transfer events with only FcR inhibited, we decided to investigate the contribution of CR, hypothesizing that it could be an alternative, less efficient cell-to-cell transfer route. Wild-type macrophages infected with guinea pig complement opsonized *C. neoformans* experienced transfer rates similar to wild-type macrophages inhibited with anti-FcR antibody and macrophages from FcR knockout mice, while neither lytic nor non-lytic exocytosis events were significantly reduced compared to control. These data support our overall hypothesis that transfer is a coordinated event of non-lytic exocytosis followed by phagocytosis. Transfer can be achieved through either FcR or CR mediated phagocytosis, though FcR mediated phagocytosis is more efficient and common.

To determine if inhibiting actin polymerization affects transfer frequency, we repeated these experiments with cytochalasin-treated macrophages. We hypothesized that if actin was required to expel cryptococcal cells, then its inhibition would result in fewer transfers. Our data supported this hypothesis but differs from a previous report¹⁸⁷ in which transfer increased after cytochalasin treatment. We tried to reproduce those findings and were unable to identify the source of the

discrepancy, although it is possibly due to the use of different types of host cells. Finally, we attempted to show that fungal cells enter the extracellular environment by adding dyes (Uvitex 2B and antibody conjugated fluorophore) to the media. Unfortunately, the time required for yeasts to acquire staining was longer than the length of transfer. Additionally, Uvitex 2B permeated certain macrophages, yielding stained *C. neoformans* cells which never exited their host cell.

A coordinated exocytosis-phagocytosis mechanism allows us to discard more complex explanations. For example, the publications which discovered cryptococcal cell-to-cell transfer hypothesized that direct “cell-to-cell bridges” formed through merging and subsequent unmerging of host cell membranes, allowing direct transfer of the cryptococcus containing organelle. This explanation was suggested without experimental data and does not explain our results as inhibition of antibody receptors should not inhibit the direct transfer of an organelle. If cryptococcal cells were retained in the phagosome throughout the transfer process, then the phagosomal membrane would separate the opsonized yeast from contact with FcR and CR on the acceptor cell surface. Another hypothesis was that cryptococcal cells are transferred via membrane tunnel structures between macrophages. A tunnel transfer explanation is unlikely given that tunnels were absent from our microscopy analysis. In fact, when tunnels form they are too small for even cytosolic molecules to traverse²⁰². In any case, a tunnel is also ruled out by the fact that transfer was abrogated by blocking cell surface opsonic receptors. Finally, due to the roles of FcR and CR in immune synapse formation, we contemplated the possibility of cryptococcal transfer between macrophages via some type of uncharacterized, macrophage specific immune

synapse but concluded this is also unlikely with respect to the data. Immune synapses allow only small molecules and dyes to directly transfer. Particles larger than 32 nm are entirely excluded²⁰³, which also excludes *C. neoformans*.

We have termed the exocytosis-phagocytosis phenomenon Dragocytosis, to denote that this is a transfer between two sentinel (Greek 'Dragot') phagocytic cells. The coupled exocytosis-phagocytosis phenomenon is a new process in microbe-macrophage interactions and warrants a new name to distinguish it from other mechanisms of cell entrance or exit, such as: Trogocytosis, non-lytic exocytosis, and phagocytosis. Dragocytosis differs from other mechanisms of cell to cell transfer mainly in that it involves the complete expulsion of yeast cells from one macrophage before engulfment by another. Furthermore, Dragocytosis differs from a simple sequence of exocytosis and phagocytosis in that the donor and acceptor cell are in physical contact before the event occurs and remain in contact through the process. Whether cell contact is involved in triggering exocytosis is an important question for future studies. Dragocytosis is anticipated to occur in other pathogenic microbes capable of triggering exocytosis such as *Candida albicans*¹⁹, *Mycobacteria tuberculosis*²⁰¹, *Serratia marcescens*²⁰⁴, provided opsonins are available.

The experiments here do not directly address the biological significance of Dragocytosis. In fact, designing an experiment to assess biological significance by interfering with Dragocytosis then measuring an outcome related to cryptococcal infection is not possible without introducing a variety of downstream changes that would raise serious doubts about any association between measured effects on virulence and this process. To interfere with Dragocytosis *in vivo* would

require preventing either phagocytosis or non-lytic exocytosis and such interference would have important secondary effects on host defense and intracellular pathogenesis, respectively. Instead, we argue for the significance of this effect from logical inference and deduction. Phagocytosis is a fundamental cellular host defense mechanism that occurs *in vivo* during cryptococcal infection, evident from the intracellular residence of cryptococci during infection^{1,101}. Non-lytic exocytosis is a complex cellular process shown to occur during cryptococcal infection in mice, zebra fish, and amoeba^{7,70,190}. Hence, both phagocytosis and non-lytic exocytosis occur both *in vivo* and *in vitro*^{70,101}. During cryptococcal infection, yeast reside in granulomatous inflammation where the cellular density of macrophages is much greater than the *in vitro* conditions where Dragocytosis was shown to occur in this study¹⁰¹. Given the occurrence of its component processes of phagocytosis and non-lytic exocytosis *in vivo* and that *C. neoformans* often resides in granulomas where macrophages exist in close apposition, it is likely that Dragocytosis occurs *in vivo*.

Dragocytosis may result in an overall benefit to *C. neoformans* rather than the host. After infecting BMDMs with *C. neoformans*, we found that inhibiting Dragocytosis through blockading FcR and CR reduced *C. neoformans* viability. This suggests that the ability of *C. neoformans* to freely move between macrophages is advantageous to the yeast. We considered the possibility that addition of blocking antibodies was activating the macrophages in some way to enhance their antifungal activity but found no evidence that receptor blockage affected transcriptional responses. We know *C. neoformans* can reside in macrophages for hours, if not days, and it is possible that antifungal effects in phagolysosomes take time to be effective in inhibiting fungal replication. Hence, moving to a younger phagolysosome by Dragocytosis could benefit fungal

cells. We confirmed that *C. neoformans* viability is essential for non-lytic exocytosis and Dragotcytosis. We recognize that if inhibition of Dragotcytosis enhances antifungal activity, and that fungal viability is needed for exocytosis, the latter alone could reduce the frequency of Dragotcytosis. However, we note non-lytic exocytosis occurs relatively early (< 4 h) in macrophage infection¹⁸⁸ while the commencement of intracellular budding occurs later, peaking at 6-10 h¹³. Indeed, we observed the initiation of Dragotcytosis events early in macrophage infection as well (approximately 6.7 h). Hence, although we cannot fully separate reduction in Dragotcytosis by receptor blocking from enhanced inhibition of *C. neoformans* in macrophages where the fungal cell cannot escape, the available data favors a temporal sequence where inhibition of Dragotcytosis is followed by inhibition of fungal replication.

In summary, three lines of evidence strongly suggest that Dragotcytosis represents sequential exocytosis-phagocytosis events: 1) we observed no cytosol transfer from donor to receptor cell; 2) the frequency of transfer events was greatly reduced by interference with phagocytic receptors; and 3) the time involved in Dragotcytosis was indistinguishable from the sum of the times involved in exocytosis and phagocytosis. The implications of Dragotcytosis for pathogenesis and host defense are uncertain and may vary with infection setting. Antibody administration can protect mice against cryptococcal infection²⁰⁵. Comparative analysis of infected tissues of antibody-treated and control mice shows that presence of antibody is associated with increased *C. neoformans* intracellular residence in macrophages²⁰⁶, which was interpreted as reflecting more efficient antibody-mediated phagocytosis. However, our results suggest that Dragotcytosis could contribute to this effect since fungal cells experiencing non-lytic exocytosis in granulomas

could be rapidly ingested by proximal macrophages, perpetuating intracellular residence. The dependence on phagocytic receptors and opsonins has the interesting implication that Dragocytosis may be more frequent in hosts with robust antibody responses. Since non-lytic exocytosis has been described with several other pathogens, Dragocytosis could theoretically occur in other infections. Whether Dragocytosis benefits the host by promoting re-ingestion of expelled cells or harms the host by promoting new cellular infections capable of disseminating in a Trojan Horse manner is not known and probably depends on the circumstances when it occurs. Future research into Dragocytosis should focus on elucidating the factors that control the frequency of transfer and the macrophage and/or fungal signals that trigger this process.

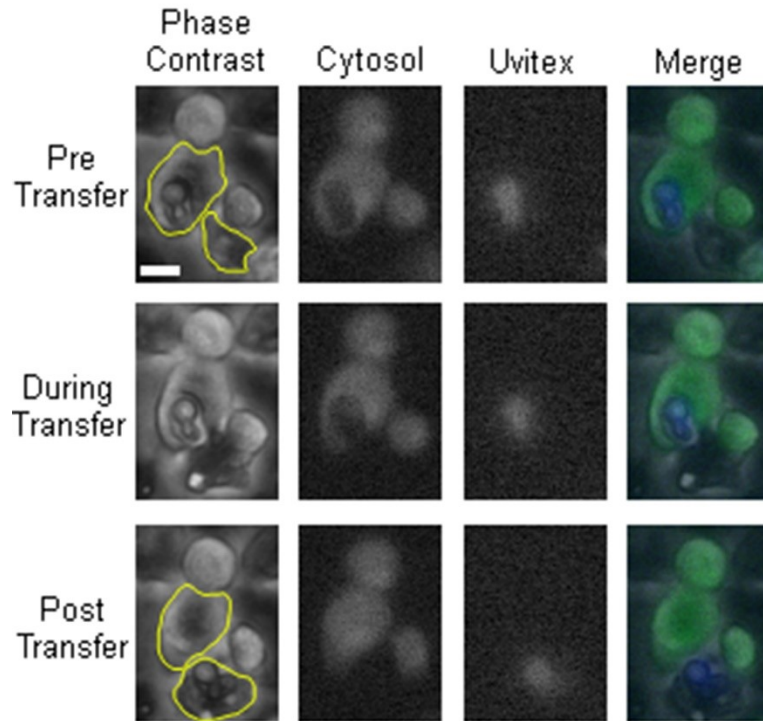


Figure 25

Dragocytosis event captured via fluorescent microscopy. Representative frames before (Pre), during, and after (Post) cryptococcal transfer. 10X Phase Contrast, Cytosolic CellTracker Green CMFDA (Green), Uvitex (Blue), and merged channels. The Scale bar represents 10 μm and is constant for all images. Pre, During, and Post Transfer images were obtained from movie frames 266, 274, and 278, respectively. Representative regions of interest have been outlined (yellow) to demonstrate areas analyzed for fluorescence. These images are from Event 4 in subsequent graphs.

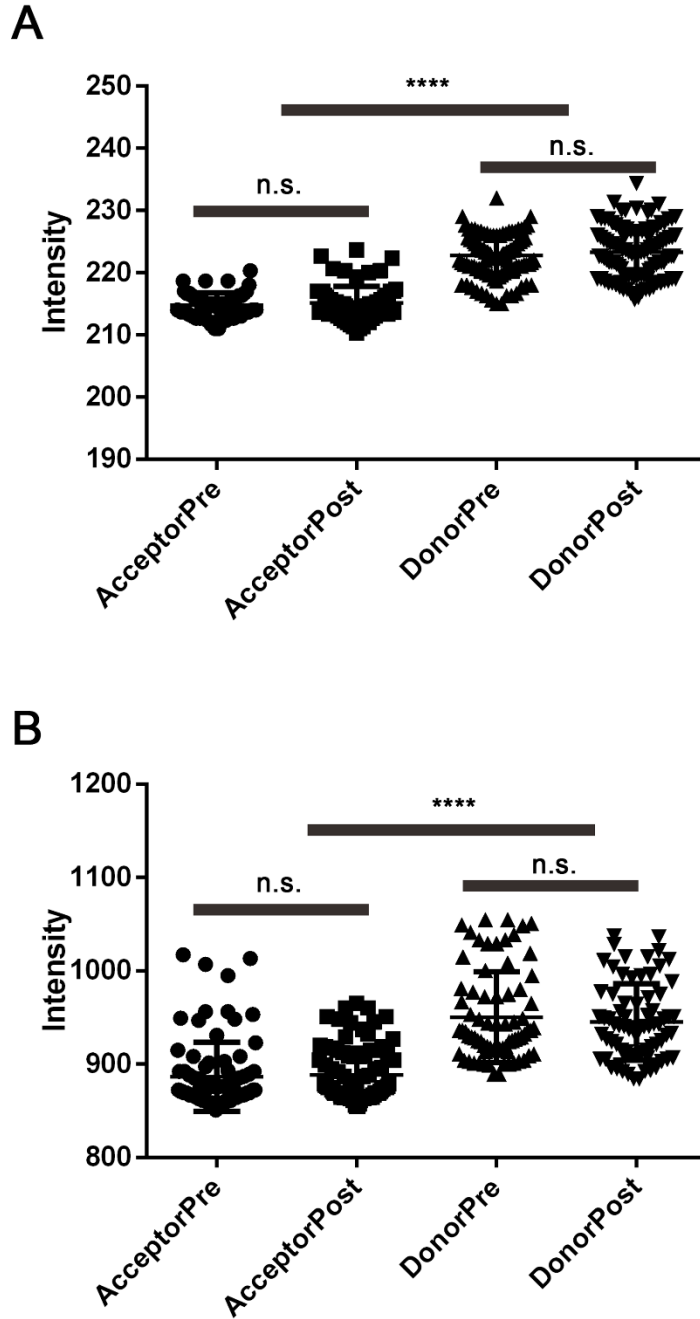


Figure 26

Visualization of cytoplasmic stain intensities for donor and acceptor cells pre and post cryptococcal transfer. **A.** Event 2 and **B.** Event 1. In each event the donor (positive) and acceptor (negative) cells are distinguishable from each other ($P < 0.0001$) but differences are not observed within cells post transfer. This difference is distinguishable even in Event 1 which was in the upper dynamic range of the stain. P values were calculated via unpaired two tailed t-test.

Figure 27

Quantifications of stains from Dragotcytosis events in biological replicates. **A.** Donor cell cytosol as measured by CellTracker Green CMFDA intensity before (blue) and after (red) transfer. **B.** Acceptor cell cytosol as measured by CellTracker Green CMFDA intensity before and after transfer. Intensity values remain at background levels in each replicate. **C.** Presence of cryptococcal cell inside Donor cell measured as Uvitex intensity before and after transfer. **D.** Presence of cryptococcal cell inside Acceptor cell measured as Uvitex intensity before and after transfer. Significance was determined by unpaired two tailed t-test with (****) representing $P < 0.0001$, (***) representing $P < 0.001$, and (**) representing $P < 0.01$. Data for each population is each individual pixel intensity measurement, with bars representing minimum-maximum spans in box-whisker format. Density (pixel intensity frequency) histograms represent pixel population data specifically for Event 4 with solid colored rectangles representing mean +/- standard error. Data for each event consists of intensity measurements from each pixel within the acceptor or donor cell. The relative fluorescence of Event 1 is higher than the other events because that measurement came from the initial experiment before dyes were titrated for optimization. Each of these events corresponds to a single event in which a single yeast is transferred from one macrophage to another with the exception of event 8 which spans two individual transfer events in which one yeast cell is transferred during each event. This was due to the necessity of acquiring clear frames for quantification.

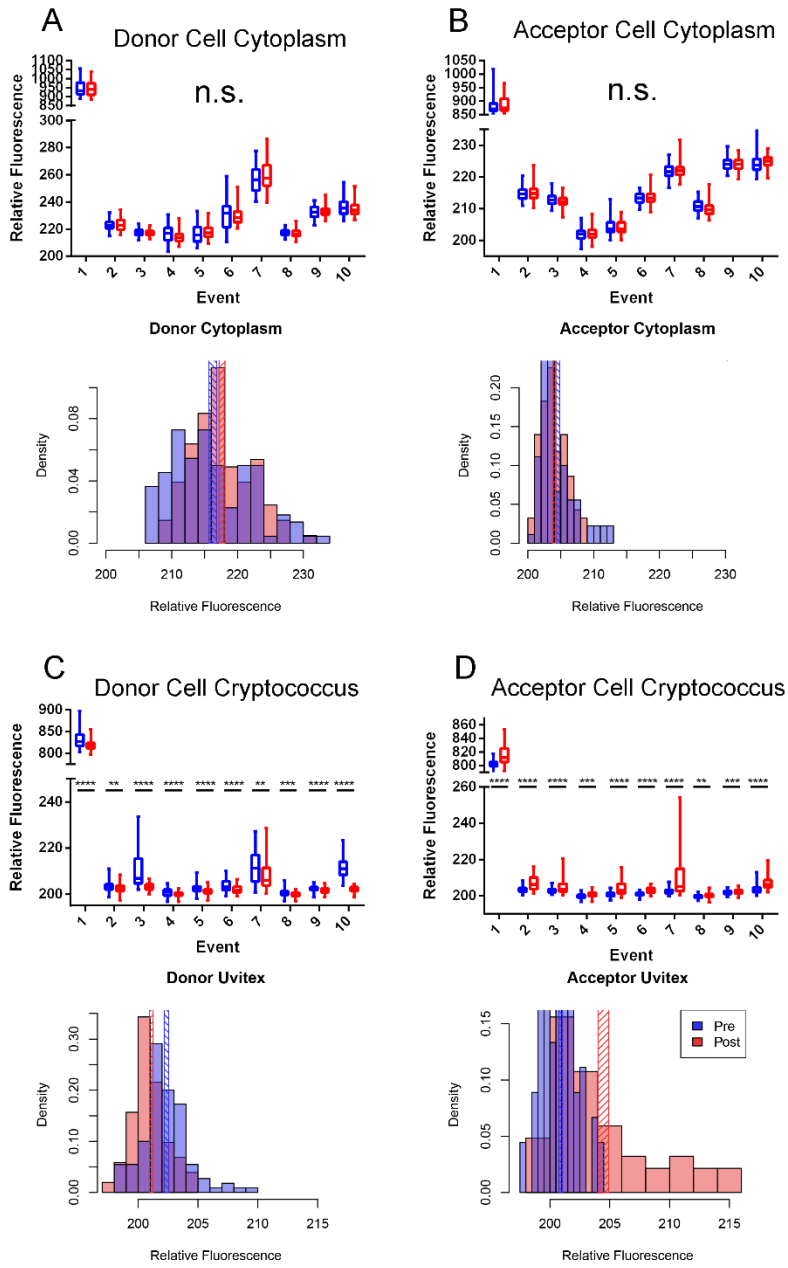
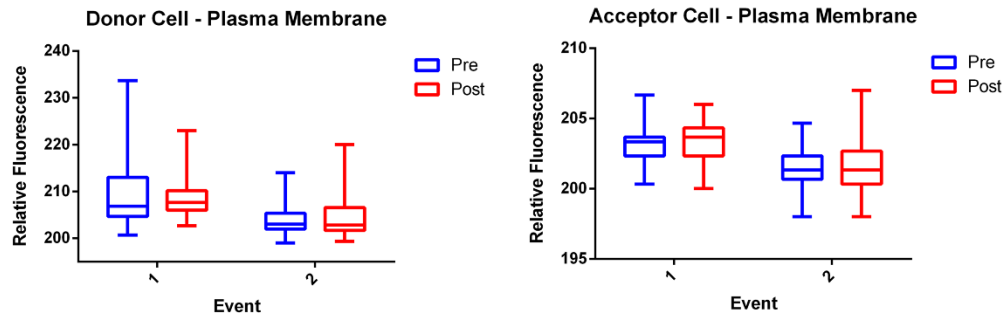
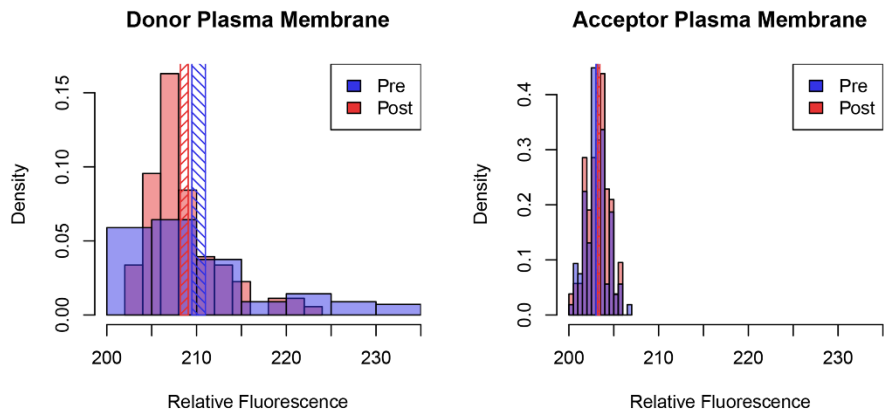


Figure 27



Event 1



Event 2

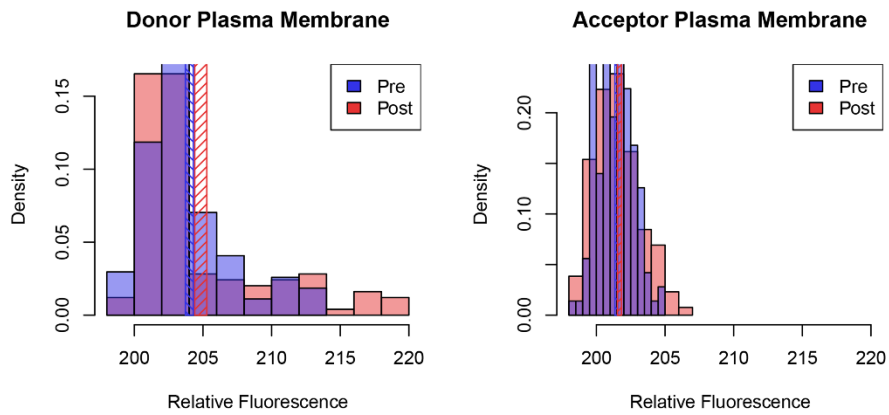


Figure 28

Quantification of a plasma membrane marker before and after transfer events for donor and acceptor macrophages.

Figure 29

Inhibition and timing of transfer events supports exocytosis-phagocytosis hypothesis. **A.** Quantification of the frequency of transfer events observed between BMDMs supplemented with different inhibitor antibody combinations. Frequency values represent frequency of events based on number of events in all infected cells, with complete information found in Table I. P values calculated via one tailed proportion test. **B.** Quantification of the total timespan of each transfer event as well as phagocytosis ingestion time determined by total frames captured. **C.** Quantification of the total timespan of transfer events compared to the addition of phagocytosis and exocytosis events. Data points represent population average with bars representing population standard deviations. P value calculated as non-significant via unpaired two tailed t-test. **D.** Timespan between the start of an experiment and the initial frame of transfer events. Events began at 392 min post infection (SD +/- 395 min) with most events occurring before 9 h.

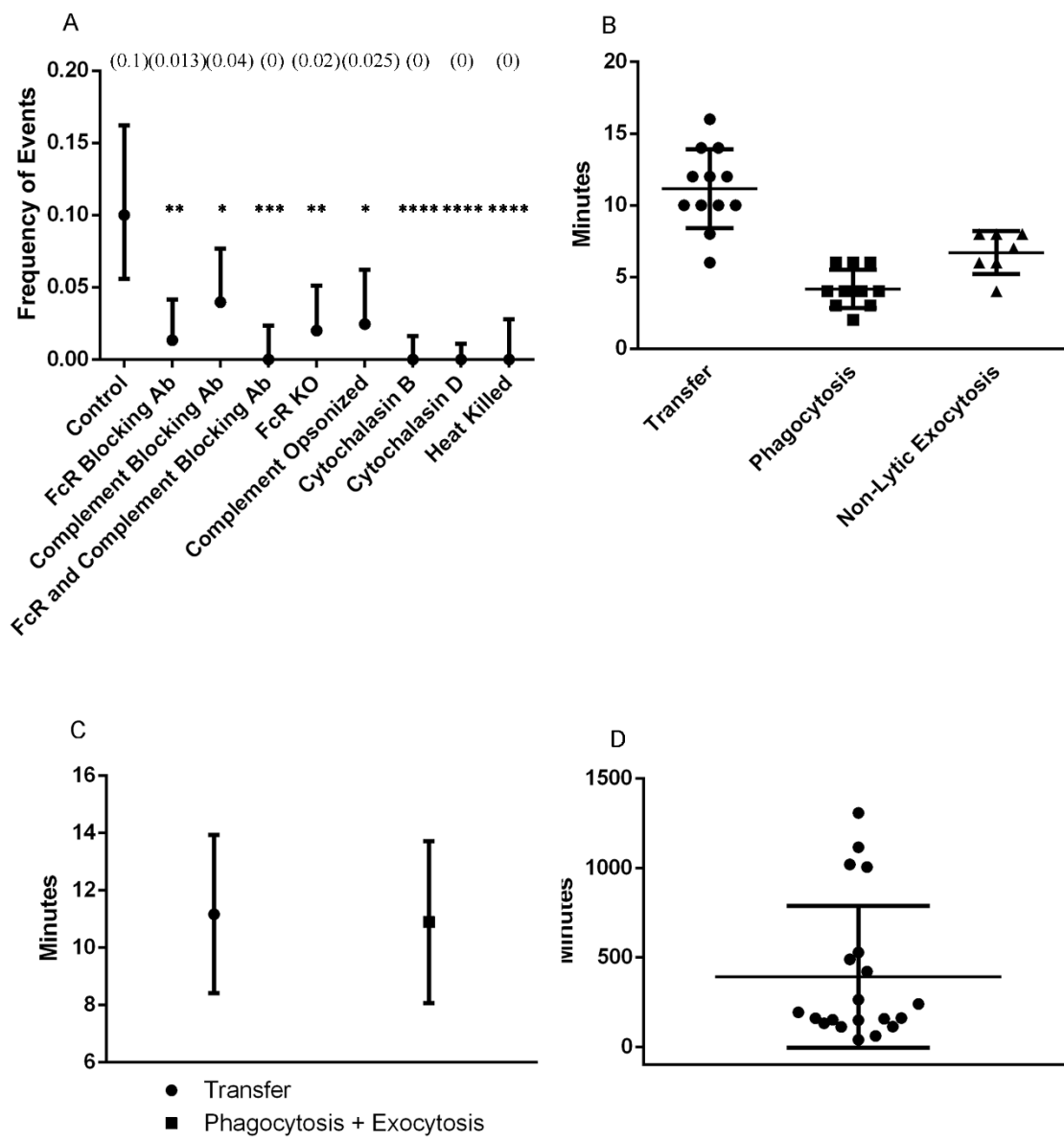


Figure 29

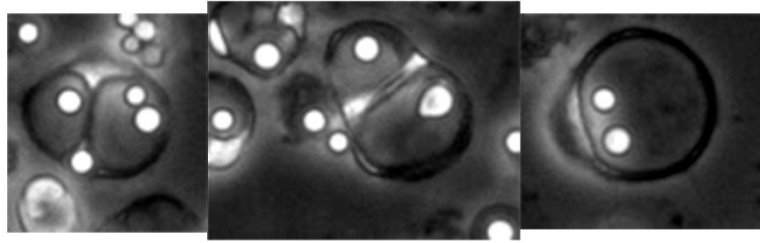


Figure 30

Examples of irregular BMDM cell morphology when incubated with cytochalasin D.

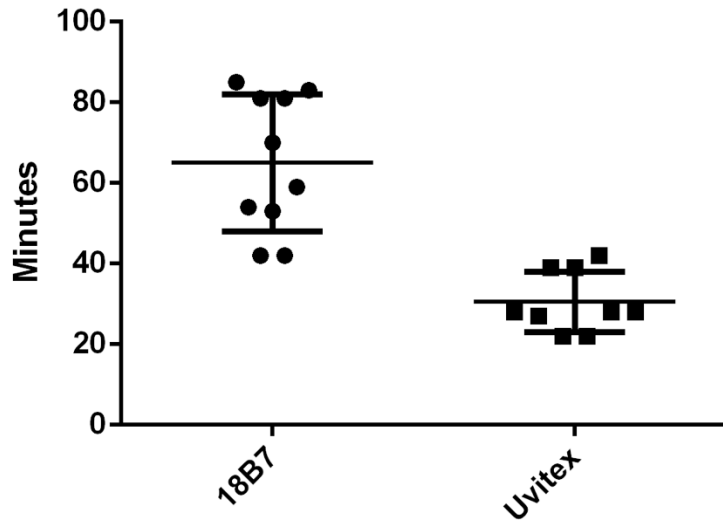


Figure 31

Temporal dynamics of dye acquisition for Uvitex 2B and 18B7-Oregon Green in BMDM ingested *C. neoformans*. Quantification of the amount of time, in minutes, required for a cryptococcal cell to be exposed to the extracellular environment in order to acquire a clear dye signal for 18B7-Oregon Green (65 min) and Uvitex 2B (30 min).

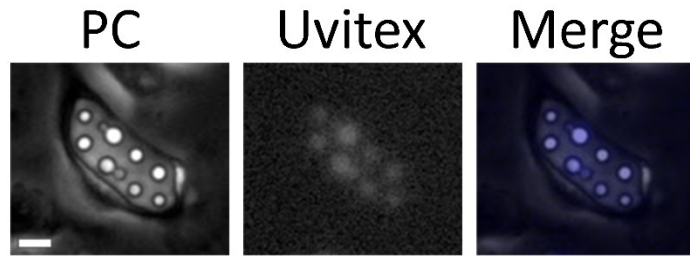


Figure 32

Phagolysosome containing many *C. neoformans* cells that has begun to acquire Uvitex staining before being expelled from their host cell. (PC) Phase Contrast, (Uvitex) Uvitex 2B, and (Merge) false color channel merged images are shown. Scale bar represents 10 μm and is consistent for each image.

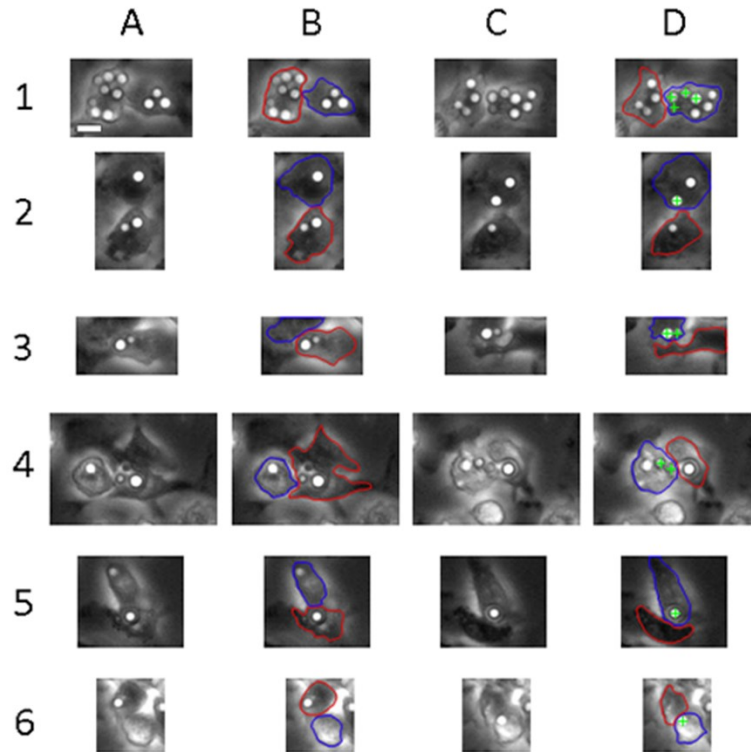


Figure 33

Visualization of donor and acceptor macrophages immediately pre- and post-transfer events. **A.** Initial image of donor and acceptor cells immediately prior to transfer. **B.** Initial image pre-transfer with donor (red) and acceptor (blue) cells outlined. **C.** Initial image of donor and acceptor cells immediately after transfer. **D.** Initial image post-transfer with donor (red), acceptor (blue), and transferred crypto (green cross) cells noted. Scale bar represents 10 μm and is consistent throughout images.

Figure 34

Proposed overarching model of cryptococcal cell-to-cell transfer. **A.** The initial step in transfer, and the point which was defined as the start of exocytosis. The moment when a phagosome (white space) containing an opsonized cryptococcal cell begins to move toward the plasma membrane of the donor macrophage. The phagosome reaches and merges with the plasma membrane of the donor macrophage in a manner which expels the cryptococcal cell. Cytosol is retained within the donor macrophage and excluded from the transfer process. The moment at which the cryptococcal cell is fully expelled from a macrophage was defined as the end of exocytosis. **B.** The next step of transfer in which the released cryptococcal cell is free to interact with the Fc receptor of the acceptor macrophage via opsonin which survives the initial phagosome. The moment of initial attachment of the cryptococcal cell to the acceptor macrophage defined as the start of phagocytosis. Note the macrophage cells remain in contact but the transfer site is not sealed to the extracellular environment. **C.** The final step of transfer, the point at which the cryptococcal cell has been fully ingested by the acceptor macrophage. This moment is also used to define the end of phagocytosis. Left. The total time of exocytosis, phagocytosis, and Dragocytosis denoted by black line and measured time. The total length of Dragocytosis roughly equals that of exocytosis plus phagocytosis.

Figure 6

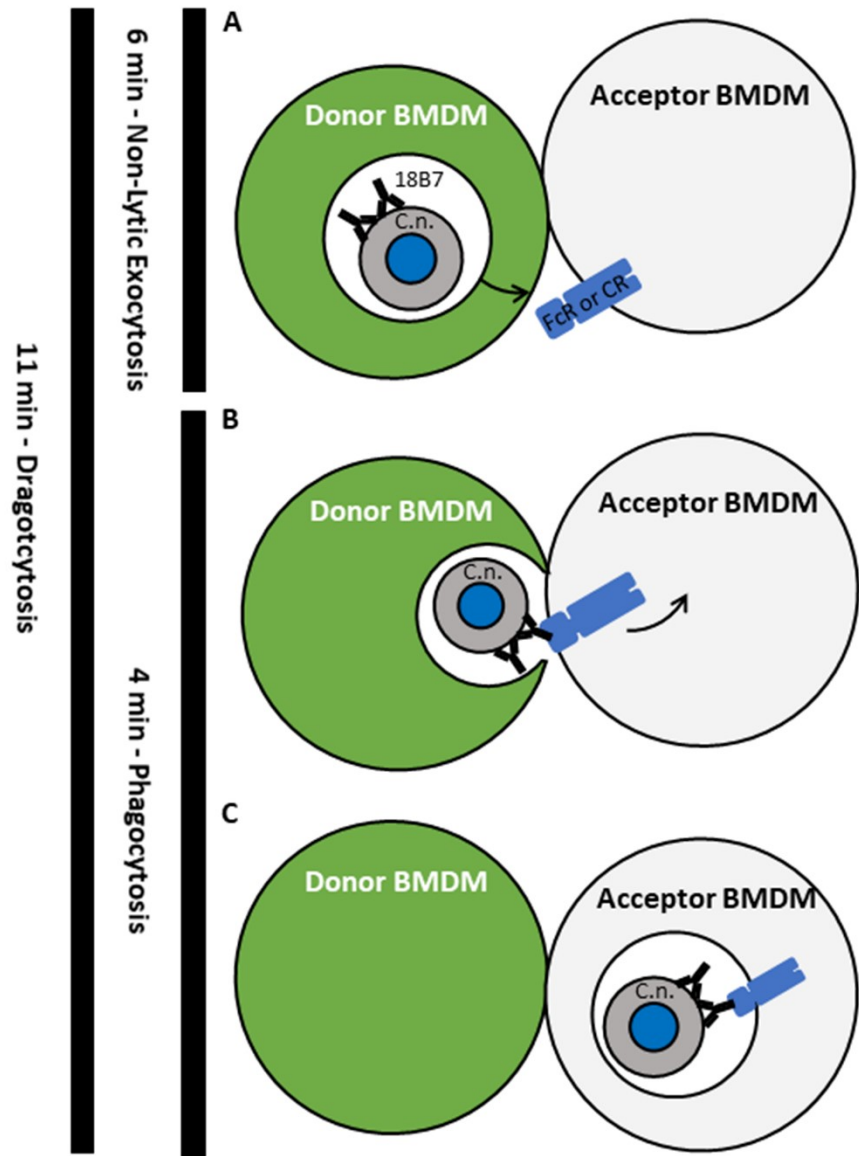


Figure 34

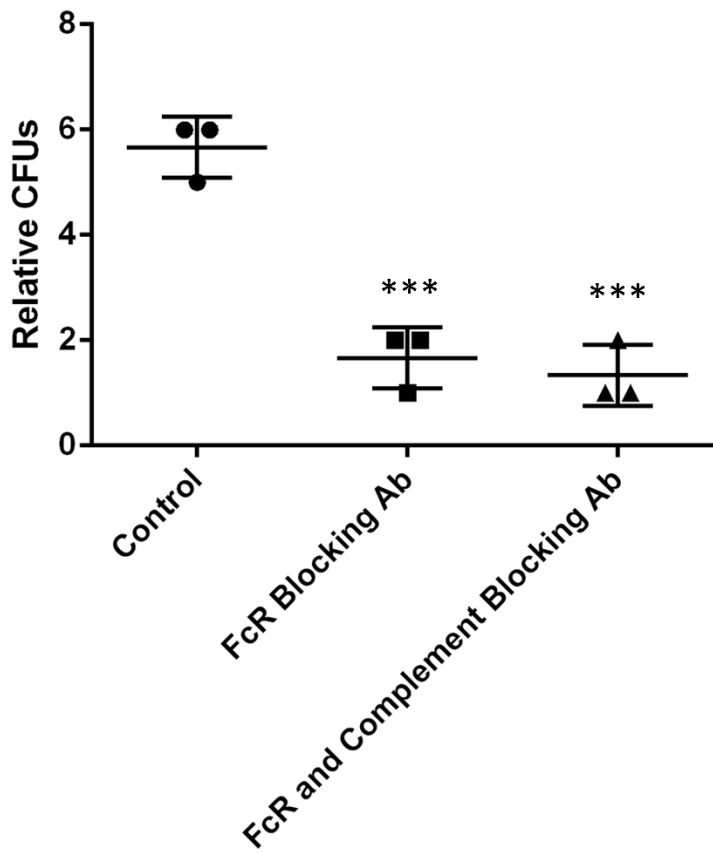


Figure 35

Relative quantification of surviving intracellular *C. neoformans*. Fungal colonies were enumerated via serial dilution after a 24 h infection period in which BMDMs were incubated with different combinations of inhibitory antibodies. *** denotes $P < 0.001$ via one-way ANOVA compared to control.

Event	Control	aCD16/32	aCD11b	aCD16/32 + aCD11b	FcR KO	Complement Opsonized	Cyto B	Cyto D	Heat Killed
Lytic Exocytosis	12 (6.9)	1 (0.67)	0	1 (0.8)	6 (4.03)	9 (7.38)	N/A	N/A	0
Non-Lytic Exocytosis	9 (5.1)	1 (0.67)	4 (2.65)	1 (0.8)	4 (2.68)	6 (4.92)	0	0	0
Transfer	14 (8)	2 (1.34)	6 (3.97)	0	3 (2.01)	3 (2.50)	0	0	0
Total Infected Cells	140	149	151	126	149	122	221	329	169

Table 3

Quantified cellular events in the presence or absence of antibody receptors. Counts are written as "Total # (Percent)". Lytic exocytosis is denoted as N/A for cytochalasin experiments because the drug results in cell death starting approximately 10 h into the experiment.

GenbankAccession	Symbol	GeneName	p-value	Fold-Change
AK164118	Phyhipl	phytanoyl-CoA hydroxylase interacting protein-like	0.043635	2.49488
NM_009140	Cxcl2	chemokine (C-X-C motif) ligand 2	0.0204045	2.37112
NM_011879	Ik	IK cytokine	0.0417661	2.015
NM_013877	Cabp5	calcium binding protein 5	0.0249099	2.59332
NM_026268	Dusp6	dual specificity phosphatase 6	0.0186441	2.28549
NM_199022	Shc4	SHC (Src homology 2 domain containing) family, member 4	0.047315	2.39855
XM_006500371	Trp53rkb	transformation related protein 53 regulating kinase B	0.0397998	2.39335

Table 4

Annotated genes differentially expressed in macrophages incubated with Fc receptor blocking antibody. Samples were compared to macrophages pre-incubation and post-incubation without antibody. Two genes are omitted due to lack of annotation.

Part III: Triggers of Dragotcytosis

Abstract

Our previous work has established that Dragotcytosis is a process triggered by, and beneficial to, ingested *C. neoformans* yeasts. Based a likely benefit to the fungus we hypothesize that Dragotcytosis is triggered by cellular stressors on the part of the yeast and that yeast containing phagolysosomes that undergo Dragotcytosis will be preceded by lower pH. Using fluorescent microscopy, qPCR, and fungal growth assays we find the dynamics of this host cell exit strategy resemble those of phagolysosome acidification, and that Dragotcytosis initiation is linked to pH and oxidative stresses.

Introduction

Cryptococcus neoformans is a pathogenic yeast which can reside in the phagolysosome of host macrophages¹. Macrophages are critical cells for the control and pathogenesis of cryptococcosis, being involved in the control and extrapulmonary dissemination of infection⁷. Macrophages are also involved in the pathogenesis of latent infection where the organism can survive for a long time in granulomas. Hence, *C. neoformans* survival in macrophages is critical for persistence and dissemination of infection. The yeasts, inhaled from the environment, manage this by modifying the phagolysosomal environment in their own favor. The capsule of *C. neoformans* is comprised of several subunits including glucuronic acid and glucuronoxylomannan (GXM) which act as weak acids capable of buffering the environment to pH ~ 5 ^{8,108}. *C. neoformans* also produces urease which disrupts phagolysosomal acidification by breaking down urea into carbon dioxide and

ammonia, a weak base¹³. Additionally, *C. neoformans* are capable of exiting host macrophages through lytic exocytosis, non-lytic exocytosis (Vomocytosis)^{20,104,187}, or lateral transfer (Dragotcytosis)¹³⁰.

We recently observed that macrophages engage in a bet hedging strategy to combat pathogens. By increasing the diversity of possible phagolysosomal pH, a population of macrophages will optimize its chances to inhibit pathogen growth based on pH alone. We also noticed that even small perturbations in this system can disrupt the betting strategy and different pathogens employ various strategies to tip the odds in their own favor. As previously discussed, *C. neoformans* directly modulates phagolysosomal pH through capsule buffering and urease activity.

A fascinating aspect of the interaction with *C. neoformans* with macrophages is the phenomenon of fungal cell transfer between two macrophages, a process we have recently termed 'Dragotcytosis'¹³⁰. Dragotcytosis, in *C. neoformans* is the result of coordinated exocytosis and phagocytosis events between adjacent macrophages¹³⁰. We also noted that Dragotcytosis is favorable to *C. neoformans* as macrophages with Dragotcytosis blockaded yield more colony forming units after 24 h than those who were not blockaded. Finally, we note that Dragotcytosis is an active process, only occurring with live *C. neoformans*. These observations are consistent with literature reports that Dragotcytosis as an active process¹⁰⁴. When taken together, these findings suggest Dragotcytosis is triggered by *C. neoformans* for a purpose beneficial to the yeast. However, it is unknown what specifically triggers Dragotcytosis or how transferring between macrophages confers a benefit even *in vitro* with only macrophages present. Notably, previous

observations have noted that phagolysosomal pH can modulate Vomocytosis frequency, supporting the idea that pH has an important and complex role in the regulation of this system^{70,102}.

Phagolysosomal pH is not the only stressor which could trigger Dragotcytosis. The oxidative burst and the release of reactive oxygen species into the phagolysosome are also potentially important. Both ROS generation and NOS activity are upregulated in M1 macrophages in response to pathogen phagocytosed pathogens^{58,77,90}. NOS metabolizes arginine into nitric oxide and citrulline. Conversely, Arg, upregulated in M2 macrophages) hydrolyzes arginine to ornithine and urea. Increased activity of either Arg or NOS will consume available arginine, resulting in lower activity of the other. Thus, M2 polarized macrophages have lower NOS activity, a less significant oxidative burst, and is thought to be one of the main reasons M2 macrophages are less effective at killing pathogens.

In this study we analyze the consequences on macrophage polarization on several aspects of *C. neoformans* pathogenesis and outcome. We anticipate that macrophages containing *C. neoformans* phagolysosomes that either acidify to a low final pH (< 4) or with a high rate of acidification are more likely to result in Dragotcytosis events than other *C. neoformans* containing phagolysosomes. Dragotcytosis being linked to *C. neoformans* attempting to escape a hostile environment would be consistent with other findings in the field that Dragotcytosis is an active process on the part of *C. neoformans*, that Dragotcytosis benefits *C. neoformans* yeasts in hostile (M1) macrophages, and that M2 macrophages are permissive to *C. neoformans* infection.

Materials and Methods

Cell Strains and Culture Conditions

Cryptococcus neoformans species complex serotype A strain H99 was originally obtained from John Perfect (Durham, NC). Culture stocks were stored at 80°C. Frozen stocks were later streaked onto SAB agar and incubated at 30°C. Liquid suspensions of cryptococcal cultures were grown in SAB overnight at 30°C. Cryptococcal cultures were heat killed by incubating at 65 °C for 1 h.

Macrophage cells were either BMDMs obtained from 6 week old C57BL/6 female mice from The Jackson Laboratory or J774.16 macrophage-like cells. BMDMs were isolated from hind leg bones and for differentiation were seeded in 10 cm tissue culture treated dishes in DMEM with 10% FBS, 1% nonessential amino acids, 1% penicillin-streptomycin, 2 mM Glutamax, 1% HEPES buffer, 20% L-929 cell conditioned supernatant, 0.1% beta-mercaptoethanol for 6 days at 37 °C and 9.5% CO₂. BMDMs were used for experiments within 5 days after differentiation. J774.16 cells were cultured in DMEM with 10% FBS, 1% nonessential amino acids, 10% NCTC109, and 1% penicillin-streptomycin at 37 °C with 9.5% CO₂. Cells were activated with 0.5 ug/mL LPS and 10 ng/mL IFN- γ for M1 polarization or 20 ng/mL IL-4 for M2 polarization.

Phagolysosomal pH measurement

Phagolysosomal pH was measured using ratiometric fluorescence imaging involving the use of pH-sensitive probe Oregon green 488 as described in prior studies¹³. The pH values analyzed here

were collected in part as described in Chapter II. Briefly, Oregon green 488 was first conjugated to mAb 18B7 using Oregon Green 488 Protein Labeling Kit. BMDMs were plated at a density of 1.25×10^5 cells/well on 24-well plate with 12 mm circular coverslip. Cells were activated with 0.5 $\mu\text{g/ml}$ LPS and 100 U/ml IFN- γ or 20 ng/mL IL-4 as previously described at 37 °C in a 9.5% CO₂ atmosphere overnight. Prior to infection, 2 d old live H99, heat killed H99, or anti-mouse IgG coated polystyrene bead (3.75×10^6 cells or beads/ml) were incubated with 10 $\mu\text{g/ml}$ Oregon green conjugated mAb 18B7 for 15 min. Macrophages were then incubated with Oregon green conjugated mAb 18B7-opsionized particles in 3.75×10^5 cryptococcal cells or beads per well. Cells were either centrifuged immediately at 350 x g for 1 min or incubated at 4 °C for 30 min to synchronize ingestion and cultures were incubated at 37 °C for 10 min to allow phagocytosis. Extracellular cryptococcal cells or beads were removed by washing three times with fresh medium, a step that prevents the occurrence of new phagocytic events. As an additional safeguard against new phagocytic events fresh media was supplemented with AlexaFluor 568 conjugated mAb 18B7 for 1 h to label extracellular particles. Samples on coverslip were collected at their respective time points after phagocytosis by washing twice with pre-warmed HBSS and placing upside down on MatTek petri dish with HBSS in the microwell. Images were taken by using Olympus AX70 microscopy with objective 40x at dual excitation 440 nm and 488 nm, and emission 520 nm. Images were analyzed using MetaFluor Fluorescence Ratio Imaging Software. Fluorescence intensities were used to determine the ratios of Ex488 nm/Ex440 nm that were converted to absolute pH values using a standard curve where the images are taken as above but intracellular pH of macrophages was equilibrated by adding 10 μM nigericin in pH buffer (140 mM KCl, 1 mM MgCl₂, 1 mM CaCl₂, 5 mM glucose, and appropriate buffer \leq pH 5.0: acetate-acetic acid;

pH 5.5-6.5: MES; \geq pH 7.0: HEPES. Desired pH values were adjusted using either 1 M KOH or 1 M HCl). The pH of buffers was adjusted at 3-7 using 0.5-pH unit increments.

Dragotcytosis Frequency Measurements

BMDMs were seeded (5×10^4 cells/well) in MatTek dishes. The cells were activated overnight (16h) with IFN γ (0.02 μ g/mL) and (0.5 μ g) LPS for M1, IL-4 (20 ng/mL) for M2, or unstimulated for M0. Cells in the MatTek dish were infected with Uvitex 2B (5 μ m/mL) stained and 18B7 (10 μ g/mL) opsonized *C. neoformans* at an MOI of 3 for 1 h, then supplemented with 2 mL fresh media and 18B7 mAb. In the case of drug trials this fresh media was also supplemented with bafilomycin A1 (100 nM) or chloroquine (6 μ m). MatTek dishes were then placed under a Zeiss axiovert 200M 10X magnification, incubated at 37 °C and 9.5% CO $_2$, and imaged every 2 min for a 24 h period. Images were then manually analyzed to identify ingested yeast cell outcomes.

Modelling

To simulate the effect of Dragotcytosis on a population of *C. neoformans* in phagolysosomes we generated 10,000 hypothetical phagolysosomal pH values based on the distribution of observed phagolysosomal pH in M1 polarized bead containing macrophage phagolysosomes. Each value < 4 was replaced one time by randomly determining a new phagolysosomal pH from the same distribution to simulate a Dragotcytosis event from the initial macrophage to a random new one.

Cryptococcal Capsule Measurements

Capsule measurements were determined by measuring exclusion zones on India Ink slides and phase contrast microscopy. To determine differences between polarized macrophage incubations, *C. neoformans* were harvested after being ingested by macrophages for 24 h. Extracellular yeasts were first removed by washing the cells 3 times with 1 mL HBSS. Macrophages were lifted from their plates, centrifuged at 350 x g for 10 min, and resuspended in 1 mL distilled H₂O. Cells were then passed through a 27 ¼ gauge needle 10 times and left incubating for 20 total min to ensure lysis. After lysis *C. neoformans* were pelleted via centrifugation at 2300 x g for 5 min and resuspended in 50 µL of PBS. Slides were prepared using 8 µL of cell mixture and 1.5 µL India Ink, then imaged on an Olympus Olympus AX70 at 20x objective. Capsules and cell bodies were measured using a previously published measuring program²⁰⁷.

NOS and Arg Activity Measurements

BMDMs were seeded at 10⁶ cell/well in 6-well treated tissue culture plates and activated overnight for M0, M1, or M2 polarization as previously described. Prior to infection, 2 d old live H99 (10⁶ cells/well) were incubated with 10 µg/ml mAb 18B7 for 10 min. Macrophages were then incubated with opsonized particles at MOI 1. Cells were either centrifuged immediately at 350 x g for 1 min or incubated at 4 °C for 30 min to synchronize ingestion and cultures were incubated at 37 °C for 10 min to allow phagocytosis. Extracellular cryptococcal cells were removed by washing three times with fresh medium, a step that prevents the occurrence of new phagocytic events. After 24 hours, cell supernatant was collected and the BMDMs were lysed with distilled water and 10 passages through a syringe with 23G needle. The supernatant was tested for NO

levels via Greiss reagent kit (Millipore-Sigma G4410). Cell lysates were tested for arginase activity with arginase activity assay kit (Millipore-Sigma MAK112).

qPCR

BMDMs were seeded at 10^6 cell/well in 6-well treated tissue culture plates and activated overnight for M0, M1, or M2 polarization as previously described. Prior to infection, 2 d old live H99 or inert beads (10^6 particles/well) were incubated with 10 $\mu\text{g/ml}$ mAb 18B7 for 10 min. Macrophages were then incubated with opsonized particles at MOI 1. Cells were either centrifuged immediately at 350 x g for 1 min or incubated at 4 °C for 30 min to synchronize ingestion and cultures were incubated at 37 °C for 10 min to allow phagocytosis. Extracellular cryptococcal cells were removed by washing three times with fresh medium, a step that prevents the occurrence of new phagocytic events. After 24 hours, BMDMs were resuspended in TRIzol reagent and frozen at -80°C before being sent to a collaborator's lab where qPCR was performed using standard TaqMan (ThermoFisher) commercial protocols.

Results

Polarization State Changes pH Dynamics

To investigate differences between pH distributions and dynamics between macrophages, we measured the pH of phagolysosomes at various times post infection. We found that, on average, M2 polarized macrophages had higher pH than M0 macrophages, which had higher pH than M1 polarized macrophages (Figure 36A). These insights were consistent at almost every time interval,

excluding at 15 min, at which time M0 was higher than M2 (Figure 36B). Additionally, the shape of the pH distributions in the different macrophage populations differed quite a bit, with only M1 macrophages reaching an approximately normal distribution while M0 was starkly bimodal, and M2 was approximately bimodal. Specifically, using empirical cumulative distribution functions of the observed data along with literature records of pH tolerance for *C. neoformans*, we found that M2 macrophages are the most hospitable with higher proportions of phagolysosomes at optimal ranges (~5.5) and few phagolysosomes at inhibitory ranges (≤ 4) for *C. neoformans* (Figure 37).

Polarization State Modulates Frequency of Host Escape Events

During our previous investigation into Dragocytosis, we never identified a single transfer event in M2 macrophages infected with *C. neoformans* and found that M0 macrophages experience Dragocytosis at a reduced rate compared to M1 (Figure 38). When taken in context with the two previously reported key insights that 1. Dragocytosis is an active process on the part of *C. neoformans* and 2. Inhibiting Dragocytosis is detrimental to *C. neoformans* survival, these data suggest that *C. neoformans* may utilize Dragocytosis in an attempt to find a less hostile phagolysosome to reside in.

Phagolysosome pH and Melanization are Associated with Dragocytosis Frequency

To further probe the role of phagolysosomal inhospitality in Dragocytosis, we measured and manipulated the phagolysosomal pH of infected macrophages. Chloroquine is a weak base which localizes to phagolysosomes and can be used to alkalize macrophage phagolysosomes *in vitro*.

bafilomycin A1 is a V-ATPase inhibitor which prevents protons from being pumped into the organelle. We found abrogated Dragotcytosis frequencies when phagolysosomes were alkalized with chloroquine or bafilomycin A1 (Figure 38). These data suggest acidification, or a downstream process, are important for triggering Dragotcytosis. Additionally, we decided to investigate if melanization modulates Dragotcytosis frequency, as melanin helps neutralize reactive oxygen species. We confirmed that melanized *C. neoformans* yeasts are significantly less likely to undergo Dragotcytosis (Figure 38).

Simulation Data Shows Dragotcytosis at low pH Benefits Cryptococcal Cells

Our hypothesis assumes that triggering Dragotcytosis, or Vomocytosis, in phagolysosomes of low pH would benefit *C. neoformans* cells by lowering the total number of inhibitory phagolysosomes. To explore this, we modeled phagolysosomal pH distributions based on observed pH measurements of bead containing BMDM phagolysosomes. Specific focus was given to Dragotcytosis events because Exocytosis events can, by nature, only result in fewer yeast cells at inhibitory pH since the extracellular environment will be at neutral pH by default. We found that if a *C. neoformans* particle were to trigger Dragotcytosis even a single time if their original phagolysosome dropped to $\text{pH} < 4$, it would be enough to drop the proportion of inhibitory phagosomes from ~15% to ~1% (Figure 39). Actual effects on *C. neoformans* survival would be even more pronounced since Dragotcytosis events are not actually limited to one event per yeast.

Cryptococcus neoformans Capsule and Cell Body Size are Unaffected by Polarization

The *C. neoformans* capsule is one of the most important virulence factors and determinants of infection outcome and a powerful modulator of phagolysosomal pH. Several aspects of cryptococcal pathology and phagolysosomal outcome are correlated to capsule size. Therefore, to determine whether capsule sizes and their effects differ, we measured capsule sizes after infection of differently polarized macrophages. We found that the average and median capsule sizes do not appreciably differ between populations of *C. neoformans* ingested by differently polarized macrophages (Figure 40A). Similarly, average and median cell body sizes also remained consistent (Figure 40B).

Time to Initiation is Stochastic for Exocytosis Events

If Vomocytosis and Dragocytosis are triggered by hostile pH and final pH is determined stochastically from a normal distribution, then these host cell exocytosis events should also display stochastic dynamics resembling those of the upstream pH trigger. To explore this hypothesis, we measured the time at which each process occurs throughout a series of videos of macrophages infected with *C. neoformans*. We found that exocytosis events do not trigger at normally distributed times and that these events are triggered stochastically, with no forbidden ordinal patterns observed (Figure 41). These data suggest that while acidification is an important upstream regulator of Dragocytosis frequency there are also likely to be other contributing determinants, skewing the distribution of initiation times away from normality.

Macrophage Polarization Modulates Oxidative Response

In addition to phagolysosomal pH, oxidative stress is an important host defense mechanism against ingested pathogens, including *C. neoformans*. To investigate potential differences in pathogen outcome due to differences in oxidative response, we first investigated the differences in oxidative response inherent to differently polarized macrophages. M2 macrophages were observed to have the lowest NOS activity, resulting from the highest Arg-1 activity (Figure 42). This data supports the notion that M2 macrophages have the most hospitable phagolysosomes for *C. neoformans*.

C. neoformans Infection Synergizes with IL-4 Stimulation

To investigate whether *C. neoformans* infection induces Th1/Th2 responses in macrophage populations, we performed qPCR on RNA harvested from differently polarized macrophages 24 h after infection. We found that *C. neoformans* infection synergistically activates the Th2 response with IL-4 stimulation (Figure 43) suggesting that *C. neoformans* may actively skew macrophages toward the most hospitable state. We did not see such synergism when macrophages were stimulated with IFN γ and LPS, or when macrophages were not stimulated.

Discussion

M2 macrophages and Th2 skewed immune responses are known to be more permissive to *C. neoformans* infection. In fact, *C. neoformans* lung infection is associated with a polarized M2 response triggered by fungal virulence factors including urease²⁴. We observed that M2 macrophages have, on average, higher pH phagolysosomes compared to M1 macrophages when

containing inert particles. Specifically, phagolysosomal pH of populations of M2 activated macrophage is more hospitable to *C. neoformans*. M2 macrophages had the fewest inhibitory macrophages (pH < 4) and the most optimal phagolysosomes (5 < pH < 6). This observation fits with, and helps explain, the established literature demonstrating M2 macrophages are more permissive to *C. neoformans* infection than their M1 counterparts.

Additionally, we found that *C. neoformans* will undergo fewer Dragocytosis events when residing in M2 macrophage phagolysosomes compared to *C. neoformans* ingested by M1 macrophages. We hypothesized that if the phagolysosomal pH drops too low for an ingested *C. neoformans* to counter with its polysaccharide capsule or urease activity, then it triggers either Vomocytosis or Dragocytosis as an escape mechanism, hoping to end up in the neutral extracellular environment or a more hospitable phagolysosome, respectively. Since, as we previously established, phagolysosomal pH is stochastically determined from a distribution in which most values are greater than pH 4, it is likely the *C. neoformans* would find a more hospitable home post-Dragocytosis. To investigate this we treated macrophage populations with multiple phagolysosome alkalizing agents, reasoning that if we keep phagolysosomal pH near optimal ingested *C. neoformans* will no longer transfer. We found that both chloroquine and bafilomycin drastically reduced or completely eliminated transfer events.

We are confident that the drug treatments did not have a direct effect on *C. neoformans* growth, virulence, or survivability but rather modulated the host macrophage response. Chloroquine has been shown not to significantly reduce *C. neoformans* growth and survivability unless ingested by

macrophages and at concentrations of at least 10 μM ²⁰⁸, higher than used in these experiments. Similarly, at high concentrations Bafilomycin A1 can have anti-fungal activity²⁰⁹ and even inhibit *C. neoformans* melanization²¹⁰. To ensure our results did not result from the anti-fungal activity of either drug, we only used each in lower concentrations that would not exhibit inhibitory behavior¹³⁴.

When taken in context with the two previously reported key insights that 1. Dragotcytosis is an active process on the part of *C. neoformans* and 2. Inhibiting Dragotcytosis is detrimental to *C. neoformans* survival, these data suggest that *C. neoformans* may utilize Dragotcytosis in an attempt to find a less hostile phagolysosome to reside in. Therefore, we probed how Dragotcytosis could modulate the effectiveness of the macrophage acidification betting strategy we established in chapter I. We found that even a single Dragotcytosis event triggered for *C. neoformans* residing in low pH phagolysosomes would significantly increase the proportion of surviving yeasts.

Unfortunately, all of our available drugs which inhibit phagosome acidification can also inhibit autophagy, and vice versa, so it is difficult to parse out whether Dragotcytosis is triggered by only one of these systems. Additionally, the generation of ROS is innately tied to these processes, and phagolysosomal pH itself, with the concentration of ROS in the phagolysosome increasing alongside pH with previously measured concentrations of 50 μM $\text{O}_2^{\bullet-}$ at pH 7.4 and 2 μM at pH 4.5⁷⁷. Thus, it is almost impossible to narrow down Dragotcytosis triggers to one specific stressor. More likely is that a combination of stresses results in Dragotcytosis, supported by previous

observations that inhibiting pH buffering via urease mutation does not increase Dragotcytosis events as would be expected if the process was triggered by pH alone¹³. Given that the frequency of Dragotcytosis appears parabolic with a dip in frequency around pH 6 and a rise in frequency on either end, ROS could be less influential than the other stressors. Future work will focus on parsing out contributions of individual stressors with focus on reactive oxygen species, pH, and a functioning autophagy pathway.

Regardless of the exact trigger(s) of Dragotcytosis, our hypothesis fits well with the known data of *C. neoformans* infection in human macrophages. It is known that human macrophage phagolysosomes acidify with different dynamics than those of mice. For example, human M2 macrophage phagolysosomes acidify to a lower pH than mouse macrophage phagolysosomes²⁷. Humans are also markedly resistant to *C. neoformans* infection, which poses little threat to most immune competent hosts. Additionally, human macrophages undergo both Vomocytosis and Dragotcytosis with much greater frequency than mouse macrophages *in vitro*.

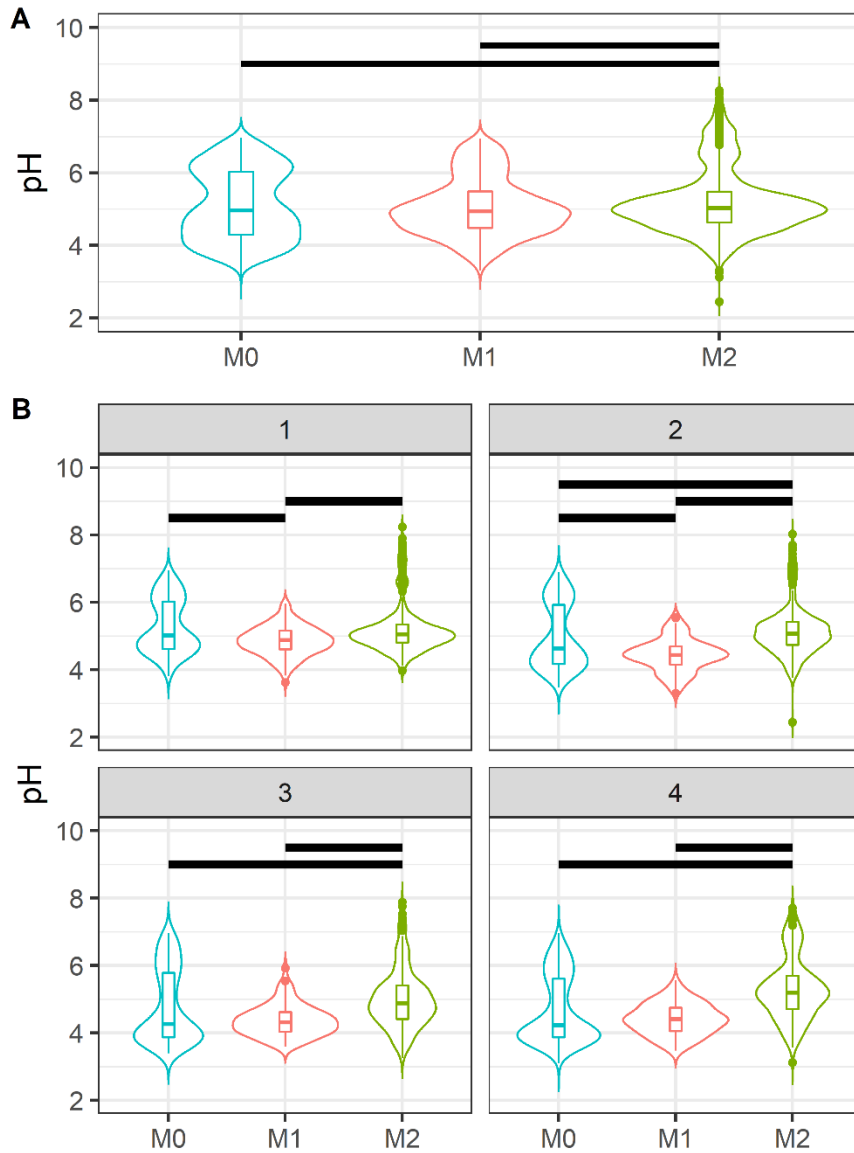


Figure 36

pH distributions observed in differently polarized BMDM populations after ingesting polystyrene beads. **A.** Compiled data for all timepoints post infection for differently polarized BMDM populations. **B.** Individual data for each hour post infection (gray box value) of measured phagolysosomal pH. Black bars represent $P < 0.0001$ via Kruskal-Wallis test with Wilcox rank pair testing.

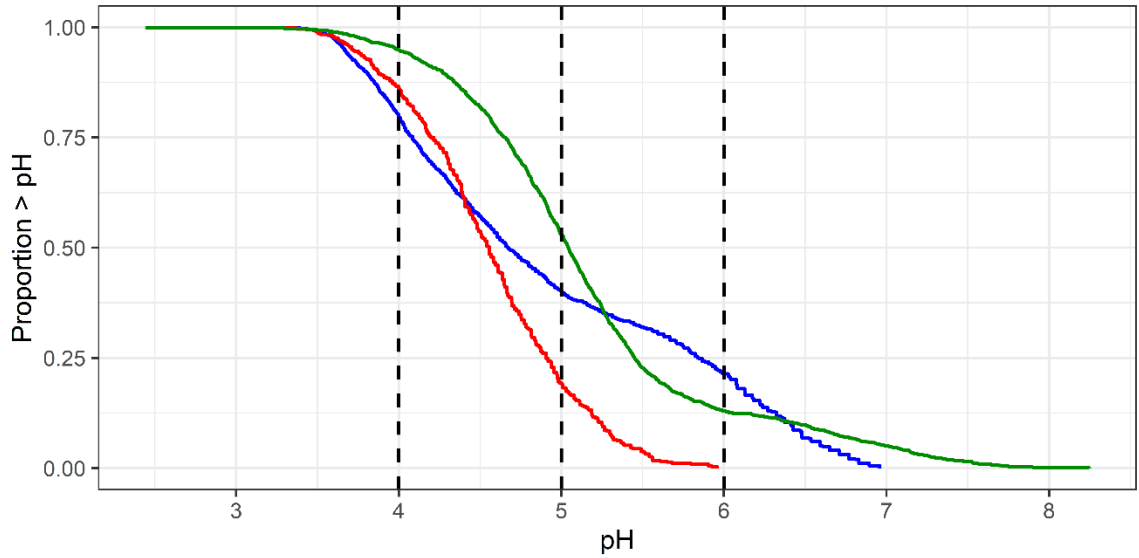


Figure 37

Inverse empirical cumulative distribution functions for bead containing phagolysosome pH data measured in M0 (blue), M1 (red), and M2 (green) macrophage populations. The dashed line at pH 4 represents the point at which pH inhibits *C. neoformans* replication while the area between the dashed lines at pH 5 and 6 represents the optimal growth pH for *C. neoformans*. Hospitality of each population is estimated by the number of phagolysosomes within each of these regions.

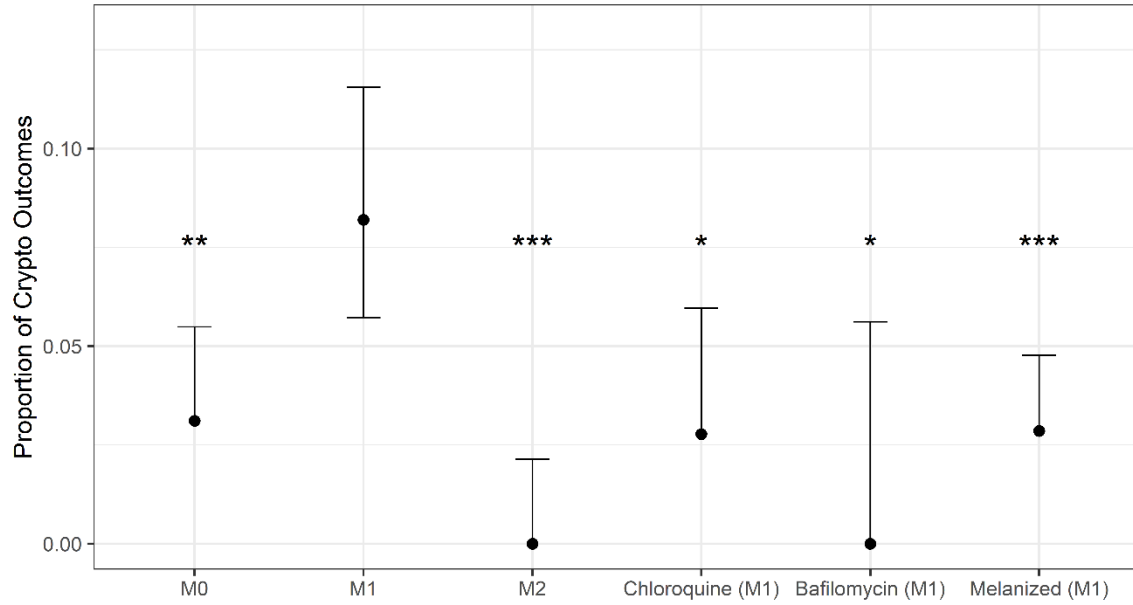


Figure 38

Dragotcytosis frequencies of *C. neoformans* ingested by BMDMs under various conditions. M0 and M2 macrophages have lower frequencies of Dragotcytosis overall compared to M1. Alkalinizing the phagolysosomes of M1 macrophages with chloroquine or bafilomycin A1 also abrogate Dragotcytosis frequency. *, **, *** denote $P < 0.05$, 0.01, 0.001 via single tailed test of equal proportions compared to M1.

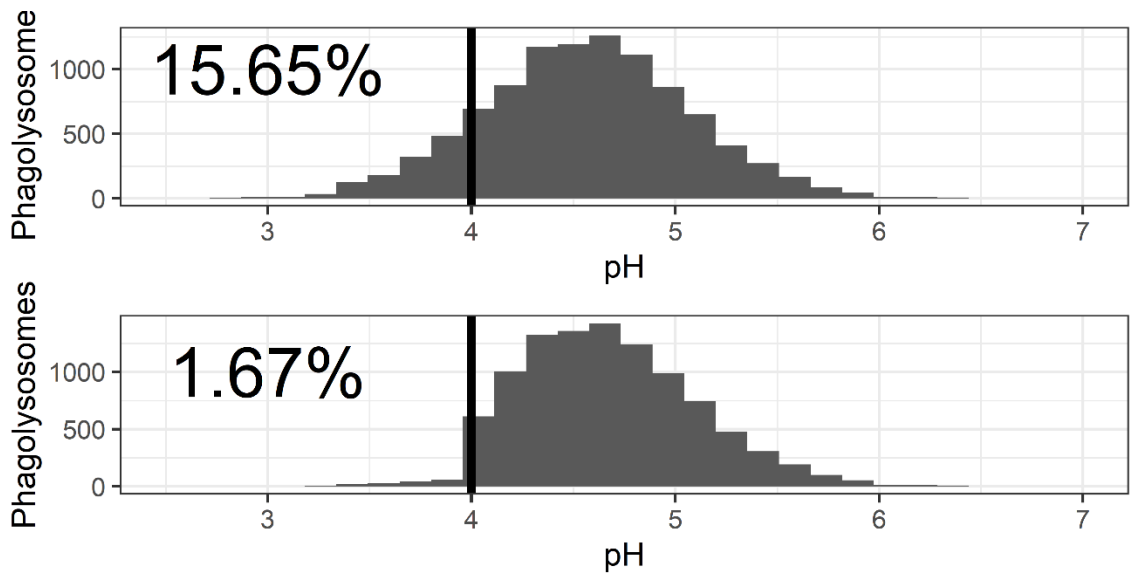


Figure 39

Hypothetical phagolysosomal pH distributions if *C. neoformans* particles were to undergo **(top)** no Dragotcytosis events or **(bottom)** a single Dragotcytosis event if the original phagolysosome acidified to $\text{pH} < 4$. Even a single round of low pH triggered Dragotcytosis drastically shifts the distribution to the right resulting in a greater proportion of *C. neoformans* hospitable phagolysosomes.

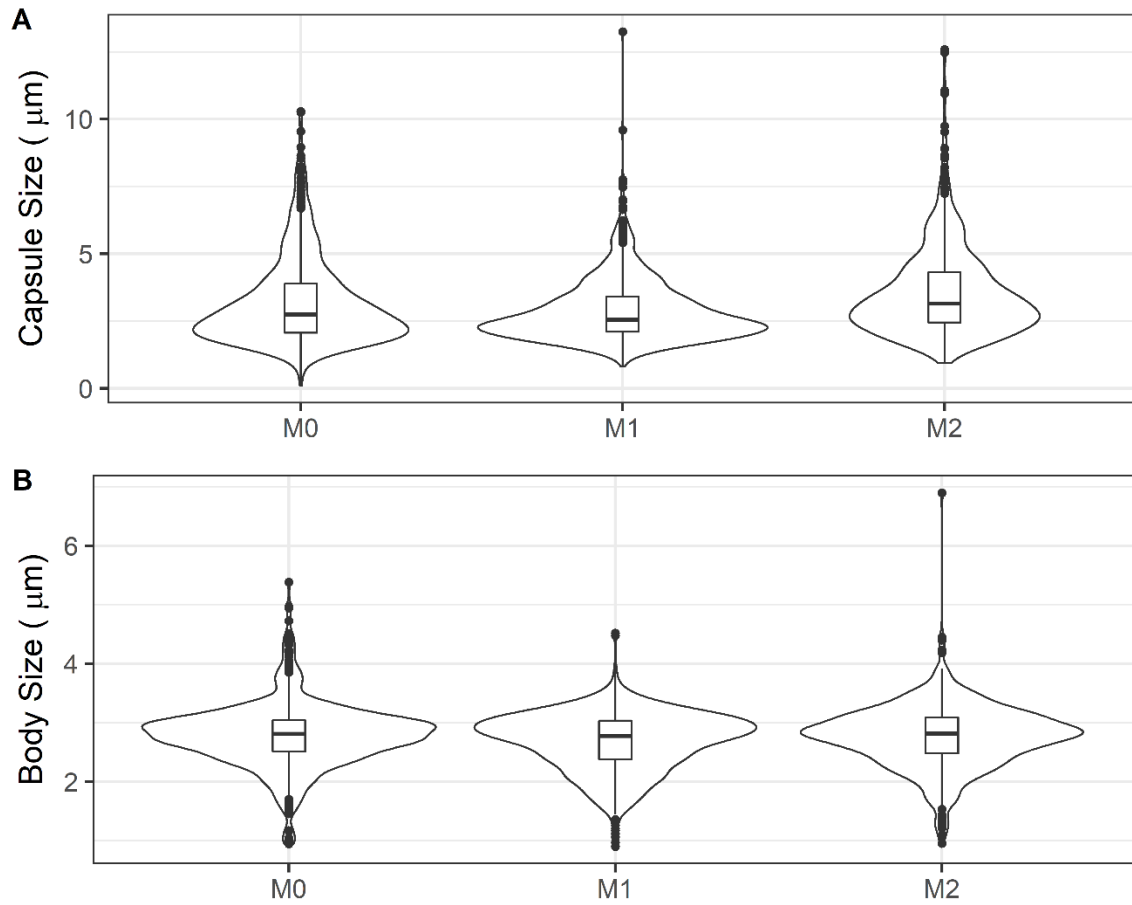


Figure 40

Capsule and cell body size of *C. neoformans* isolated 24 hours after ingestion by BMDMs. Capsules and cell bodies are measured by preparing and imaging India Ink slides and a previously established measuring code. No significant differences were found between the polarization states of host macrophages.

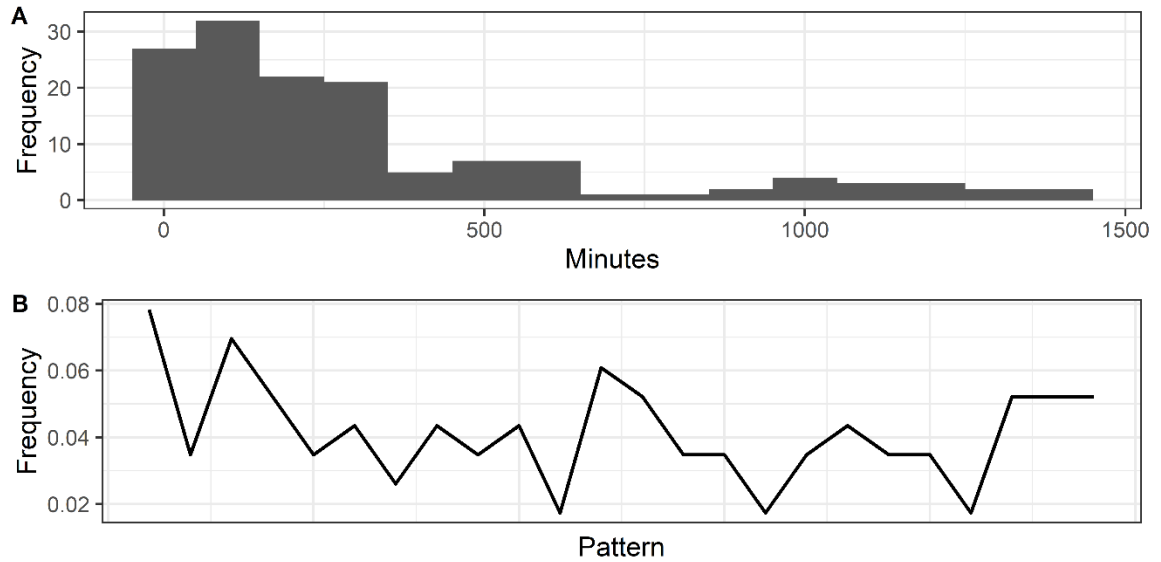


Figure 41

Dynamics of the initiation of host cell exit events by *C. neoformans* from M1 BMDMs. **A.** Distribution of the times at which *C. neoformans* yeasts initiated host cell exit strategies. Both Vomocytosis and Dragocytosis events are represented here. Bin widths are set to 100 and the data depicted spans 139 samples from 12 experiments. **B.** Ordinal pattern analysis for the intervals between events. Intervals were gathered and analyzed within experiments and total proportions of individual ordinal patterns summed between experiments.

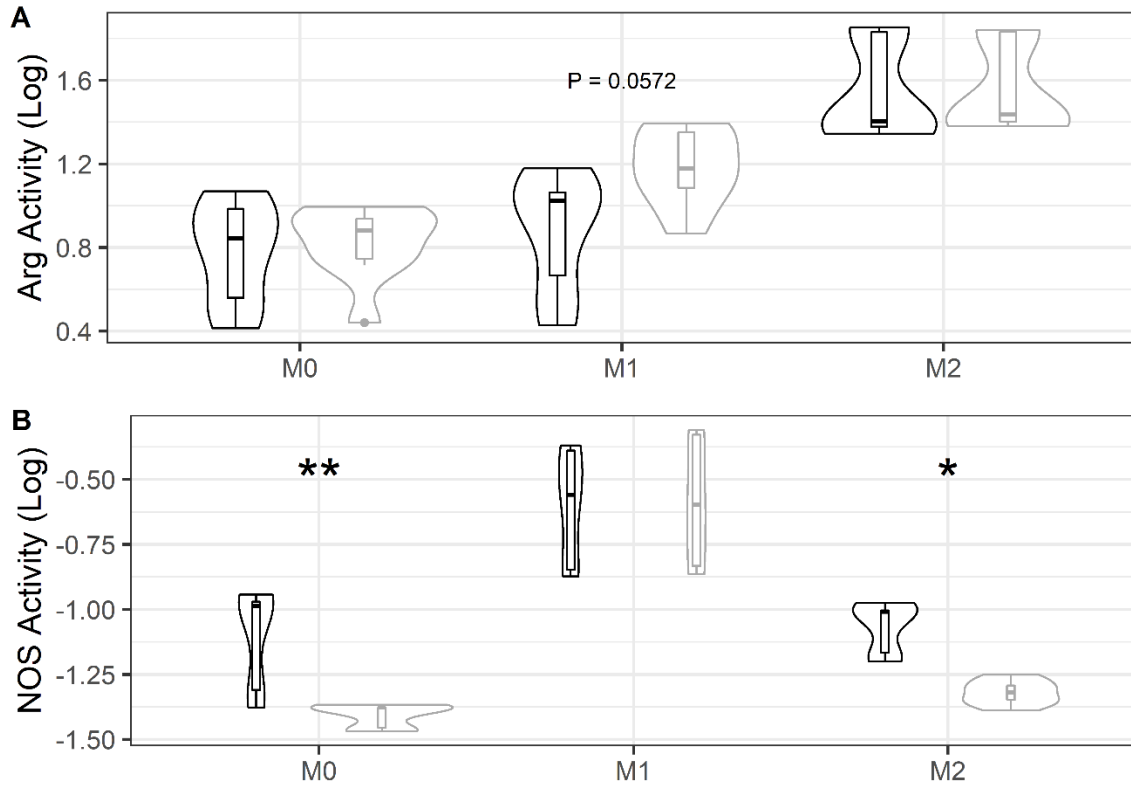


Figure 42

Oxidative response in BMDM populations measured by the activity of associated enzymes in uninfected (black) BMDMs or BMDMs infected with H99 (gray). **A.** Arg-1 activity of differently polarized and infected BMDMs. M2 have the highest overall activity, and activity is promoted with infection in M1 populations. **B.** NOS activity of differently polarized and infected BMDMs. M1 have the highest overall activity, and activity is decreased with infection in both M0 and M2 populations. *, ** represent $P < 0.05$ and 0.01 , respectively. Significance determined by 2-way ANOVA with Tukey's HSD comparisons.

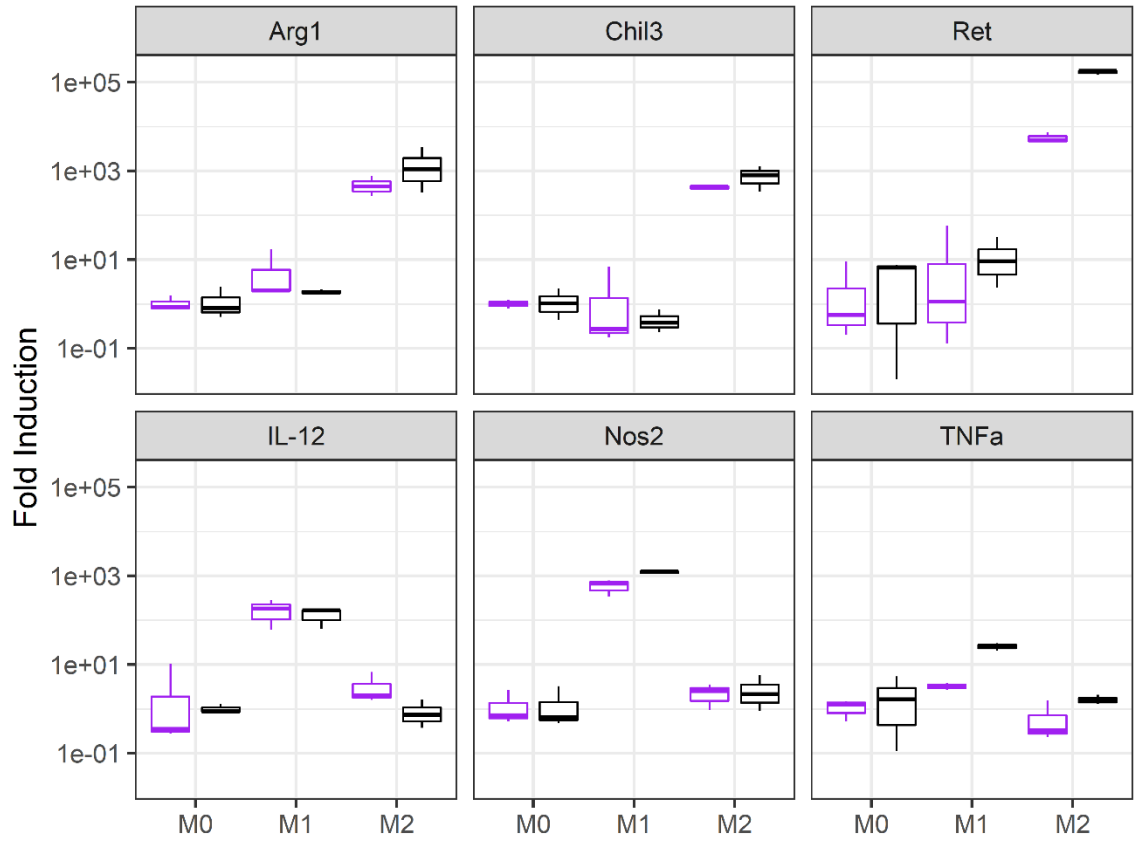


Figure 43

qPCR data from differently polarized BMDMs uninfected (purple) and infected (black) with *C. neoformans* 24 HPI. Values are normalized to the respective M0 uninfected fold induction.

Discussion

Summary

In-depth investigation of *C. neoformans*-macrophage interactions at the phagolysosome has allowed us to identify a key host defense mechanism and to elucidate one strategy how *C. neoformans* circumvents this system, offering a new perspective on host pathogen interactions specific to *C. neoformans* but with implications to a wide array of intracellular human pathogens which interact with the phagolysosome. Our original goals were to characterize the underlying mechanics of macrophage phagolysosome acidification and investigate how a macrophage can combat a pathogen of unknown pH tolerance, to determine the mechanism by which *C. neoformans* can transfer between host cells and place it within known cellular processes, and to explore whether Dragocytosis is modulated or triggered by changes in phagolysosomal/environmental pH. The main findings of this thesis are as follows:

First, macrophages utilize a bet-hedging strategy to increase their efficacy against inhibition of unknown pathogens via pH. By increasing the variation of possible phagolysosomal pH macrophages can optimize their bets against unknown pathogen pH susceptibilities. This system sacrifices a small amount of average fitness during any given pathogen challenge to drastically reduce the overall variation fitness between pathogen challenges. This, in turn, drastically increases the mean log fitness, representative of the long-term survivability of the macrophage population in the context of all pathogens. Simply put, the macrophages increase the diversity of their pH range to “not put their eggs in one basket”.

We had originally hypothesized that the acidification process, while complex, would be deterministic in nature, specifically chaotic determinism. The lack of underlying forbidden ordinal patterns in the data suggested a different answer: that the final pH of a given phagolysosome is randomly determined. Additionally, we are confident this betting system is not a coincidental result of stochasticism in cellular machinery because the variation in phagolysosomal pH is markedly larger than that of comparable biological and cellular pH systems. Blood and organelle luminal pH, for example, are both regulated much more tightly than what is observed in phagolysosomal acidification. Furthermore, we found that macrophages engage in bet-hedging at the cellular level, generating this stochastic diversity on a “per phagosome” basis rather than “per cell”. Multiple phagolysosomes within a single macrophage which were synchronized in formation yield different final pHs normally distributed and centered around 0.

Early interactions between the immune system and encountered pathogens are often extremely important to disease outcome and our data suggests this bet hedging strategy is a potent and early contributor to host defense. The importance of pH itself as a pathogen inhibition mechanism has been downplayed and overlooked in general, with emphasize placed on the activation or optimization of hydrolases and other protein players in the phagolysosome rather than considering the effect pH can have on inhibiting pathogen replication. However, the mechanisms behind this system are still not understood and more work is required to fully understand the interplay between host and pathogen within the phagolysosome. For example, our model does not account for all possibilities or all possible aspects of the host response and an updated version

should include considerations such as the benefits of a subpopulation of macrophages dying to infection (release of alarmins, antigens, etc.) or potential cellular damage caused by certain extreme lows and highs of phagolysosomal pH. We also did not consider protease function or reactive oxygen species, which would be optimized or inhibited depending on the phagolysosomal pH and both have important roles in pathogen inhibition. Also, our data suggests the variety in pH is generated, at least in part, by the number or efficacy of V-ATPase complexes on a given phagolysosome but we do not currently have the technology to investigate this further. Future studies should endeavor to discover the cellular and molecular pathways responsible for operating this betting system.

Our next major finding was that pathogens combat the bet hedging system by disrupting or altering acidification, taking advantage of the fact that even small perturbations in acidification can drastically shift the odds in favor of the pathogen. A wide variety of pathogen evasion mechanisms have been reported in the literature, and we confirm that several significant pathogens disrupt the macrophage bet hedging strategy while residing in the phagolysosome. *C. neoformans* for example can both actively and passively disrupt phagolysosome acidification through mechanisms including buffering via capsular subunits, urease activity, and disruption of the phagolysosomal membrane. According to our model we predict that these effects drastically reduce overall macrophage fitness by increasing the mean and decreasing the variation of phagolysosomal pH. The wider literature supports our model, reporting decreased macrophage fitness when these pathogen systems are functional. *C. neoformans* is able to manipulate the macrophage population into focusing their acidities around a region of pH more hospitable to the

pathogen. *Mycobacterium avium* shows a similar pH buffering ability. Using previously reported literature data we were able to model *M. avium* infection with our model as well, with multiple experiments agreeing that phagolysosomes containing live *M. avium* had lower overall log mean fitness compared to phagolysosomes containing killed *M. avium*. Many more human pathogens are known to modulate the pH of their resident phagolysosome and any microbe engulfed by a macrophage will encounter this acidification defense strategy. It is likely one of the most widely encountered and broadly applicable innate host defense mechanisms and will likely have an important role in the early outcome of many human pathogens.

Third, *C. neoformans* utilize a coordinated exocytosis-phagocytosis process, herein named Dragocytosis, to transfer from one macrophage to another without the sharing of cytoplasmic contents. Should a cryptococcal yeast need to escape a host phagolysosome it has the capability to initiate the Dragocytosis process alongside nonlytic exocytosis or lytic escape. We found that the FcR and/or CR must be intact and functional for Dragocytosis to occur, and that the involved macrophages remain in contact throughout the process. The fact that this system is an active process on the part of *C. neoformans*, as we found Dragocytosis inhibited when the yeasts are killed, implies this process is biologically beneficial to the yeast. Indeed, we found that inhibiting this system in M1 polarized macrophages reduced the amount of recoverable *C. neoformans* after infection, implying more yeasts are inhibited if they are unable to transfer host cells. While the process itself appears to be within the context of known phagocytic and exocytic pathways, neither the trigger nor the method by which the phagolysosome is shuttled to the plasma membrane are known. Given these insights future work should focus on identifying key molecular

or transcriptional changes to the yeast and macrophage cells prior to and during transfer to elucidate this mechanism.

Fourth, we have acquired data suggesting that Dragocytosis may be triggered in response to cellular stressors, with an emphasis on extremely low or quickly decreasing pH. Initially we observed that differently polarized macrophage populations induce Dragocytosis at different frequencies, and that hospitality toward *C. neoformans* in terms of phagolysosomal pH correlated with decreased Dragocytosis frequencies. M2 macrophages have the highest average phagolysosomal pH, resulting in a high likelihood that engulfed *C. neoformans* yeasts are under less stress. Furthermore, we found that *C. neoformans* infection encourages macrophages to skew toward M2 polarization and this effect is synergistic with IL-4 supplementation. *C. neoformans* will initially encourage higher pH phagolysosomes via combination of M2 skewing and phagolysosome pH buffering. Aside from which *C. neoformans* may also disrupt this bet-hedging strategy and significantly increase their chances of survival by increasing transfer frequency when phagolysosomal pH is low. We found that even a single Dragocytosis event when *C. neoformans* encounters an inhibitory phagolysosomal pH can increase the proportion of uninhibited *C. neoformans* in a population from 0.85 to 0.985. However, while initiation of Dragocytosis is stochastic in nature, the distribution of initiation times is not normal. Thus, we cannot narrow down the trigger to pH alone, oxidative stress likely also plays a role in triggering Dragocytosis, supported by our findings that melanized *C. neoformans* undergo Dragocytosis at reduced frequencies..

Relationship to Field

Our work aligns well with the existing field of literature. Stochastic signals have been identified and referenced with regard to several steps of the phagolysosome maturation progress, such as the kinetics of kinesin and dynein molecular motors¹²⁸. Our results agree with reports that phagolysosomes within a single cell are extremely heterogeneous in nature and may even offer a partial explanation for why the heterogeneity is beneficial¹²⁷. Indeed, the stochastic nature of phagolysosome generation could explain other downstream stochastic signals in pathogenesis, for example the number of *F. tularensis* particles in a given phagolysosome¹³⁹ which, in turn, offer more avenues through which the host cell could be bet hedging.

M1 macrophages have been thoroughly reported on as resistant to *C. neoformans* infection while M2 macrophages are reported as permissive. Our data supports these conclusions as we found that M2 macrophages are the most hospitable to *C. neoformans* growth and replication in terms of pH while M1 macrophages are least hospitable, with M0 macrophages between the two. Additionally, when modeling the observed pH distributions in the context of our bet hedging model the results show the M1 population of macrophages having the highest mean log fitness, followed by M0, followed by M2, agreeing with the literature which places M1 most resistant and M2 most permissive.

Limitations

The work we have done here is novel in many respects and explores some areas either not well defined or too far past our current abilities to properly investigate, which leaves us with some limitations. The bet-hedging strategy model is based on several assumptions and simplifications of an extremely complicated system. In our model we only consider pH itself and only use reported inhibitory minimum pH values as a threshold for pathogen inhibition. We do not consider other relevant biological aspects such as protease function at different pH, extreme pH damage to the phagolysosomal membrane, expended energy of hydrogen pumps to maintain pH, etc. all of which would have relevant effects on pathogen outcome and host resource expenditure. We also make the assumption that if the phagolysosomal final pH is below the reported minimum for a respective pathogen, that pathogen is completely inhibited. We do not make allowances for pathogens which circumvent the lowering pH, acid tolerant subpopulations, etc. While pH is an important aspect of organism growth and inhibiting pathogens allows the immune system an advantage, it is not actually a guarantee that a pathogen will be fully inhibited by the host cell, despite our assumption. With more time, resources, and viewpoints contributed to this model we can improve it to more accurately reflect real infections.

Further limiting our investigation of this bet hedging strategy is the temperamental nature of the system. Any attempt to study the system via knockouts or mutants, any perturbation of the system, will inherently alter the dynamics of the system. The model we create and any conclusions we draw have to be based on logical arguments and cannot necessarily be tested for in the

biological system itself. At our current level we simply lack the knowledge, technical finesse, or both, to fully analyze this system.

Similarly, the processes of phagolysosomal maturation and acidification are intertwined and too closely related for us to parse out individual contributions. The observed stochastic dynamical system of acidification may arise from, or in part due to, underlying stochasticism of the maturation process. We probed this question in Part I using markers of phagolysosomal maturation to show that maturation is also a stochastic process but does not approximate a normal distribution. The data is interesting in that it suggests the observed heterogeneity in phagolysosomal pH is not determined by the number of V-ATPase molecules present in the phagolysosomal membrane and is instead regulated through some other mechanism. Unfortunately, we lack the required resolution and knowledge to fully separate these processes and are not sure specifically how V-ATPase pump efficacy is regulated to generate pH heterogeneity. There are many recorded mechanisms of V-ATPase regulation via assembly of the V1 and V0 domains, in turn regulated by the activity of other proteins such as PI3K. Intuitively it is likely that macrophage recognition of PAMPs upon ingestion triggers downstream regulation of PI3K and differences in V1/V0 assembly via stochastic expression of regulatory elements. At this time however we cannot point to which specific regulator would likely be at play.

Future Directions

Future endeavors into this line of research would focus on teasing out the subtleties of the bet hedging system. The bet-hedging strategy is apparent for M1 polarized macrophages while M0 and M2 macrophages seemingly lack acidification coordination. Surprisingly, M0 and M2 macrophages yielded bimodal pH distributions and fully understanding their contributions in a potential betting strategy would require optimization of our current simulation model. Explorations into the *in vivo* contributions of this bet-hedging mechanism will have to account for the fact that all three states of macrophages are present along with the fact that macrophage populations can present as a spectrum of polarization rather than binary extremes.

As previously explored, the bet hedging modelling could be improved by expanding the input parameters. Factors such as host energy expenditure in maintaining pH, the benefits of a sacrificial population of macrophages, and hydrolase function could all increase the accuracy of our model and more fully replicate *in vivo* scenarios.

Amoebas and macrophages share many morphological and functional similarities and are a natural environmental predator of *C. neoformans*. Acidification in amoebas is known to resemble that of macrophages and we therefore hypothesize amoebas would display the same, or a similar, bet hedging strategy as they also ingest various unknown microbes with unknown pH tolerances^{145,146}. We unfortunately were unable to repeat these experiments in the time we had with amoeba samples due to low phagocytic index.

Our results indicate that even among M1 polarized macrophages, differences in host genetics could result in different bet-hedging strategies. Thus, correlating host haplotypes or other biomarkers to pH distributions could allow us to use expected pH distributions as risk factors for certain diseases as well as allow us to custom prescribe treatments. Referencing our human data from Part III, host 1 could benefit from a drug to increase phagolysosome acidity in the context of a *C. neoformans* infection, but host 3 would likely suffer from that same medication with their phagolysosome pH dropping too low to be biologically sustainable, further damaging the phagolysosome.

We have established that Dragocytosis is a relevant and important escape mechanism for *C. neoformans* within hostile macrophage phagolysosomes. Non-lytic exocytosis has been reported in several other human intracellular pathogenic microbes, including microbes sequestered in alveolar macrophages and granulomas like *C. neoformans*. Dragocytosis may be a conserved strategy between intracellular pathogens and the experiments from Part II should be replicated with these pathogens to investigate whether they undergo the transfer process as well. Since Dragocytosis is an active process on the part of the pathogen and is likely unimportant to other human host cells, inhibiting the process could be a potential drug target for new therapies. Transfer is likely important to the hypothesized Trojan Horse strategy of *C. neoformans* disseminating to the brain and inhibiting that process could help prevent meningoencephalitis. If we can inhibit *C. neoformans* from transferring between host macrophages via Dragocytosis we could potentially inhibit them from being able to escape granulomas or disseminate. Alternatively,

if we could increase the frequency of Vomocytosis we could reduce the overall amount of *C. neoformans* hiding within macrophages, lowering their likelihood of traversing the blood brain barrier.

Final Note

In this thesis we have discovered and explored two aspects of host-pathogen interaction between *C. neoformans* and macrophages. We established that macrophages use a bet-hedging strategy while acidifying their phagolysosomes to maximize effectiveness against ingested pathogens, akin to spreading bets on a roulette table. We determined that transfer of *C. neoformans* between proximal macrophages is via a coordination of exocytosis and phagocytosis. Finally, we built a foundation of evidence suggesting that Dragocytosis is triggered by cellular stressors on *C. neoformans* while in the phagolysosome, likely a combination of low pH and oxidative stress. Additionally, our work has raised new questions about the field to be addressed by future studies.

References

1. Levitz, S. M.; Nong, S. H.; Seetoo, K. F.; Harrison, T. S.; Speizer, R. A.; Simons, E. R. *Cryptococcus neoformans* resides in an acidic phagolysosome of human macrophages. *Infection and Immunity* **67**, 885–890 (1999).
2. Brown, G. D.; Denning, D. W.; Gow, N. A. R.; Levitz, S. M.; Netea, M. G.; White, T. C. Hidden killers: human fungal infections. *Sci. Transl. Med* **4**, 165rv13 (2012). [PMID:23253612]
3. Perfect, J. R.; Casadevall, A. Cryptococcosis. *Infect. Dis. Clin. North Am* **16**, 837-8vi (2002).
4. Casadevall, A. Cryptococci at the brain gate: break and enter or use a Trojan horse? *The Journal of Clinical Investigation* **120**, 1389–1392 (2010).
5. Chrétien, F.; Lortholary, O.; Kansau, I.; Neuville, S.; Gray, F.; Dromer, F. Pathogenesis of Cerebral *Cryptococcus neoformans* Infection after Fungemia. *The Journal of Infectious Diseases* **186**, 522–530 (2002).
6. Charlier, C.; Nielsen, K.; Daou, S.; Brigitte, M.; Chretien, F.; Dromer, F. Evidence of a role for monocytes in dissemination and brain invasion by *Cryptococcus neoformans*. *Infect. Immun* **77**, 120–127 (2009). [PMID:18936186]
7. Bojarczuk, A.; Miller, K. A.; Hotham, R.; Lewis, A.; Ogryzko, N. V.; Kamuyango, A. A.; Frost, H.; Gibson, R. H.; Stillman, E.; May, R. C.; Renshaw, S. A.; Johnston, S. A. *Cryptococcus neoformans* Intracellular Proliferation and Capsule Size Determines Early Macrophage Control of Infection. *Scientific Reports* **6**, 21489 (2016). [PMID:26887656]
8. De Leon-Rodriguez, C. M.; Fu, M. S.; Corbali, M. O.; Cordero, R. J. B.; Casadevall, A. The Capsule of *Cryptococcus neoformans* Modulates Phagosomal pH through Its Acid-Base Properties. *mSphere* **3**, (2018). [PMID:30355667]
9. Zaragoza, O.; Chrisman, C. J.; Castelli, M. V.; Frases, S.; Cuenca-Estrella, M.; Rodriguez-Tudela, J. L.; Casadevall, A. Capsule enlargement in *Cryptococcus neoformans* confers resistance to oxidative stress suggesting a mechanism for intracellular survival. *Cell Microbiol* **10**, 2043–2057 (2008).
10. DeLeon-Rodriguez, C. M.; Casadevall, A. *Cryptococcus neoformans*: Tripping on Acid in the Phagolysosome. *Frontiers in Microbiology* **7**, 164 (2016).
11. Vecchiarelli, A. Immunoregulation by capsular components of *Cryptococcus neoformans*. *Med. Mycol* **38**, 407–417 (2000).
12. Fromtling, R. A.; Shadomy, H. J.; Jacobson, E. S. Decreased virulence in stable, acapsular mutants of *cryptococcus neoformans*. *Mycopathologia* **79**, 23–29 (1982). [PMID:6750405]
13. Fu, M. S.; Coelho, C.; De Leon-Rodriguez, C. M.; Rossi, D. C. P.; Camacho, E.; Jung, E. H.; Kulkarni, M.; Casadevall, A. *Cryptococcus neoformans* urease affects the outcome of intracellular pathogenesis by modulating phagolysosomal pH. *PLOS Pathogens* **14**,

- e1007144 (2018).
14. Blackstock, R.; Buchanan, K. L.; Adesina, A. M.; Murphy, J. W. Differential regulation of immune responses by highly and weakly virulent *Cryptococcus neoformans* isolates. *Infection and immunity* **67**, 3601–3609 (1999). [PMID:10377145]
 15. Blackstock, R.; Murphy, J. W. Secretion of the C3 component of complement by peritoneal cells cultured with encapsulated *Cryptococcus neoformans*. *Infection and immunity* **65**, 4114–4121 (1997). [PMID:9317016]
 16. Kwon-Chung, K. J.; Polacheck, I.; Popkin, T. J. Melanin-lacking mutants of *Cryptococcus neoformans* and their virulence for mice. *J. Bacteriol* **150**, 1414–1421 (1982).
 17. Wang, Y.; Aisen, P.; Casadevall, A. Melanin, melanin “ghosts,” and melanin composition in *Cryptococcus neoformans*. *Infect. Immun* **64**, 2420–2424 (1996).
 18. De Leon-Rodriguez, C. M.; Rossi, D. C. P.; Fu, M. S.; Dragotakes, Q.; Coelho, C.; Guerrero Ros, I.; Caballero, B.; Nolan, S. J.; Casadevall, A. The Outcome of the *Cryptococcus neoformans*–Macrophage Interaction Depends on Phagolysosomal Membrane Integrity. *The Journal of Immunology* **201**, 583–603 (2018).
 19. Bain, J. M.; Lewis, L. E.; Okai, B.; Quinn, J.; Gow, N. A. R.; Erwig, L.-P. Non-lytic expulsion/exocytosis of *Candida albicans* from macrophages. *Fungal genetics and biology: FG & B* **49**, 677–678 (2012).
 20. Ma, H.; Croudace, J. E.; Lammas, D. A.; May, R. C. Direct cell-to-cell spread of a pathogenic yeast. *BMC immunology* **8**, 15 (2007). [PMID:17705831]
 21. Hoag, K. A.; Lipscomb, M. F.; Izzo, A. A.; Street, N. E. IL-12 and IFN-gamma are required for initiating the protective Th1 response to pulmonary cryptococcosis in resistant C.B-17 mice. *Am. J. Respir. Cell. Mol. Biol* **17**, 733–739 (1997).
 22. Chen, G.-H.; McDonald, R. A.; Wells, J. C.; Huffnagle, G. B.; Lukacs, N. W.; Toews, G. B. The Gamma Interferon Receptor Is Required for the Protective Pulmonary Inflammatory Response to *Cryptococcus neoformans*. *Infection and Immunity* **73**, 1788–1796 (2005). [PMID:15731080]
 23. Decken, K.; Kohler, G.; Palmer-Lehmann, K.; Wunderlin, A.; Mattner, F.; Magram, J.; Gately, M. K.; Alber, G. Interleukin-12 is essential for a protective Th1 response in mice infected with *Cryptococcus neoformans*. *Infect. Immun* **66**, 4994–5000 (1998).
 24. Osterholzer, J. J.; Surana, R.; Milam, J. E.; Montano, G. T.; Chen, G.-H. H.; Sonstein, J.; Curtis, J. L.; Huffnagle, G. B.; Toews, G. B.; Olszewski, M. A. Cryptococcal urease promotes the accumulation of immature dendritic cells and a non-protective T2 immune response within the lung. *Am J Pathol* **174**, 932–943 (2009). [PMID:19218345]
 25. Mills, C. D.; Kincaid, K.; Alt, J. M.; Heilman, M. J.; Hill, A. M. M-1/M-2 macrophages and the Th1/Th2 paradigm. *Journal of immunology (Baltimore, Md. : 1950)* **164**, 6166–6173 (2000). [PMID:10843666]

26. Tarique, A. A.; Logan, J.; Thomas, E.; Holt, P. G.; Sly, P. D.; Fantino, E. Phenotypic, Functional, and Plasticity Features of Classical and Alternatively Activated Human Macrophages. *American Journal of Respiratory Cell and Molecular Biology* **53**, 676–688 (2015). [PMID:25870903]
27. Canton, J.; Khezri, R.; Glogauer, M.; Grinstein, S. Contrasting phagosome pH regulation and maturation in human M1 and M2 macrophages. *Molecular biology of the cell* **25**, 3330–3341 (2014). [PMID:25165138]
28. Lukacs, G. L.; Rotstein, O. D.; Grinstein, S. Determinants of the phagosomal pH in macrophages. In situ assessment of vacuolar H(+)-ATPase activity, counterion conductance, and H+ “leak”. *The Journal of biological chemistry* **266**, 24540–24548 (1991). [PMID:1837024]
29. Mantegazza, A. R.; Savina, A.; Vermeulen, M.; Pérez, L.; Geffner, J.; Hermine, O.; Rosenzweig, S. D.; Faure, F.; Amigorena, S. NADPH oxidase controls phagosomal pH and antigen cross-presentation in human dendritic cells. *Blood* **112**, 4712–4722 (2008). [PMID:18682599]
30. Savina, A.; Jancic, C.; Hugues, S.; Guermonprez, P.; Vargas, P.; Moura, I. C.; Lennon-Duménil, A.-M.; Seabra, M. C.; Raposo, G.; Amigorena, S. NOX2 Controls Phagosomal pH to Regulate Antigen Processing during Crosspresentation by Dendritic Cells. *Cell* **126**, 205–218 (2006).
31. Rybicka, J. M.; Balce, D. R.; Khan, M. F.; Krohn, R. M.; Yates, R. M. NADPH oxidase activity controls phagosomal proteolysis in macrophages through modulation of the luminal redox environment of phagosomes. *Proceedings of the National Academy of Sciences of the United States of America* **107**, 10496–10501 (2010).
32. Flannagan, R. S.; Harrison, R. E.; Yip, C. M.; Jaqaman, K.; Grinstein, S. Dynamic macrophage “probing” is required for the efficient capture of phagocytic targets. *Journal of Cell Biology* **191**, 1205–1218 (2010).
33. van Lookeren Campagne, M.; Wiesmann, C.; Brown, E. J. Macrophage complement receptors and pathogen clearance. *Cellular Microbiology* **9**, 2095–2102 (2007).
34. Park, H.; Cox, D. Cdc42 Regulates Fc γ Receptor-mediated Phagocytosis through the Activation and Phosphorylation of Wiskott-Aldrich Syndrome Protein (WASP) and Neural-WASP. *Molecular Biology of the Cell* **20**, 4500–4508 (2009).
35. Hall, A. B.; Gakidis, M. A. M.; Glogauer, M.; Wilsbacher, J. L.; Gao, S.; Swat, W.; Brugge, J. S. Requirements for Vav Guanine Nucleotide Exchange Factors and Rho GTPases in Fc γ R- and Complement-Mediated Phagocytosis. *Immunity* **24**, 305–316 (2006).
36. Abram, C. L.; Lowell, C. A. The Ins and Outs of Leukocyte Integrin Signaling. *Annual Review of Immunology* **27**, 339–362 (2009).
37. Colucci-Guyon, E.; Niedergang, F.; Wallar, B. J.; Peng, J.; Alberts, A. S.; Chavrier, P. A role for mammalian diaphanous-related formins in complement receptor (CR3)-mediated phagocytosis in macrophages. *Current Biology* **15**, 2007–2012 (2005).

38. Freeman, S. A.; Grinstein, S. Phagocytosis: Receptors, signal integration, and the cytoskeleton. *Immunological Reviews* **262**, 193–215 (2014).
39. Johnston, S. A.; May, R. C. Cryptococcus interactions with macrophages: evasion and manipulation of the phagosome by a fungal pathogen. *Cellular Microbiology* **15**, 403–411 (2013).
40. Bajno, L.; Peng, X. R.; Schreiber, A. D.; Moore, H. P.; Trimble, W. S.; Grinstein, S. Focal exocytosis of VAMP3-containing vesicles at sites of phagosome formation. *Journal of Cell Biology* **149**, 697–705 (2000).
41. Li, G.; Barbieri, M. A.; Colombo, M. I.; Stahl, P. D. Structural features of the GTP-binding defective Rab5 mutants required for their inhibitory activity on endocytosis. *The Journal of biological chemistry* **269**, 14631–14635 (1994). [PMID:8182071]
42. Desjardins, M.; Celis, J. E.; Van Meer, G.; Dieplinger, H.; Jahraus, A.; Griffiths, G.; Huber, L. A. Molecular characterization of phagosomes. *Journal of Biological Chemistry* **269**, 32194–32200 (1994). [PMID:7798218]
43. Vieira, O. V.; Bucci, C.; Harrison, R. E.; Trimble, W. S.; Lanzetti, L.; Gruenberg, J.; Schreiber, A. D.; Stahl, P. D.; Grinstein, S. Modulation of Rab5 and Rab7 Recruitment to Phagosomes by Phosphatidylinositol 3-Kinase. *Molecular and Cellular Biology* **23**, 2501–2514 (2003). [PMID:12640132]
44. Vieira, O. V.; Botelho, R. J.; Rameh, L.; Brachmann, S. M.; Matsuo, T.; Davidson, H. W.; Schreiber, A.; Backer, J. M.; Cantley, L. C.; Grinstein, S. Distinct roles of class I and class III phosphatidylinositol 3-kinases in phagosome formation and maturation. *Journal of Cell Biology* **155**, 19–25 (2001).
45. Simonsen, A.; Lippé, R.; Christoforidis, S.; Gaullier, J. M.; Brech, A.; Callaghan, J.; Toh, B. H.; Murphy, C.; Zerial, M.; Stenmark, H. EEA1 links PI(3)K function to Rab5 regulation of endosome fusion. *Nature* **394**, 494–498 (1998).
46. Wozniak, K. L.; Levitz, S. M. Cryptococcus neoformans enters the endolysosomal pathway of dendritic cells and is killed by lysosomal components. *Infection and Immunity* **76**, 4764–4771 (2008).
47. Christoforidis, S.; McBride, H. M.; Burgoyne, R. D.; Zerial, M. The rab5 effector EEA1 is a core component of endosome docking. *Nature* **397**, 621–625 (1999).
48. Kissing, S.; Hermsen, C.; Repnik, U.; Nasset, C. K.; Von Bargen, K.; Griffiths, G.; Ichihara, A.; Lee, B. S.; Schwake, M.; De Brabander, J.; Haas, A.; Saftig, P. Vacuolar ATPase in phagosome-lysosome fusion. *Journal of Biological Chemistry* **290**, 14166–14180 (2015).
49. Harrison, R. E.; Bucci, C.; Vieira, O. V.; Schroer, T. A.; Grinstein, S. Phagosomes Fuse with Late Endosomes and/or Lysosomes by Extension of Membrane Protrusions along Microtubules: Role of Rab7 and RILP. *Molecular and Cellular Biology* **23**, 6494–6506 (2003). [PMID:12944476]
50. Mottola, G. The complexity of Rab5 to Rab7 transition guarantees specificity of pathogen

subversion mechanisms. *Frontiers in Cellular and Infection Microbiology* **4**, (2014).

51. Vitelli, R.; Santillo, M.; Lattero, D.; Chiariello, M.; Bifulco, M.; Bruni, C. B.; Bucci, C. Role of the small GTPase RAB7 in the late endocytic pathway. *Journal of Biological Chemistry* **272**, 4391–4397 (1997).
52. Jeschke, A.; Zehethofer, N.; Lindner, B.; Krupp, J.; Schwudke, D.; Haneburger, I.; Jovic, M.; Backer, J. M.; Balla, T.; Hilbi, H.; Haas, A. Phosphatidylinositol 4-phosphate and phosphatidylinositol 3-phosphate regulate phagolysosome biogenesis. *Proceedings of the National Academy of Sciences of the United States of America* **112**, 4636–4641 (2015).
53. Eskelinen, E. L.; Tanaka, Y.; Saftig, P. *Trends in Cell Biology*. Elsevier Ltd March 1, 2003, pp 137–145
54. Huynh, K. K.; Eskelinen, E. L.; Scott, C. C.; Malevanets, A.; Saftig, P.; Grinstein, S. LAMP proteins are required for fusion of lysosomes with phagosomes. *EMBO Journal* **26**, 313–324 (2007).
55. Flannagan, R. S.; Cosío, G.; Grinstein, S. *Nature Reviews Microbiology*. 2009, pp 355–366
56. Sun-Wada, G. H.; Tabata, H.; Kawamura, N.; Aoyama, M.; Wada, Y. Direct recruitment of H⁺-ATPase from lysosomes for phagosomal acidification. *J Cell Sci* **122**, 2504–2513 (2009). [PMID:19549681]
57. Botelho, R. J.; Hackam, D. J.; Schreiber, A. D.; Grinstein, S. Role of COPI in phagosome maturation. *Journal of Biological Chemistry* **275**, 15717–15727 (2000).
58. Nguyen, G. T.; Green, E. R.; Meccas, J. *Frontiers in Cellular and Infection Microbiology*. Frontiers Media S.A. August 25, 2017
59. Helfinger, V.; Palfi, K.; Weigert, A.; Schröder, K. The NADPH oxidase Nox4 controls macrophage polarization in an NFκB-dependent manner. *Oxidative Medicine and Cellular Longevity* **2019**, (2019).
60. Cross, A. R.; Segal, A. W. *Biochimica et Biophysica Acta - Bioenergetics*. June 28, 2004, pp 1–22
61. Panday, A.; Sahoo, M. K.; Osorio, D.; Batra, S. *Cellular and Molecular Immunology*. Chinese Soc Immunology January 8, 2015, pp 5–23
62. Braun, V.; Fraisier, V.; Raposo, G.; Hurbain, I.; Sibarita, J. B.; Chavrier, P.; Galli, T.; Niedergang, F. TI-VAMP/VAMP7 is required for optimal phagocytosis of opsonised particles in macrophages. *EMBO Journal* **23**, 4166–4176 (2004).
63. Conus, S.; Simon, H. U. *Swiss Medical Weekly*. EMH Swiss Medical Publishers Ltd. 2010
64. Turk, V.; Stoka, V.; Vasiljeva, O.; Renko, M.; Sun, T.; Turk, B.; Turk, D. *Biochimica et Biophysica Acta - Proteins and Proteomics*. January 2012, pp 68–88
65. Conus, S.; Perozzo, R.; Reinheckel, T.; Peters, C.; Scapozza, L.; Yousefi, S.; Simon, H. U. Caspase-8 is activated by cathepsin D initiating neutrophil apoptosis during the

- resolution of inflammation. *Journal of Experimental Medicine* **205**, 685–698 (2008).
66. Hole, C. R.; Bui, H.; Wormley, F. L.; Wozniak, K. L. Mechanisms of dendritic cell lysosomal killing of cryptococcus. *Scientific Reports* **2**, (2012).
 67. Rodriguez-Franco, E. J.; Cantres-Rosario, Y. M.; Plaud-Valentin, M.; Romeu, R.; Rodríguez, Y.; Skolasky, R.; Meléndez, V.; Cadilla, C. L.; Melendez, L. M. Dysregulation of macrophage-secreted cathepsin B contributes to HIV-1-linked neuronal apoptosis. *PLoS ONE* **7**, (2012).
 68. Kaplan, A.; Achord, D. T.; Sly, W. S. Phosphohexosyl components of a lysosomal enzyme are recognized by pinocytosis receptors on human fibroblasts. *Proceedings of the National Academy of Sciences of the United States of America* **74**, 2026–2030 (1977). [PMID:266721]
 69. Qin, Q.-M.; Luo, J.; Lin, X.; Pei, J.; Li, L.; Ficht, T. A.; de Figueiredo, P. Functional analysis of host factors that mediate the intracellular lifestyle of *Cryptococcus neoformans*. *PLoS pathogens* **7**, e1002078 (2011).
 70. Nicola, A. M.; Robertson, E. J.; Albuquerque, P.; Derengowski, L. da S.; Casadevall, A. Nonlytic Exocytosis of *Cryptococcus neoformans* from Macrophages Occurs In Vivo and Is Influenced by Phagosomal pH. *mBio* **2**, e00167-11 (2011). [PMID:21828219]
 71. Klionsky, D. J.; Eskelinen, E. L.; Deretic, V. *Autophagy*. Taylor and Francis Inc. 2014, pp 549–551
 72. Stukes, S.; Coelho, C.; Rivera, J.; Jedlicka, A. E.; Hajjar, K. A.; Casadevall, A. The Membrane Phospholipid Binding Protein Annexin A2 Promotes Phagocytosis and Nonlytic Exocytosis of *Cryptococcus neoformans* and Impacts Survival in Fungal Infection. *J Immunol* (2016). [PMID:27371724]
 73. Nicola, A. M.; Albuquerque, P.; Martinez, L. R.; Dal-Rosso, R. A.; Saylor, C.; De Jesus, M.; Nosanchuk, J. D.; Casadevall, A. Macrophage autophagy in immunity to *Cryptococcus neoformans* and *Candida albicans*. *Infect. Immun* **80**, 3065–3076 (2012).
 74. Warris, A.; Ballou, E. R. *Seminars in Cell and Developmental Biology*. Elsevier Ltd May 1, 2019, pp 34–46
 75. Dupré-Crochet, S.; Erard, M.; Nüße, O. ROS production in phagocytes: why, when, and where? *Journal of Leukocyte Biology* **94**, 657–670 (2013).
 76. Nathan, C.; Sciences, M. S. the N. A. of; 2000, undefined. Reactive oxygen and nitrogen intermediates in the relationship between mammalian hosts and microbial pathogens. *National Acad Sciences*
 77. Slauch, J. M. How does the oxidative burst of macrophages kill bacteria? Still an open question. *Molecular Microbiology* **80**, 580–583 (2011).
 78. Aratani, Y.; Kura, F.; Watanabe, H.; Akagawa, H.; Takano, Y.; Suzuki, K.; Dinauer, M. C.; Maeda, N.; Koyama, H. Relative contributions of myeloperoxidase and NADPH-oxidase

to the early host defense against pulmonary infections with *Candida albicans* and *Aspergillus fumigatus*. *Medical Mycology* **40**, 557–563 (2002).

79. Brovkovich, V.; Gao, X. P.; Ong, E.; Brovkovich, S.; Brennan, M. L.; Su, X.; Hazen, S. L.; Malik, A. B.; Skidgel, R. A. Augmented inducible nitric oxide synthase expression and increased NO production reduce sepsis-induced lung injury and mortality in myeloperoxidase-null mice. *American Journal of Physiology - Lung Cellular and Molecular Physiology* **295**, (2008).
80. Das, P.; Lahiri, A.; Lahiri, A.; Chakravorty, D. Modulation of the Arginase Pathway in the Context of Microbial Pathogenesis: A Metabolic Enzyme Moonlighting as an Immune Modulator. *PLoS Pathogens* **6**, e1000899 (2010).
81. Liemburg-Apers, D. C.; Willems, P. H. G. M.; Koopman, W. J. H.; Grefte, S. *Archives of Toxicology*. Springer Verlag August 25, 2015, pp 1209–1226
82. Cox, G. M.; Harrison, T. S.; McDade, H. C.; Taborda, C. P.; Heinrich, G.; Casadevall, A.; Perfect, J. R. Superoxide dismutase influences the virulence of *Cryptococcus neoformans* by affecting growth within macrophages. *Infect. Immun* **71**, 173–180 (2003).
83. Chaturvedi, V.; Wong, B.; Newman, S. L. Oxidative killing of *Cryptococcus neoformans* by human leukocytes. Evidence that fungal mannitol protects by scavenging reactive oxygen intermediates. *J. Immunol* **156**, 3836–3840 (1996).
84. Silva, M. B.; Thomaz, L.; Marques, A. F.; Svidzinski, A. E.; Nosanchuk, J. D.; Casadevall, A.; Travassos, L. R.; Taborda, C. P. Resistance of melanized yeast cells of *Paracoccidioides brasiliensis* to antimicrobial oxidants and inhibition of phagocytosis using carbohydrates and monoclonal antibody to CD18. *Mem. Inst. Oswaldo Cruz* **104**, 644–648 (2009).
85. Tsai, H. F.; Chang, Y. C.; Washburn, R. G.; Wheeler, M. H.; Kwon-Chung, K. J. The developmentally regulated *alb1* gene of *Aspergillus fumigatus*: Its role in modulation of conidial morphology and virulence. *Journal of Bacteriology* **180**, 3031–3038 (1998). [PMID:9620950]
86. Missall, T. A.; Moran, J. M.; Corbett, J. A.; Lodge, J. K. Distinct stress responses of two functional laccases in *Cryptococcus neoformans* are revealed in the absence of the thiol-specific antioxidant Tsa1. *Eukaryot. Cell* **4**, 202–208 (2005).
87. Brown, S. M.; Campbell, L. T.; Lodge, J. K. *Cryptococcus neoformans*, a fungus under stress. *Curr. Opin. Microbiol* **10**, 320–325 (2007).
88. Doering, T. L.; Nosanchuk, J. D.; Roberts, W. K.; Casadevall, A. Melanin as a potential cryptococcal defence against microbicidal proteins. *Medical mycology* **37**, 175–181 (1999). [PMID:10421849]
89. Narasipura, S. D.; Ault, J. G.; Behr, M. J.; Chaturvedi, V.; Chaturvedi, S. Characterization of Cu,Zn superoxide dismutase (SOD1) gene knock-out mutant of *Cryptococcus neoformans* var. *gattii*: Role in biology and virulence. *Molecular Microbiology* **47**, 1681–1694 (2003).
90. Nordenfelt, P.; Tapper, H. Phagosome dynamics during phagocytosis by neutrophils.

- Journal of Leukocyte Biology* **90**, 271–284 (2011). [PMID:21504950]
91. Cornet, M.; Gaillardin, C. *Eukaryotic Cell*. March 2014, pp 342–352
 92. Alanio, A.; Vernel-Pauillac, F.; Sturny-Leclère, A.; Dromer, F. *Cryptococcus neoformans* host adaptation: toward biological evidence of dormancy. *mBio* **6**, (2015).
 93. Sorrell, T. C.; Juillard, P. G.; Djordjevic, J. T.; Kaufman-Francis, K.; Dietmann, A.; Milonig, A.; Combes, V.; Grau, G. E. Cryptococcal transmigration across a model brain blood-barrier: evidence of the Trojan horse mechanism and differences between *Cryptococcus neoformans* var. *grubii* strain H99 and *Cryptococcus gattii* strain R265. *Microbes Infect* **18**, 57–67 (2016). [PMID:26369713]
 94. Santiago-Tirado, F. H.; Onken, M. D.; Cooper, J. A.; Klein, R. S.; Doering, T. L. Trojan Horse Transit Contributes to Blood-Brain Barrier Crossing of a Eukaryotic Pathogen. *mBio* **8**, (2017).
 95. Broderick, N. A. A common origin for immunity and digestion. *Front Immunol* **6**, 72 (2015). [PMID:25745424]
 96. Rosales, C.; Uribe-Querol, E. Phagocytosis: A Fundamental Process in Immunity. *Biomed Res Int* **2017**, 9042851 (2017). [PMID:28691037]
 97. Kinchen, J. M.; Ravichandran, K. S. Phagosome maturation: going through the acid test. *Nat Rev Mol Cell Biol* **9**, 781–795 (2008). [PMID:18813294]
 98. Jankowski, A.; Scott, C. C.; Grinstein, S. Determinants of the phagosomal pH in neutrophils. *J Biol Chem* **277**, 6059–6066 (2002). [PMID:11744729]
 99. Bouvier, G.; Benoliel, A. M.; Foa, C.; Bongrand, P. Relationship between phagosome acidification, phagosome-lysosome fusion, and mechanism of particle ingestion. *J Leukoc Biol* **55**, 729–734 (1994). [PMID:8195699]
 100. Geisow, M. J.; D’Arcy Hart, P.; Young, M. R. Temporal changes of lysosome and phagosome pH during phagolysosome formation in macrophages: studies by fluorescence spectroscopy. *J Cell Biol* **89**, 645–652 (1981). [PMID:6166620]
 101. Feldmesser, M.; Kress, Y.; Novikoff, P.; Casadevall, A. *Cryptococcus neoformans* is a facultative intracellular pathogen in murine pulmonary infection. *Infection and Immunity* **68**, 4225–4237 (2000).
 102. Ma, H.; Croudace, J. E.; Lammas, D. A.; May, R. C. Expulsion of Live Pathogenic Yeast by Macrophages. *Current Biology* **16**, 2156–2160 (2006). [PMID:17084701]
 103. Alvarez, M.; Casadevall, A. Phagosome fusion and extrusion, and host cell survival following *Cryptococcus neoformans* phagocytosis by macrophages. *Current Biology* **16**, 2161–2165 (2006).
 104. Alvarez, M.; Casadevall, A. Cell-to-cell spread and massive vacuole formation after *Cryptococcus neoformans* infection of murine macrophages. *BMC immunology* **8**, 16 (2007).

105. Freij, J. B.; Fu, M. S.; De Leon Rodriguez, C. M.; Dziejczak, A.; Jedlicka, A. E.; Dragotakes, Q.; Rossi, D. C. P.; Jung, E. H.; Coelho, C.; Casadevall, A. Conservation of Intracellular Pathogenic Strategy among Distantly Related Cryptococcal Species. *Infection and Immunity* **86**, (2018).
106. Zunino, L.; Soriano, M. C.; Rosso, O. A. Distinguishing chaotic and stochastic dynamics from time series by using a multiscale symbolic approach. *Phys. Rev. E. Stat. Nonlin. Soft. Matter Phys* **86**, 46210 (2012).
107. Kulp, C. W.; Zunino, L. Discriminating chaotic and stochastic dynamics through the permutation spectrum test. *Chaos* **24**, 33116 (2014). [PMID:25273196]
108. Smith, L. M.; Dixon, E. F.; May, R. C. The fungal pathogen *Cryptococcus neoformans* manipulates macrophage phagosome maturation. *Cellular Microbiology* **17**, 702–713 (2015). [PMID:25394938]
109. Davis, M. J.; Eastman, A. J.; Qiu, Y.; Gregorka, B.; Kozel, T. R.; Osterholzer, J. J.; Curtis, J. L.; Swanson, J. A.; Olszewski, M. A. *Cryptococcus neoformans*-induced macrophage lysosome damage crucially contributes to fungal virulence. *J Immunol* **194**, 2219–2231 (2015). [PMID:25637026]
110. McCullough, M.; Sakellariou, K.; Stemler, T.; Small, M. Counting forbidden patterns in irregularly sampled time series. I. The effects of under-sampling, random depletion, and timing jitter. *Chaos* **26**, 123103 (2016).
111. Sakellariou, K.; McCullough, M.; Stemler, T.; Small, M. Counting forbidden patterns in irregularly sampled time series. ii. reliability in the presence of highly irregular sampling. *Chaos* **26**, 123104 (2016).
112. Rosso, O. A.; Carpi, L. C.; Saco, P. M.; Ravetti, M. G.; Larrondo, H. A.; Plastino, A. Noisy-chaotic time series and the forbidden/missing patterns paradigm. (2011).
113. Skiadas, C. H.; Skiadas, C. *Handbook of applications of chaos theory*
114. McCullough, M.; Sakellariou, K.; Stemler, T.; Small, M. Counting forbidden patterns in irregularly sampled time series. I. The effects of under-sampling, random depletion, and timing jitter. *Chaos* **26**, 123103 (2016).
115. Sakellariou, K.; McCullough, M.; Stemler, T.; Small, M. Counting forbidden patterns in irregularly sampled time series. ii. reliability in the presence of highly irregular sampling. *Chaos* **26**, 123104 (2016).
116. Rosso, O. A.; Carpi, L. C.; Saco, P. M.; Ravetti, M. G.; Larrondo, H. A.; Plastino, A. Noisy-chaotic time series and the forbidden/missing patterns paradigm. (2011).
117. Fierer, N.; Jackson, R. B. The diversity and biogeography of soil bacterial communities. *Proc Natl Acad Sci U S A* **103**, 626–631 (2006). [PMID:16407148]
118. Baath K., E. ;Arnebrand. Growth rate and response of bacterial communities to pH in limed and ash treated forest soils. *Soil Biol. Biochem.* **26**, 995–1001 (1994).

119. Baath, E.; Frostegard, A.; Fritze, H. Soil Bacterial Biomass, Activity, Phospholipid Fatty Acid Pattern, and pH Tolerance in an Area Polluted with Alkaline Dust Deposition. *Appl Environ Microbiol* **58**, 4026–4031 (1992). [PMID:16348828]
120. Karlin, S.; Lieberman, U. Random temporal variation in selection intensities: case of large population size. *Theoretical population biology* **6**, 355–382 (1974). [PMID:4460262]
121. Quintin, J.; Saeed, S.; Martens, J. H. A.; Giamarellos-Bourboulis, E. J.; Ifrim, D. C.; Logie, C.; Jacobs, L.; Jansen, T.; Kullberg, B.-J.; Wijmenga, C.; Joosten, L. A. B.; Xavier, R. J.; van der Meer, J. W. M.; Stunnenberg, H. G.; Netea, M. G. *Candida albicans* infection affords protection against reinfection via functional reprogramming of monocytes. *Cell host & microbe* **12**, 223–232 (2012). [PMID:22901542]
122. Sau, K.; Mambula, S. S.; Latz, E.; Henneke, P.; Golenbock, D. T.; Levitz, S. M. The Antifungal Drug Amphotericin B Promotes Inflammatory Cytokine Release by a Toll-like Receptor- and CD14-dependent Mechanism. *Journal of Biological Chemistry* **278**, 37561–37568 (2003). [PMID:12860979]
123. Casadevall, A.; Coelho, C.; Alanio, A. Mechanisms of *Cryptococcus neoformans*-Mediated Host Damage. *Front Immunol* **9**, 855 (2018). [PMID:29760698]
124. Coelho, C.; Souza, A. C. O.; Derengowski, L. da S.; de Leon-Rodriguez, C.; Wang, B.; Leon-Rivera, R.; Bocca, A. L.; Gonçalves, T.; Casadevall, A. Macrophage mitochondrial and stress response to ingestion of *Cryptococcus neoformans*. *Journal of Immunology (Baltimore, Md.: 1950)* **194**, 2345–2357 (2015).
125. Alspaugh, J. A.; Granger, D. L. Inhibition of *Cryptococcus neoformans* replication by nitrogen oxide supports the role of these molecules as effectors of macrophage-mediated cystostasis. *Infect. Immun* **59**, 2291–2296 (1991).
126. Oh, Y. K.; Straubinger, R. M. Intracellular fate of *Mycobacterium avium*: use of dual-label spectrofluorometry to investigate the influence of bacterial viability and opsonization on phagosomal pH and phagosome-lysosome interaction. *Infect Immun* **64**, 319–325 (1996). [PMID:8557358]
127. Griffiths, G. On phagosome individuality and membrane signalling networks. *Trends Cell Biol* **14**, 343–351 (2004). [PMID:15246427]
128. Mallik, K. C. B.; Banerjee, P. L.; Chatterjee, B. D.; Pramanick, M. An experimental study of the course of infection in mice after intranasal insufflation with *Cryptococcus neoformans*. *Ind. J. Med. Res* **54**, 608–610 (1966).
129. Paul, D.; Achouri, S.; Yoon, Y.-Z.; Herre, J.; Bryant, C. E.; Cicuta, P. Phagocytosis dynamics depends on target shape. *Biophysical journal* **105**, 1143–1150 (2013). [PMID:24010657]
130. Dragotakes, Q.; Fu, M. S.; Casadevall, A. Dragocytosis: Elucidation of the Mechanism for *Cryptococcus neoformans* Macrophage-to-Macrophage Transfer. *The Journal of Immunology* **ji1801118** (2019). [PMID:30877168]
131. Cherniak, R.; Valafar, H.; Morris, L. C.; Valafar, F. *Cryptococcus neoformans* chemotyping

by quantitative analysis of ¹H NMR spectra of glucuronoxylomannans using a computer simulated artificial neural network. *Clin. Diagn. Lab. Immunol* **5**, 146–159 (1998).

132. Westman, J.; Moran, G.; Mogavero, S.; Hube, B.; Grinstein, S. Candida albicans Hyphal Expansion Causes Phagosomal Membrane Damage and Luminal Alkalinization. *MBio* **9**, (2018). [PMID:30206168]
133. Weber, S. M.; Levitz, S. M. Chloroquine antagonizes the proinflammatory cytokine response to opportunistic fungi by alkalinizing the fungal phagolysosome. *J Infect Dis* **183**, 935–942 (2001). [PMID:11237811]
134. Harrison, T. S.; Griffin, G. E.; Levitz, S. M. Conditional lethality of the diprotic weak bases chloroquine and quinacrine against *Cryptococcus neoformans*. *J. Infect. Dis* **182**, 283–289 (2000).
135. Artavanis-Tsakonas, K.; Love, J. C.; Ploegh, H. L.; Vyas, J. M. Recruitment of CD63 to *Cryptococcus neoformans* phagosomes requires acidification. *Proc. Natl. Acad. Sci. U. S. A* **103**, 15945–15950 (2006).
136. Yates, R. M.; Russell, D. G. Phagosome Maturation Proceeds Independently of Stimulation of Toll-like Receptors 2 and 4. *Immunity* **23**, 409–417 (2005).
137. Rathman, M.; Sjaastad, M. D.; Falkow, S. Acidification of phagosomes containing *Salmonella typhimurium* in murine macrophages. *Infect Immun* **64**, 2765–2773 (1996). [PMID:8698506]
138. Queval, C. J.; Brosch, R.; Simeone, R. The Macrophage: A Disputed Fortress in the Battle against *Mycobacterium tuberculosis*. *Front Microbiol* **8**, 2284 (2017). [PMID:29218036]
139. Gillard, J. J.; Laws, T. R.; Lythe, G.; Molina-Paris, C. Modeling early events in *Francisella tularensis* pathogenesis. *Front Cell Infect Microbiol* **4**, 169 (2014). [PMID:25566509]
140. Darwin, C. *The Foundation of the Origin of Species: Two Essays Written in 1842 and 1844*. ; Cambridge University Press: Cambridge, UK, 1909
141. Slatkin, M. Cascading speciation. *Nature* **252**, 701–702 (1974). [PMID:4437620]
142. Philippi, T.; Seger, J. Hedging one's evolutionary bets, revisited. *Trends Ecol Evol* **4**, 41–44 (1989). [PMID:21227310]
143. Bergman, A. . T. M. On the Natural Selection of Market Choice. *Autonomous Agents and Multi-Agent Systems* **5**, 387–395 (2002).
144. Olofsson, H.; Ripa, J.; Jonzén, N. Bet-hedging as an evolutionary game: the trade-off between egg size and number. *Proceedings. Biological sciences* **276**, 2963–2969 (2009). [PMID:19474039]
145. Heiple, J. M.; Taylor, D. L. pH changes in pinosomes and phagosomes in the ameba, *Chaos carolinensis*. *The Journal of Cell Biology* **94**, 143–149 (1982). [PMID:7119011]
146. Watts, C.; Marsh, M.; Martin, J. B.; Satre, M.; Martin, J. B.; Satre, M. Endocytosis: what

- goes in and how? *Journal of cell science* **103 (Pt 1)**, 1–8 (1992). [PMID:1429899]
147. Curran, R. E.; Claxton, C. R. J.; Hutchison, L.; Harradine, P. J.; Martin, I. J.; Littlewood, P. Control and Measurement of Plasma pH in Equilibrium Dialysis: Influence on Drug Plasma Protein Binding. *Drug Metabolism and Disposition* **39**, 551–557 (2011). [PMID:21098647]
 148. Davis, M. J.; Tsang, T. M.; Qiu, Y.; Dayrit, J. K.; Freij, J. B.; Huffnagle, G. B.; Olszewski, M. A. Macrophage M1/M2 polarization dynamically adapts to changes in cytokine microenvironments in *Cryptococcus neoformans* infection. *mBio* **4**, e00264-00213 (2013). [PMID:23781069]
 149. Leopold Wager, C. M.; Wormley, F. L. Classical versus alternative macrophage activation: the Ying and the Yang in host defense against pulmonary fungal infections. *Mucosal Immunology* **7**, 1023–1035 (2014). [PMID:25073676]
 150. Leung, C.-Y.; Palmer, L. C.; Kewalramani, S.; Qiao, B.; Stupp, S. I.; Olvera de la Cruz, M.; Bedzyk, M. J. Crystalline polymorphism induced by charge regulation in ionic membranes. *Proceedings of the National Academy of Sciences of the United States of America* **110**, 16309–16314 (2013). [PMID:24065818]
 151. Jacobsohn, M. K.; Lehman, M. M.; Jacobsohn, G. M. Cell membranes and multilamellar vesicles: Influence of pH on solvent induced damage. *Lipids* **27**, 694–700 (1992).
 152. Weber, S. M.; Levitz, S. M.; Harrison, T. S. Chloroquine and the fungal phagosome. *Current Opinion in Microbiology* **3**, 349–353 (2000).
 153. Casadevall, A.; Pirofski, L. A. What Is a Host? Attributes of Individual Susceptibility. *Infect Immun* **86**, (2018). [PMID:29084893]
 154. Zhan, H.; Wang, H.; Liao, L.; Feng, Y.; Fan, X.; Zhang, L.; Chen, S. Kinetics and Novel Degradation Pathway of Permethrin in *Acinetobacter baumannii* ZH-14. *Front Microbiol* **9**, 98 (2018). [PMID:29456525]
 155. Raevuori, M.; Genigeorgis, C. Effect of pH and sodium chloride on growth of *Bacillus cereus* in laboratory media and certain foods. *Appl Microbiol* **29**, 68–73 (1975). [PMID:234158]
 156. Chenoweth, M. R.; Somerville, G. A.; Krause, D. C.; O'Reilly, K. L.; Gherardini, F. C. Growth characteristics of *Bartonella henselae* in a novel liquid medium: primary isolation, growth-phase-dependent phage induction, and metabolic studies. *Appl Environ Microbiol* **70**, 656–663 (2004). [PMID:14766538]
 157. Tamimi, H. A.; Hiltbrand, W.; Loercher, H. Some growth requirements of *Bacteroides fragilis*. *J Bacteriol* **80**, 472–476 (1960). [PMID:13775103]
 158. Venkatesh G.; Debral, A. K.; Kirpan, P.; Reers, M.; Murthy, P. V. V. S.; Swarupa, V.; Srikanth, L.; Sarma, P. V. G. K., K. ; Reine. pH Optimization and Production of High Potent Cellular Vaccine by *Bordetella pertussis*. *International Journal of Biotechnology and Bioengineering Research* **3**, 17–25 (2012).

159. *Bergey's Manual of Bacteriology. The Proteobacteria*, 2nd ed.; Brenner N.R.; Staley, J.T., D. J. ; Krie., Ed.; Springer: New York; Vol. 2
160. Jordan S.E., R. C. ; Jacob. The Effect of pH at Different Temperatures on the Growth of Bacterium coli with a Constant Food Supply. *J.Gen.Microbiol.* **2**, 15–24 (1948).
161. Silva, J.; Leite, D.; Fernandes, M.; Mena, C.; Gibbs, P. A.; Teixeira, P. Campylobacter spp. as a Foodborne Pathogen: A Review. *Front Microbiol* **2**, 200 (2011). [PMID:21991264]
162. Fisher, K.; Phillips, C. The ecology, epidemiology and virulence of Enterococcus. *Microbiology* **155**, 1749–1757 (2009). [PMID:19383684]
163. Gera, K.; McIver, K. S. Laboratory growth and maintenance of Streptococcus pyogenes (the Group A Streptococcus, GAS). *Curr Protoc Microbiol* **30**, Unit 9D.2. (2013). [PMID:24510893]
164. Savic, D. J.; McShan, W. M. Long-term survival of Streptococcus pyogenes in rich media is pH-dependent. *Microbiology* **158**, 1428–1436 (2012). [PMID:22361943]
165. Yang, Q.; Porter, A. J.; Zhang, M.; Harrington, D. J.; Black, G. W.; Sutcliffe, I. C. The impact of pH and nutrient stress on the growth and survival of Streptococcus agalactiae. *Antonie Van Leeuwenhoek* **102**, 277–287 (2012). [PMID:22527623]
166. Goodman, N. L.; Larsh, H. W. Environmental factors and growth of Histoplasma capsulatum in soil. *Mycopathol Mycol Appl* **33**, 145–156 (1967). [PMID:5585327]
167. Wadowsky, R. M.; Wolford, R.; McNamara, A. M.; Yee, R. B. Effect of temperature, pH, and oxygen level on the multiplication of naturally occurring Legionella pneumophila in potable water. *Appl Environ Microbiol* **49**, 1197–1205 (1985). [PMID:4004233]
168. Tienungoon, S.; Ratkowsky, D. A.; McMeekin, T. A.; Ross, T. Growth limits of Listeria monocytogenes as a function of temperature, pH, NaCl, and lactic acid. *Appl Environ Microbiol* **66**, 4979–4987 (2000). [PMID:11055952]
169. Conner, D. E.; Brackett, R. E.; Beuchat, L. R. Effect of temperature, sodium chloride, and pH on growth of Listeria monocytogenes in cabbage juice. *Appl Environ Microbiol* **52**, 59–63 (1986). [PMID:3089158]
170. Piddington, D. L.; Kashkouli, A.; Buchmeier, N. A. Growth of Mycobacterium tuberculosis in a defined medium is very restricted by acid pH and Mg(2+) levels. *Infect Immun* **68**, 4518–4522 (2000). [PMID:10899850]
171. Portaels, F.; Pattyn, S. R. Growth of mycobacteria in relation to the pH of the medium. *Ann Microbiol (Paris)* **133**, 213–221 (1982). [PMID:7149523]
172. Pettit, R. K.; McAllister, S. C.; Hamer, T. A. Response of gonococcal clinical isolates to acidic conditions. *J Med Microbiol* **48**, 149–156 (1999). [PMID:9989642]
173. Brookes, R.; Sikyta, B. Influence of pH on the growth characteristics of Neisseria gonorrhoeae in continuous culture. *Appl Microbiol* **15**, 224–227 (1967). [PMID:4961768]

174. Kohman, E. F. The So-called Reduced Oxygen Tension for Growing the Meningococcus. *J Bacteriol* **4**, 571–584 (1919). [PMID:16558853]
175. Tsuji, A.; Kaneko, Y.; Takahashi, K.; Ogawa, M.; Goto, S. The effects of temperature and pH on the growth of eight enteric and nine glucose non-fermenting species of gram-negative rods. *Microbiol Immunol* **26**, 15–24 (1982). [PMID:7087800]
176. Stokes, J. L.; Bayne, H. G. Growth rates of Salmonella colonies. *J Bacteriol* **74**, 200–206 (1957). [PMID:13475221]
177. Valero, A.; Perez-Rodriguez, F.; Carrasco, E.; Fuentes-Alventosa, J. M.; Garcia-Gimeno, R. M.; Zurera, G. Modelling the growth boundaries of Staphylococcus aureus: Effect of temperature, pH and water activity. *Int J Food Microbiol* **133**, 186–194 (2009). [PMID:19523705]
178. Dernby, K. G.; Avery, O. T. THE OPTIMUM HYDROGEN ION CONCENTRATION FOR THE GROWTH OF PNEUMOCOCCUS. *J Exp Med* **28**, 345–357 (1918). [PMID:19868263]
179. Williams, R. P.; Gott, C. L.; Qadri, S. M.; Scott, R. H. Influence of temperature of incubation and type of growth medium on pigmentation in Serratia marcescens. *J Bacteriol* **106**, 438–443 (1971). [PMID:4929859]
180. Giri, A. V.; Anandkumar, N.; Muthukumaran, G.; Pennathur, G. A novel medium for the enhanced cell growth and production of prodigiosin from Serratia marcescens isolated from soil. *BMC Microbiol* **4**, 11 (2004). [PMID:15113456]
181. Erlandson Jr., A. L.; Mackey, W. H. Nutrition of Shigella: growth of Shigella flexneri in a simple chemically defined medium. *J Bacteriol* **75**, 253–257 (1958). [PMID:13513593]
182. Patel M.;Gouws,E., M. ;Isaacso. Effect of Iron and pH on the survival of Vibrio cholerae in water. *Transactions of the Royal Society of Tropical Medicine and Hygiene* **89**, 175–177 (1995).
183. Huq, A.; West, P. A.; Small, E. B.; Huq, M. I.; Colwell, R. R. Influence of water temperature, salinity, and pH on survival and growth of toxigenic Vibrio cholerae serovar 01 associated with live copepods in laboratory microcosms. *Appl Environ Microbiol* **48**, 420–424 (1984). [PMID:6486784]
184. Adams, M. R.; Little, C. L.; Easter, M. C. Modelling the effect of pH, acidulant and temperature on the growth rate of Yersinia enterocolitica. *J Appl Bacteriol* **71**, 65–71 (1991). [PMID:1894580]
185. Brubaker, R. R. Influence of Na(+), dicarboxylic amino acids, and pH in modulating the low-calcium response of Yersinia pestis. *Infect Immun* **73**, 4743–4752 (2005). [PMID:16040987]
186. Perry, R. D.; Fetherston, J. D. Yersinia pestis--etiologic agent of plague. *Clin. Microbiol. Rev* **10**, 35–66 (1997).
187. Alvarez, M.; Casadevall, A. Phagosome Extrusion and Host-Cell Survival after

- Cryptococcus neoformans Phagocytosis by Macrophages. *Current Biology* **16**, 2161–2165 (2006).
- 188.** Stukes, S. A.; Cohen, H. W.; Casadevall, A. Temporal Kinetics and Quantitative Analysis of Cryptococcus neoformans Nonlytic Exocytosis. *Infection and Immunity* **82**, 2059–2067 (2014).
 - 189.** Davis, J. M.; Huang, M.; Botts, M. R.; Hull, C. M.; Huttenlocher, A. A Zebrafish Model of Cryptococcal Infection Reveals Roles for Macrophages, Endothelial Cells, and Neutrophils in the Establishment and Control of Sustained Fungemia. *Infection and Immunity* **84**, 3047–3062 (2016).
 - 190.** Chrisman, C. J.; Alvarez, M.; Casadevall, A. Phagocytosis of Cryptococcus neoformans by, and Nonlytic Exocytosis from, Acanthamoeba castellanii. *Applied and Environmental Microbiology* **76**, 6056–6062 (2010). [PMID:20675457]
 - 191.** Vergunst, A. C.; Meijer, A. H.; Renshaw, S. A.; O’Callaghan, D. Burkholderia cenocepacia creates an intramacrophage replication niche in zebrafish embryos, followed by bacterial dissemination and establishment of systemic infection. *Infection and Immunity* **78**, 1495–1508 (2010).
 - 192.** Hagedorn, M.; Rohde, K. H.; Russell, D. G.; Soldati, T. Infection by tubercular mycobacteria is spread by nonlytic ejection from their amoeba hosts. *Science (New York, N.Y.)* **323**, 1729–1733 (2009).
 - 193.** Syme, R. M.; Bruno, T. F.; Kozel, T. R.; Mody, C. H. The capsule of Cryptococcus neoformans reduces T-lymphocyte proliferation by reducing phagocytosis, which can be restored with anticapsular antibody. *Infection and immunity* **67**, 4620–4627 (1999). [PMID:10456908]
 - 194.** Kozel, T. R.; Gotschlich, E. C. The capsule of cryptococcus neoformans passively inhibits phagocytosis of the yeast by macrophages. *Journal of immunology (Baltimore, Md. : 1950)* **129**, 1675–1680 (1982). [PMID:7050244]
 - 195.** Heitman, J.; Kozel, T. R.; Kwon-Chung, K.; Perfect, J.; Casadevall, A. The Interaction of Cryptococcus neoformans with Host MacroPhages and Neutrophils. *ASM Press* 373–385 (2011).
 - 196.** Alvarez, M.; Saylor, C.; Casadevall, A. Antibody action after phagocytosis promotes Cryptococcus neoformans and Cryptococcus gattii macrophage exocytosis with biofilm-like microcolony formation. *Cellular Microbiology* **10**, 1622–1633 (2008).
 - 197.** Tabora, C. P.; Casadevall, A. CR3 (CD11b/CD18) and CR4 (CD11c/CD18) are involved in complement-independent antibody-mediated phagocytosis of Cryptococcus neoformans. *Immunity* **16**, 791–802 (2002).
 - 198.** Edelson, B. T.; Unanue, E. R. Intracellular antibody neutralizes Listeria growth. *Immunity* **14**, 503–512 (2001). [PMID:11371353]
 - 199.** Joly, E.; Hudrisier, D. What is trogocytosis and what is its purpose? *Nature Immunology* **4**,

- 815 (2003).
200. Steele, S.; Radlinski, L.; Taft-Benz, S.; Brunton, J.; Kawula, T. H. Trophocytosis-associated cell to cell spread of intracellular bacterial pathogens. *Elife* **5**, e10625 (2016).
 201. Quigley, J.; Hughitt, V. K.; Velikovskiy, C. A.; Mariuzza, R. A.; El-Sayed, N. M.; Briken, V. The Cell Wall Lipid PDIM Contributes to Phagosomal Escape and Host Cell Exit of *Mycobacterium tuberculosis*. *mBio* **8**, (2017). [PMID:28270579]
 202. Rustom, A.; Saffrich, R.; Markovic, I.; Walther, P.; Gerdes, H.-H. Nanotubular Highways for Intercellular Organelle Transport. *Science* **303**, 1007–1010 (2004).
 203. Cartwright, A. N. R.; Griggs, J.; Davis, D. M. The immune synapse clears and excludes molecules above a size threshold. *Nature Communications* **5**, 5479 (2014).
 204. Di Venanzio, G.; Lazzaro, M.; Morales, E. S.; Krapf, D.; García Vescovi, E. A pore-forming toxin enables *Serratia* a nonlytic egress from host cells. *Cellular Microbiology* **19**, e12656 (2017). [PMID:27532510]
 205. Casadevall, A.; Pirofski, L.-A. Immunoglobulins in defense, pathogenesis, and therapy of fungal diseases. *Cell Host & Microbe* **11**, 447–456 (2012).
 206. Feldmesser, M.; Casadevall, A. Effect of serum IgG1 to *Cryptococcus neoformans* glucuronoxylomannan on murine pulmonary infection. *Journal of Immunology (Baltimore, Md.: 1950)* **158**, 790–799 (1997).
 207. Dragotakes, Q.; Casadevall, A. Automated measurement of cryptococcal species polysaccharide capsule and cell body. *Journal of Visualized Experiments* **2018**, (2018).
 208. Levitz, S. M.; Harrison, T. S.; Tabuni, A.; Liu, X. Chloroquine induces human mononuclear phagocytes to inhibit and kill *Cryptococcus neoformans* by a mechanism independent of iron deprivation. *Journal of Clinical Investigation* **100**, 1640–1646 (1997).
 209. WERNER, G.; HAGENMAIER, H.; DRAUTZ, H.; BAUMGARTNER, A.; ZÄHNER, H. Metabolic products of microorganisms. 224. Bafilomycins, a new group of macrolide antibiotics. Production, isolation, chemical structure and biological activity. *The Journal of Antibiotics* **37**, 110–117 (1984).
 210. Erickson, T.; Liu, L.; Gueyikian, A.; Zhu, X.; Gibbons, J.; Williamson, P. R. Multiple virulence factors of *Cryptococcus neoformans* are dependent on VPH1. *Molecular Microbiology* **42**, 1121–1131 (2001).

Curriculum Vitae

Quigly Dragotakes

Email: dragotakes55@gmail.com

Education

Ithaca College

Ithaca, NY, May 2014

Degree: B.S. **Major:** Biochemistry **GPA:** 3.78

Awards and Honors: Dean's List (2010, 2011, 2012, 2013), Newton Award (2011), Magna Cum Laude (2014)

Johns Hopkins University Bloomberg School of Public Health

Baltimore, MD, May 2020

Degree: Ph.D. **Focus:** Molecular Microbiology and Immunology **GPA:** 3.98

Awards and Honors: Centennial Scholar (2017-2019), Predoctoral Training Grant T32 (2018-2020), Frederick B. Bang Award (2019-2020)

Scientific Contributions

Dragotakes Q, Casadevall A. Automated Measurement of *Cryptococcal* Species Polysaccharide Capsule and Cell Body. *Journal of Visualized Experiments* (2018).

Casadevall A, Coelho C, Cordero RJB, Dragotakes Q, Jung E, Vij R, Wear MP. The Capsule of *Cryptococcus neoformans*. *Virulence* (2018).

Freij JB, Fu MS, De Leon-Rodriguez CM, Dziedzic A, Jedlicka AE, Dragotakes Q, Rossi DCP, Jung EH, Coelho C, Casadevall A. Conservation of intracellular pathogenic strategy among distantly related cryptococcal species. *Infection and Immunity* (2018).

De Leon-Rodriguez CM, Rossi DCP, Fu MS, Dragotakes Q, Coelho C, Ros IG, Caballero B, Nolan SJ, Casadevall A. The outcome of the *Cryptococcus neoformans*-macrophage interaction depends on phagolysosomal membrane integrity. *The Journal of Immunology* (2018).

Dragotakes Q, Fu MS, Casadevall A. Dragotocytosis: Elucidation of the Mechanism for *Cryptococcus neoformans* Macrophage-to-Macrophage Transfer. *The Journal of Immunology* (2019).

Vij R, Danchik C, Crawford C, Dragotakes Q, Casadevall A. Variation in cell surface hydrophobicity among *Cryptococcus neoformans* strains influences interactions with amoeba. *mSphere* (2020).

Dragotakes Q, Stouffer K, Christine Youn, Fu MS, Leon-Rodriguez C, Freij J, Bergman A, Casadevall A: Macrophages utilize a bet-hedging strategy for antimicrobial activity in phagolysosomal acidification. *Journal of Clinical Investigations* (2020).

Patents

Dragotakes Q, Cordero RJB, Casadevall, A. "Melanin-based biocomposite for 3D-printing" Non-provisional Patent. JHU Ref. No. C15833. Dec 2019.

Cordero RJB, Casadevall A. "Fungal-based air-cooling system" Invention ID: D15946

Dragotakes Q, Cordero RJB, Casadevall, A. "Fungal carbon fixation" Invention ID: D15628

Research and Work Experience

Chief Science Officer, 2020

MelaTech LLC.

Upon graduation from my Ph.D. I have accepted a position as CSO at MelaTech LLC. I will oversee and manage research projects relating to the production of melanin and investigation into its uses as a biomaterial. Our main focus is developing products and materials to use in radiation shielding.

Research Assistant, June 2014 – June 2016

Greengard Lab of Molecular and Cellular Neuroscience, Rockefeller University

Investigating the role of a gene of interest in cellular Alzheimer's Disease pathology utilizing primary cell culture and mouse models.

Student Researcher, August 2013 – May 2014

Biochemistry Department, Ithaca College

Honors Research Thesis. Topic: Development of an *in-vitro* enzymatic assay of LuxI and AinS, two proteins involved in *Vibrio fischeri* quorum sensing.

Student Researcher, January 2011 – May 2014

Chemistry Department, Ithaca College, Scott Ulrich Ph.D.

Research topic: Synthesizing and assaying potential regulators of bacterial quorum sensing involving the Lux, Las, and Ain quorum sensing pathways.

Student Researcher, August 2013 – May 2014

Biology Department, Ithaca College, Te-Wen Lo Ph.D.

Research topic: Determining the role of Xol1 and Her1 in *C. briggsae* dosage compensation via genome editing with CRISPR/Cas and TALENs.

Student Researcher, August 2011 – May 2013

Chemistry Department, Ithaca College, Emily Garcia Segal Ph.D.

Research topic: Synthesis and assay of the TP-1 Revised quorum triggering molecule and new derivatives as inducers of the *Pseudomonas aeruginosa* LasR pathway.

Fellowships and Support

ARCS Foundation, Metropolitan Washington Chapter, 2018-2019

NIH T32 Training Grant, 2018-2020

Frederick B. Bang Award, JHSPH, 2019-2020

Research in the ability of melanized fungi to fix inorganic, environmental carbon. Utilizing modern technology to confirm fungi are capable of carbon fixation and elucidate the molecular pathway responsible for this phenomenon.

Internships and Scholarships

Ithaca College Dana Student Internship Summer of 2012

Research Associate, Summer 2012

Chemistry Department, Ithaca College, Emily Garcia Segal Ph.D.

Research topic: Synthesis and assay of TP-Br hybrid molecule and new derivatives as potential regulators of the *Pseudomonas aeruginosa* LasR quorum sensing pathway.

Teaching Experience

Private Science Tutor, August 2011 – May 2014

Academic Enrichment Services, Ithaca College

Academically engaging students struggling in biology, chemistry, and biochemistry classes in one-on-one and small group environments. Assisted students with understanding concepts, problem solving, and developing strong academic skills for the future.

Teaching Assistant, August 2011 – May 2014

Academic Enrichment Services, Ithaca College

Assisted professors in both laboratory and classroom settings for classes I had previously taken and scored well in. Throughout my four undergraduate years I assisted with Genetics (lecture), Principles of Chemistry (Lab), Organic and Biochemistry (lecture). In addition to the classroom portion, I was also responsible for hosting my own after-hour review sessions for students seeking extra help.